1982

End plate connections for steel beams.

Mona Ali. Hafez
University of Windsor

CANADIAN THESES ON MICROFICHE

I.S.B.N.

THESES CANADIENNES SUR MICROFICHE

National Library of Canada
Collections Development Branch

Canadian Theses on
Microfiche Service

Ottawa, Canada
K1A 0N4

Bibliothèque nationale du Canada
Direction du développement des collections

Service des thèses canadiennes
sur microfiche

NOTICE

The quality of this microfiche is heavily dependent upon the quality of the original thesis submitted for microfilming. Every effort has been made to ensure the highest quality of reproduction possible.

If pages are missing, contact the university which granted the degree.

Some pages may have indistinct print especially if the original pages were typed with a poor typewriter ribbon or if the university sent us a poor photocopy.

Previously copyrighted materials (journal articles, published tests, etc.) are not filmed.

Reproduction in full or in part of this film is governed by the Canadian Copyright Act, R.S.C. 1970, c. C-30. Please read the authorization forms which accompany this thesis.

THIS DISSERTATION
HAS BEEN MICROFILMED
EXACTLY AS RECEIVED

AVIS

La qualité de cette microfiche dépend grandement de la qualité de la thèse soumise au microfilmage. Nous avons tout fait pour assurer une qualité supérieure de reproduction.

S'il manque des pages, veuillez communiquer avec l'université qui a conféré le grade.

La qualité d'impression de certaines pages peut laisser à désirer, surtout si les pages originales ont été dactylographiées à l'aide d'un ruban usé ou si l'université nous a fait parvenir une photocopie de mauvaise qualité.

Les documents qui font déjà l'objet d'un droit d'auteur (articles de revue, examens publiés, etc.) ne sont pas microfilmés.

La reproduction, même partielle, de ce microfilm est soumise à la Loi canadienne sur le droit d'auteur, SRC 1970, c. C-30. Veuillez prendre connaissance des formules d'autorisation qui accompagnent cette thèse.

LA THÈSE A ÉTÉ
MICROFILMÉE TELLE QUE
NOUS L'AVONS REÇUE

NL-339 (r. 82/08)

Canada

END PLATE CONNECTIONS FOR STEEL BEAMS

by

© Mona Ali Hafez

A Thesis
submitted to the Faculty of Graduate Studies
through the Department of
Civil Engineering in Partial Fulfillment
of the requirements for the degree of
Master of Applied Science at
The University of Windsor

Windsor, Ontario, Canada

1982.

773927

To my family

ABSTRACT

END PLATE CONNECTIONS FOR STEEL BEAMS

An end plate welded transversely to the web of a beam and then bolted to the supporting member should provide an effective simple connection to transmit shear. However, under loading, the end of the beam rotates and moments are developed in the connection. It is essential that the end plate connection be sufficiently flexible so that the factored moment can be attained in the beam without fracture of the connection and without the development of excessive moments in the connection itself.

Based on the behaviour of T-sections, where the flange of the T simulates the end plate and stem simulates the web of the beam, both when the stem is loaded in tension and compression, analytical procedures have been developed to predict the moment-rotation behavior of end plate connections.

Good agreement has been obtained between the predicted moment-rotation curves and experimental curves for eight connections covering a practical range of end plate thicknesses, gage distances between bolt holes and connection depths. With the analytical curves the designer is thus able to predict the behavior of a proposed connection to ensure it has sufficient strength and flexibility.

ACKNOWLEDGEMENTS

The author wishes to express her sincere gratitude to Dr. D.J.L. Kennedy who kindly supervised this research, for his guidance, suggestions and continuous encouragement through the preparation of this thesis. The author expresses her deepest appreciation to the Civil Engineering Faculty members at the University of Windsor for their direct and indirect inspiration through their valuable courses.

Thanks are due to the technicians of the Civil Engineering laboratory, especially Mr. George Michalczuk; the technicians of the Central Shop at the University of Windsor; the Computer Centre at the University of Windsor for running the computer programs; Mrs. Zeleney for typing the manuscript.

The author is grateful to the financial support provided by the National Research Council of Canada.

The author's special deepest thanks go to her husband for his guidance and continuous encouragement.

TABLE OF CONTENTS

CHAPTER

LIST OF TABLES

LIST OF FIGURES

NOMENCLATURE

a	movement of the plate element in T-section tension tests away from the loading block, inches
b	width of the plate, inches
C	applied compressive force on the T-section compression test specimens, kips
c	half the thickness of the tensile zone, inches
d	depth of the beam, inches
d'	length of the flange of the T in a T-section compression test, inches
E	modulus of elasticity, ksi
e	one half the horizontal movement between the centre of the bolt holes in the flange plate for the T-section tension tests, inches
h_b	distance from the bottom of the beam to the spindle of the bottom dial gage, inches
h_t	distance from the top of the beam to the spindle of the top dial gage, inches
I	moment of inertia of the cross-section of the simulated end plate in the T-section tension tests, inches
ℓ	initial average distance between toe of the fillet weld and adjacent edge of the bolt hole of the end plate, inches
ℓ_b	distance from the neutral axis to the bottom flange of the beam, inches

L	span length, inches
M	moment acting on the section, inch-kips
M_u	maximum moment resistance of the section under pure moment, inch-kips
P	tensile force on the cross-section of the simulated end plate in the T-section tension test, kips
P_u	maximum tensile resistance under axial tension, kips
r_b	contraction given by the bottom gage in the end plate tests, inches
r_t	extension given by the top gage, inches
S	section modulus, in^3
s	the length over which spreading out occurs, inches
T	the applied tension force in the T-section tension test, kips
t	thickness of the end plate, inches
w	web thickness, inches
α	angle of deformation for the T-section tension tests, radians
Δ	deformation of the web plate of the T-section compression specimen, inches
Δ_b	distance between the end of the bottom flange of the beam and the face of the column during applying the end moment, inches

θ	the angle of rotation of the beam, radians
σ	maximum stress on the cross section of the simulated end plate in the T-section tension test, ksi
σ'	the average compresive stress at one inch (24.5 mm) from the flange force, ksi
σ_c	the applied compressive stress, ksi
σ_u	ultimate stress, ksi
σ_y	yield stress, ksi

CHAPTER I

INTRODUCTION

1.1 General

An end plate for beam-to-column connections is a relatively new type of simple connection. It consists solely of a vertical plate shop welded to the end of the web transverse to the axis of the beam with fillet welds on each side of the web. The field connection is made by bolting the end plate to the flange or web of the supporting member.

In simple end connections for beams, it is assumed that the connection allows rotation of the beam and transmits shear only. The very common simple connection has consisted of two angles, either bolted or welded to the beam web, and most frequently bolted to the supporting member.

One of the advantages of the angle connection is the possibility of making small adjustments in length or out-of-squareness. For example, if the beam is cut to the wrong length, the longitudinal position of the angles can be adjusted to make the length correct from back-to-back of angles. On the other hand, the angle connection has the disadvantage that two pieces of material have to be handled. It is, also, difficult to use when a skew connection is required.

The end plate connection is a simpler shear connection with only one piece to be fastened to the web and as well can be set at the skew angle easily. The beam must however be cut to the required length within close tolerances, but this can be done easily with automatic sawing equipment which also provides square ends.

1.2 Purpose of Research

The purpose of this research is:

1. to establish an analytical method for predicting the moment-rotation relationship for the end plate connection, at least up to the point where the end rotation causes the bottom flange of the beam to bear against the column,

2. to investigate the behaviour of the end plate, in tension and compression, and

3. to predict the moment at which the beam comes in contact with the column.

1.3 Method and Scope of Work

Three series of experimental studies have been conducted:

1. a study of the whole end plate connection was carried out. Static tests were performed on a series of end plate connections with varying geometry by subjecting the connections to shear and moment while measuring the rotation. These tests simulate the actual conditions as-

sociated with a beam connected to a column,

2. a study of the end plate connection detail in tension by testing short segments subjected to tension only,

3. a study of the end plate connection detail in compression by testing short segments of the end plate connection in compression.

The relationship between moment and rotation for the end plate connection can be derived by integrating the behaviour of elemental lengths of T-sections, under tension or compression, where the T is comprised of a stem modelling the beam web and a flange modelling the end plate. Fig. 1.1 shows an elevation and horizontal section of an end plate connection. By subdividing the end plate into a sufficient number of constituent short segments of finite length, a combined effect, equivalent to that of the total length of end plate, can be found.

1.4 Previous Work

Kennedy (1966), carried out some tests to determine the practicability of end plate connections. The limited tests indicated that the connection would perform satisfactorily, but the tests were insufficient in number to assess the behaviour of the connections with differing geometries.

Sommer (1969), investigated the effect of varying some geometric parameters. Parameters investigated included

the thickness of the end plate, thickness of web, gage between bolt holes and the overall depth of the connection. These tests led to:

1. the development of a standardized moment rotation curve within the limits of these tests,

2. the realization that end plate connections are relatively flexible limiting the moment transmitted,

3. the demonstration that the shear capacity is not appreciably affected by the moment on the connection, and

4. the realization that previous representations of the beam-line, on moment-rotation curves for end connections, as a single straight line (McGuire 1968) were incorrect.

CHAPTER II

EXPERIMENTAL PROGRAM

2.1 General

In devising the experimental program, chief consideration was given to the behaviour of the end plate connections themselves when subject to shear and moment. Previous work by Sommer (1969) had shown that the moment rotation behaviour, which depends on the depth of connection (or the number of rows of bolts), the thickness of the end plate, and the gage distance between the vertical rows of bolts fastening the end plate to the column, was independent of the moment-shear ratio. Therefore, in the main series of tests reported here, the load was applied to the beam cantilevering from the test frame at one lever arm only of 38.5 inches (978 mm) as shown in Fig. 2.1.

It is recognized, when end plate connections are used for framing a simple beam, that the bending moment changes from the negative moment developed in the connection at the face of the column to zero and then to a positive moment a short distance along the length of the beam. Assuming the usual case of a uniformly distributed load, the position where the moment reverses depends both on the ratio of the end moment developed to the maximum moment in the beam and the beam span. For the connections tested the location of zero moment was always within the beam as given in Section 4.4.5.

Under load, the top of the end plate deforms and is pulled away from the column. To determine the relationship between this deformation, that is, the amount the plate pulled away from the column, and the tensile load, a series of tension tests on T-sections, to simulate an incremental length of the top of the end plate connection in tension, was performed as described in Section 2.3.

In the lower portion of the end plate connection, as the moment is increased, the end plate is pushed into the beam web. To simulate this behaviour, and to arrive at an understanding of how the loads were transferred, a series of compression tests was performed, again on a simulated part of the end plate connection in the form of T-section as described in Section 2.4.

In addition to the main series of tests on the end plate connections themselves, the tension and compression tests on the T-sections to simulate the behaviour of the end plate above and below the neutral axis, ancillary tests were conducted to determine fundamental material properties of the steel used for the end plates and for the beam web. These tests are reported in Section 2.2.

2.2 Ancillary Tests

The beam and plate material was specified to be general purpose structural steel, C.S.A. Grade G40.21 44W (grade G40.21 300W). Static tension tests were carried out in

accordance with ASTM Standard A370 on coupons of two inch (51 mm) gage length, cut from the plates and beam web.

Three plate thicknesses of 1/4, 3/8 and 1/2 inches (6.3, 9.5, and 12.7 mm) plates and three tension tests were conducted on each thickness.

One beam size, WWF 27x106 (WWF 690x158)* was used throughout the program and six tension tests were conducted on coupons cut from the 7/16 inch (11.1 mm) thick web.

2.3 Tension Tests on T-Sections

2.3.1 Test Specimens

The top portion of the end plate of the beam-column connection is subject to a tensile load when the beam is loaded with transverse loads. To simulate this behaviour, T-section specimens were tested under tension.

The flanges for the specimens were cut from the same steel that was used for the end plate in the main tests on end plate connections.

Twenty-seven specimens were tested to represent the different dimensions that were tested in the main end plate connection tests.

Each specimen consisted of two pieces of steel welded to form a T with E 7018 electrodes, the same type as used for welding the end plates to the beam web. The stem of

---

*Not available in SI units.

the T represented part of the web of the beam, and the flange a short segment of the end plate. Fig. 2.2 shows a tensile T-section specimen.

The width of the stems and flanges of all specimens was 3 inches (76 mm), corresponding to the pitch of the bolt holes used in the end plates of the main connection tests, thus representing one pitch length of end plate. The length of the stems of all T-section specimens was 12 inches (305 mm), to enable each specimen to be held firmly in the jaws of the Universal Testing Machine used for testing, and leaving a portion of the stem free for access to the test piece for measurements during testing.

Two different widths of 6 1/2 or 8 inches (165 or 203 mm) representing the two different widths of the end plates in the main tests were used. Two 13/16 inch (20.6 mm) diameter holes were drilled in each flange at a gage of either 4 or 5 1/2 inches (102 or 140 mm) according to the flange width with the edge distance in both cases held constant at 1 1/4 inches (31.8 mm), the same as for the main tests.

The thickness of the flanges of the tension specimens 1/4, 3/8 or 1/2 inch (6.3, 9.5 or 12.7 mm) corresponded to the end plate thickness in the main tests.

Table 2.1 shows the combinations of plate thickness and gages of the tension tests conducted. A typical test

was designated at T-9-3/8-4, where the T signifies a tension test, the 9 the sequential test number the 3/8 the plate flange thickness in inches of the T-section and the 4 the gage distance in inches.

The specimens for test number 1 to 12 were welded at the Civil Engineering Laboratory of the University of Windsor, while specimens for test numbers 13 to 27 were welded in a steel fabricator's shop.

2.3.2 Test Equipment and Instrumentation

A Universal Testing Machine, Fig. 2.3, with a capacity of 120 kips (534 kN) was used to load the T-section tension specimens. The jaws of the machine grasped the end portion of the stem of the specimen on the one end and a heavy rectangular loading block with a gage of 4 or 5 1/2 inches (102 or 140 mm) was bolted to the flange of the T-section on the other as shown in Fig. 2.4.

The movement of the flange of the T away from the loading block, - the latter simulating the flange of the column - was measured by two dial gages with bases attached to the stem of the T-section and spindles resting against the loading block. The least reading of the dial gages with a range of one inch (25.4 mm) was 0.001 inches (0.025 mm).

As the test progressed, the distance between the centers of the holes of the flange decreased, and this change was measured on both sides to the nearest 0.001 inches

(0.025 mm) using calipers held in place by a magnet bearing against the 1/8 inch (3 mm) diameter pins installed opposite the holes.

2.3.3 Testing Procedure

The specimen, bolted to the loading block with two 3/4 inch (19 mm) diameter A 325 bolts torqued to 360 ft. lbs. (488 N.m), was firmly grasped in the testing machine, the calipers and dial gages were mounted and zero readings were taken.

The load was applied in increments based on the anticipated behaviour and readings were taken.

Tests were terminated when the plate or the weld failed.

2.4 Compression Tests on T-Sections

2.4.1 Test Specimens

The bottom portion of the end plate connection is subject to compressive forces as the end plate is forced into the web of the beam. The force in the end plate spreads downward into the web. To simulate this behaviour and to determine how the load spreads out, twelve T-section specimens, cut from the 1/2 inch (12.7 mm) thick steel plate that was used for the end plates in the main tests, were tested under compression.

Each specimen consisted of two pieces of steel welded perpendicular to each other with E 7018 electrode as shown

in Fig. 2.5. The stem of the T-section represents part of the web of the beam while the flange simulates a segment of the end plate. By testing 3 different lengths of simulated end plate as shown in Fig. 2.5 it was hoped to be able to distinguish between the compressive force transmitted per unit length of end plate and the compressive force resulting from the spreading out in the web.

Following preliminary tests, conducted to get an appreciation of the behaviour of the compression zone at the ends of the end plate, the deformation measurement system evolved from that shown in Fig. 2.5.1 to that in Fig. 2.5.3. In all cases measurements were made using dial gages supported on the platten with spindles against long 1/8 inch diameter pins snug fitted in the holes drilled in the simulated web plate at several points.

Table 2.2 gives the matrix of compression tests on T-sections. A typical compression test was designated as C-5-3-2, where the C signifies a compression test, the 5 the sequential test number, the 3 the length of the end plate in inches and 2 the second pattern of gaging.

The specimens for test numbers 1 to 6 were welded at the Civil Engineering Laboratory of the University of Windsor, while specimens for test number 7 to 12 were welded at a fabricator's shop.

2.4.2 Test Equipment and Instrumentation

The Universal testing machine shown in Fig. 2.3 with a maximum capacity of 120 kips (534 kN) was used for the first three tests and thereafter the specimens were tested using a compression testing machine of capacity of 300 kips (1334 kN).

A steel loading plate 10 inches (254 mm) long by 5 inches (127 m) wide by 1.25 inches (31.7 mm) thick with a central longitudinal rectangular groove 1/4 inches (6.3 mm) deep by 9/16 inches (14.3 mm) wide was placed on top of the specimen and a swivel base was placed beneath for testing. The spindles of the dial gages were placed against portions of the steel rods (snugly fitted into the holes drilled into the specimens as shown in Fig. 2.5) that were ground flat.

2.4.3 Testing Procedure

Before testing a stress coating was applied to the two sides of the web of the specimen.

A relatively small load, less than 500 pounds (2.2 kN) was applied to the specimen to hold it in place without movement while the dial gages were positioned and initial readings were taken.

The load was applied in increments and readings of the dial gages were taken.

The maximum applied compressive load recorded in each

test was when the extreme ends of the web on both sides of the flange plate of the specimen had deformed sufficiently to bear on the swivel plate.

Fig. 2.6 shows a T-section compression specimen placed in the testing machine between the swivel and the special loading block.

2.5 Tests on End Plate Connections

2.5.1 Test Specimens

Ordinary shop procedures were used to fabricate the end plate connection test specimens. No special care or technique was called for, so that the test specimens would be of the same standard as those normally fabricated.

One size of beam WWF 27x106 (WWF 690x158)* was used. With a span to depth ratio of 24 this beam could be used on a span of 54 feet (16.46 m). Limiting the live load deflection to 1/300 of the span and using dead and live load factors of 1.25 and 1.50 the yield moment is attained on this simple beam span when the dead load of 44% of the live load of 1.30 klf (19.0 kN/m). The corresponding factored shear is 72 kips (320 kN). Four beams each 44 inches (1118 mm) long were prepared with an end plate welded at each end to enable each beam to be used for two tests.

The end plates were saw cut to the different sizes

*Not available in SI units.

and the bolt holes were drilled at the required pitch and gage. The vertical pitch of all 13/16 inch (20.6 mm) diameter holes for the 3/4 inch (19 mm) diameter bolts was 3 inches (76 mm) while the horizontal gage distance was either 4 or 5 1/2 inches (102 mm or 140 mm). Beam and plate details are given in Figs. 2.7 to 2.10.

The deepest connections - 24 inches (610 mm) in depth - have 48 inches (1219 mm) of 1/4 inch (6.35 mm) weld with 16 A 325 bolts of 3/4 (19.0 mm) diameter. Such a connection could develop the full factored shear capacity of the web, for when using nominal values for the yield strength of the web, and the ultimate strengths of the bolts and welds, the factored capacity of the bolts and welds are 111% and 122% of the factored web shear capacity respectively.

By equating the uniformly distributed load to cause the attainment of the yield moment, $8\ \sigma_y S/L^2$ to that causing shear yield of the web $2 \times 0.66\ \sigma_y\ d.w/L$ the the simple span, L, can be found for which both conditions occur simultaneously. This is computed to be 12.62 feet (38.47 mm).

The shallowest connection, 1/2 of the deepest, has a factored shear capacity controlled by the capacity of the bolts of 55% of the factored web shear capacity. For this capacity to be reached simultaneously with the yield

moment in the centre of a simple supported beam with a uniformly distributed load the span length is 24.53 feet (7477 mm). The shear capacity of this connection is more than twice that needed for a beam of span to depth ratio of 24 spanning 54 feet when its capacity is simultaneously controlled by a live load deflection of 1/300 and yield attainment of the moment at the centre line.

End plates were welded, using E 7018 electrodes, at right angles to the end of the beam with a 1/4 inch (6.3 mm) fillet weld running the full depth of the plate on each side of the web of the beam.

Dial gages, affixed to the web by bolting through 1/8 inch (3.2 mm) diameter holes located in a vertical line 3 inches (76 mm) from the end of the beam, were used to measure the relative movement of the beam (and hence the distortion of the end plate assembly) with respect to the testing face. In particular two gages were mounted 1/4 inch (6.3 mm) above and below the bottom end of the end plate.

Table 2.3 presents the matrix of end plate connection tests. For a test designated as E-5-4-3/8-5 1/2 the E signifies an end plate connection test; the 5, the sequential test number; the 4, the number of rows of bolts connecting the end plate to the column; the 3/8, the thickness of the end plate tested in inches; the

5 1/2, the horizontal gage distance between the two vertical rows of bolts in inches.

2.5.2 Test Set-Up and Equipment

Figure 2.1 shows the test set-up to determine the moment-rotational behaviour of the end plate connections, with the beam bolted through the end plate to the column of the test frame.

The frame was held in place by tack welding to the floor and supporting the top laterally by connections to a fixed rigid loading frame. The frame was positioned such that the hydraulic loading jack, reacting against the beam, was located at 38.5 inches (97.8 mm) from the column flange face.

The flange of the column had holes drilled to receive the bolts on a horizontal gage of 4 inches and 5 1/2 inches (102 mm and 140 mm) and a vertical pitch of 3 inches (76 mm).

By putting shim plates between the end plates and the column flange the same length of bolts - 3.5 inches (89 mm) - as used in the T-section tension tests could be used.

Between the hydraulic jack and the beam a hardened spherical head and a nest of hardened rollers were provided to allow rotation and lateral movement of the beam with respect to the jack which was maintained in a vertical direction a constant distance from the column flange

as shown in Fig. 2.11.

2.5.3 Instrumentation

2.5.3.1 Load Measurement

A previously calibrated Universal flat load cell with a capacity of 100 kips (445 kN) interposed between the jack and the spherical head was used to measure the load applied by the hydraulic jack as shown in Fig. 2.11.

2.5.3.2 Beam Deflection

The deflection of the free end of the beam during loading was measured by two dial gages with 3 inch (176 mm) travel mounted on the top of the bottom flange of the beam as shown in Fig. 2.12. These deflection readings were used to monitor the behaviour of the connection during testing, to decide on load increments to be used and to assist in detecting when the bottom flange of the beam touched the column.

2.5.3.2 Beam Rotation

The rotation of the beam relative to the column was obtained from the measurements of the movements of the top flange of the beam away from the column and of the bottom flange toward the column. Four dial gages, two at the top and two at the bottom were used for this purpose. The bases of the gages were fastened magnetically to the upper surface of the top flange of the beam and to the lower surface of the bottom flange, on each side of the web with the

spindles resting against the column.

Figure 2.13 shows the positioning of these dial gages as well as many dial gages affixed at intermediate locations. These latter gages were subsequently abandoned.

2.5.3.4 Plate Deformation

As the upper part of the end plate connection was pulled outward from the column during loading there was a tendency for the vertical edges of the end plate to move horizontally toward each other.

This horizontal movement was measured by three dial gages placed on each side of the end plate with their bases fixed to the column and their spindles resting against the edges of the end plate, spaced 3 inches apart vertically starting from the top of the end plate as shown in Fig. 2.13.

2.5.4 Testing Procedure

Each test beam was hoisted into place using the laboratory crane and the end plate was bolted to the column using 3/4 inch (19 mm) diameter A 325 bolts torqued to 360 ft. lbs. (488 Nm) using a torque wrench. The head end of the bolt was against the end plate and the nut on the inside of the column flange. A washer was placed under the nut.

The end plate and adjoining web area were sprayed with a stress coating material so that local yielding

could be observed.

With the dial gages in place, initial readings were recorded and the load was applied in increments according to the anticipated behaviour of the connection and readings of all the dial gages were taken.

Tests were terminated when either the plate or the weld exhibited failure causing the applied load to decrease with increasing deformation.

CHAPTER III

EXPERIMENTAL RESULTS

3.1 General

The quantitative results of the various experiments are first presented in the form of tables or curves that relate, in general terms, the load to deformation. A qualitative presentation of the overall behaviour is also given. The results of the ancillary tests on tension coupons are given in Section 3.2. Section 3.3 gives the results of the tension tests on the T-specimens; section 3.4, the results of the tests on the compression tests on the T-specimens and section 3.5 gives the results of the tests on the end plate connections themselves. In Appendix I detailed observations of each of the end plate connection tests are presented.

3.2 Ancillary Tests

The results of all the static tension tests on coupons cut from the steel plates used for end plates and beam webs are summarized in Table 3.1. All deformations were measured on a 2 inch (51 mm) gage length.

The average yield stress and ultimate strength for the 1/4 inch (6.3 mm) plate were 52.5 ksi (363.6 MPa) and

78.5 ksi (541.2 MPa) respectively, while for the 3/8 inch (9.5 mm) thick plate the values are 42.2 and 65.5 ksi (291 and 451.6 MPa) and for the 1/2 inch (12.7 mm) plate 42.2 and 64.1 ksi (291 and 442.6 MPa). The modulus of elasticity was determined to be 30,000 + 359, -385 ksi (206, 841 + 2475, -2654 MPa) for all the plate tests.

The beam web on the basis of six tests, has a yield strength of 47.4 ksi (326.8 MPa) and an ultimate strength of 76.5 ksi (527.4 MPa) with a modulus of elasticity of 30,000 + 3,500, - 1,700 ksi (206 841 + 24 131, - 11 720 MPa).

Figure 3.1 shows a typical stress-strain curve as obtained on a test on the 3/8 inch (9.5 mm) thick end plate material.

3.3 Tension Tests on T-Sections

3.3.1 Tension Versus Angle of Deformation

In Figs. 3.2 through 3.11 are plotted the tension developed versus the angle of deformation of the end plate, as discussed later, for the tension tests on the T-sections for flange thicknesses and gage lengths respectively as follows, with 2 figures for each combination: 1/2 inch (12.7 mm) and 5.5 inches (140 mm); 3/8 inch (9.5 mm) and 5.5 inches (140 mm); 3/8 inch (9.55 mm) and 4 inches (102 mm); 1/4 inch (6.3 mm) and 5.5 inches (140 mm); 1/4 inch (6.3 mm) and 4 inches (102 mm). In all, 27 tests were conducted. Also shown in the figures are analytical curves derived as discussed in Chapter IV.

From Fig. 3.12, showing an undeformed and deformed plate, the angle of deformation is calculated as,

$$\alpha = \tan^{-1} \frac{a}{\ell - e}$$

where,

a = movement of the plate element away from the loading block, the average of the two dial gage readings.

ℓ = initial average distance between the toe of the fillet weld and the adjacent edge of the hole in the plate, and

e = one half the horizontal movement between the centres of the bolt holes in the flange plate.

3.3.2 Overall Behaviour

The tension tests performed on T-sections specimens all exhibited the same general overall behaviour:

1) At very low loads deformations appeared to be elastic with a linear relationship between the applied load and the angle of deformation, α.

2) At still relatively low loads, yielding was observed near the toe of the welds and on a line approximately at the inner edge of the bolt holes indicating the formation of plastic hinges along these lines.

3) With further loading the gap between the T-Section and the loading block increased significantly. Inward lateral movement of the extreme edges of the flange of the T-section was observed as slip took place at the bolts and inelastic deformation of the bolt holes occurred. At this stage it appeared that the tensile load T is being carried by the plate acting predominantly as a membrane.

4) Failure of the specimens generally occurred with the formation of a longitudinal crack at the outer toe of the fillet weld on one or both sides of the specimen. Attempts to increase the load would lead to propagation of the crack along the plate until rupture occurred.

Figure 3.13 illustrates the large gap that developed between the T-section and the loading block and a fracture line. To locate the position where plastic yield lines form as discussed above, three specimens of the T-Section tension tests were sectioned by cutting the 3 inch (76 mm) length into 5 portions 0.6 inch (15 mm) wide.

Traces of the cross section given in Fig. 3.14 show that the hinges can be considered to form at the toe of the fillet weld and at the inner edge of the bolt hole.

3.4 Compression Tests on T-Sections

3.4.1 Compression Versus Deformation

On Figs. 3.15 to 3.21 are plotted the compressive

load in kips applied to the T-section versus the deformation Δ, in inches as measured between the gage locations indicated and the supporting platten of the loading machine. Each curve on a figure represents the average of the four measurements taken at the same distance from the edge of the end plate, two on the obverse and two on the reverse face of the web plate. On Fig. 3.21 the results for tests 7, 8, 9, 10, 11 and 12 are summarized. Here are plotted the deformations, found to be most significant taken at a location 1/4 inches (6.3 mm), (locations 1, 4, 5, 8), away from the edge of the end plate.

3.4.2 Overall Behaviour

The general behaviour of the T-sections when tested in compression is as follows:

i) At low loads the specimens deform elastically as evidenced by linear load deformation curves and the observation of no cracking of the stress coating;

ii) As the load is increased yielding of the simulated web plate (the upper plate) begins at the ends of the end (lower) plate;

iii) With further loading the yielding of the web plate spreads to eventually cover the entire length of the end plate (lower plate) and beyond both its ends;

iv) The end plate is pushed up into the web plate until the extreme edges of the web plate touch the machine

platten. Figure 3.22 shows a compression test after testing.

Two specimens, the test results of which are not represented here, failed by buckling of the web plate before the web plate was deformed sufficiently to touch the platten. This behaviour resulted because the web plates were not welded at right angles to the end plate and the specimens were therefore loaded eccentrically.

3.5 Tests on End Plate Connections

3.5.1 The Moment Rotation Curves

The results of the tests on the end plate connection is presented in the form of the moment rotation curves plotted in Figs. 3.23 to 3.30. Experimental data are also given in Tables 3.2 to 3.9 where is also tabled the theoretical moment as determined in Section 4.4.3.

The moment is the cantilever moment resulting from the dead weight of the loading system and the applied load of the hydraulic jack acting at the lever arm "L".

Figure 3.31 shows schematically dial gage spindles at distances h_t and h_b above the top and below the bottom flanges of the beam respectively from which the angle of rotation is determined to be:

$$\theta = \tan^{-1} \frac{r_t + r_b}{d + h_t + h_b}$$

in which r_t is the extension given by the top gage, r_b is the contraction given by the bottom gage and d is the depth of the beam.

3.5.2 Overall Behaviour

All the moment rotation curves exhibit the same characteristics from which the overall behaviour of the connection when subject to shear and moment can be summarized as follows:

i) Even at very low loads inelastic action occurs as the curves have very limited if any linear portions;

ii) With increased loading as the moment rotation curves become flattened, cracking of the stress coating occurs on the upper part of the end plate adjacent to the toes of the welds and between the bolts. Yield lines at these locations are forming and gradually progress downwards as shown in Fig. 3.32 for Test 7.

iii) Further loading causes spalling of the coating on the web adjacent to the bottom end of the end plate as shown in Fig. 3.33.

iv) The outward movement of the top portion of the plate from the column becomes very evident and the yielded zones in the end plate increase in size;

v) The rotation of the connection is now relatively large and is attributed also in part to the end plate being pushed into the web plate with very severe inelastic distortions of the latter. The bottom flange of the beam comes in contact with the column;

vi) Further loading causes little deformation at the

bottom of the beam with the flange bearing against the column and subsequent rotation results almost entirely from the outward movement of the top of the connection. Rotation now essentially takes place about the bottom flange of the beam. With the shift in the neutral axis and the increased effective depth of the connection it becomes much stiffer as shown by the sharply increased slope of the moment rotation curves;

vii) Cracking at the toe of the welds in the end plates starting at the top finally occurs. With continued deformation the cracks progress downward and the connection is only capable of carrying a reduced load.

At low loads plastic hinges (yield lines) tend to develop in the upper portion of the end plate at the toe of the welds and near the line of the bolts, as the end plate moves away from the column.

The thinner the end plate, the less its yield capacity and conversely the greater is its flexibility. Thus this action occurs at relatively low loads with the 1/4 inch thick end plate. In the end plate connection tests with plate thickness of 3/8 and 1/2 inches plates, pronounced prying action on the bolts in the tension zone occurs with significant deformation of the bolts, although no bolts fractured. The bolts' deformation, of course, increases the rotation of the connection and compensated partly for the

decreased flexibility of the thicker plates.

Figure 3.34 shows deformed bolts for test E 6-4-1/2-5.5. Figure 3.35 shows the large gap that develops between the end of the beam and the column at the top of the connection.

3.5.3 Deformation of Connection as a Function of Depth

In some tests measurements of movement of the beam web with respect to the column face were made by fixing a series of dial gages on a vertical line 3 inches away from the column face. Fig. 3.36 presents the results of such measurements for test E-6-1/2-5.5 at loads of 5, 10, 15, 20, 25, 30, 50 and 60 kips (22.2, 44.5, 66.7, 90, 112.2, 133.4, 222.4, 266.9 kN) and shows that the movement varies linearly with depth.

3.5.4 Position of Centre of Rotation

The location of the centre of rotation of a flexible end plate connection subjected to moment, appears to depend on the depth of the connection and to vary with load even before the beam flange bears against the column. After the beam flange contacts the column the centre of rotation shifts to a point near the bottom of the beam. When the beam flange is about to come into contact with the column the centre of rotation is from 65 to 95% of

the depth of the connection below the top end as shown on Fig. 3.37 to Fig. 3.41, where are plotted the variation of the neutral axis measured from the top of the end plate as a function of the end rotation for the eight beam tests. These data are also presented in tabular form in Table 3.10.

CHAPTER IV

ANALYSIS AND DISCUSSION

4.1 General

The experimental results of tension tests on the T-sections are discussed and analytical relationships between force and deformation are developed. A study and analysis of the compression test results on T-sections leads to the development of a stress displacement relationship applicable to all of the compression tests. The analytical relationships for the tension and compression tests are then used to establish an analytical method for the prediction of moment-rotation behaviour for end plate connections. The method of analysis presented includes the determination of the position of centre of rotation of the end plate and the corresponding moment and rotation for all moments up to that which causes the bottom flange of the beam to come into contact with the column.

4.2 Tension Tests on T-sections

4.2.1 Analytical Relationship Between Force and Angle of Deformation

Visual observations incidicate that two limiting modes of behaviour of the T-sections exist. As load is first

applied to the T-specimen, the flange of the T, (simulating the end plate) bends at the toe of weld and near the edge of bolt hole and plastic hinges - yield lines - are formed at these two locations. The plate is being subject to bending moments and a flexural analysis would be appropriate. With increased loading, tensile straining of the plate becomes dominant, indicating that the plate is now acting as a membrane.

The shift from one mode to the other is gradual as the tensile strains, due to membrane action, gradually erase the flexural strains. An analysis, taking into account both the flexural and membrane action, is therefore appropriate.

4.2.1.1 Elastic Flexural Analysis

The observed location of the yield lines when the T-section exhibits flexural action are shown schematically on Fig. 4.1.

From the free body diagram of the half plate shown in Fig. 4.2

$$T = \frac{4M}{\ell} \qquad (4.1)$$

For elastic conditions the displacement, a, in the direction of the web is

$$a = \frac{T\ell^3}{24EI} \qquad (4.2)$$

where

E = modulus of elasticity, ksi

$I = \frac{bt^3}{12}$

= moment of inertia of the rectangular cross section of the plate, in^4

b = width of plate, inches, and

t = thickness of plate, inches.

The angle of deformation is

$$\alpha = \tan^{-1} \frac{a}{\ell} \tag{4.3}$$

and thus

$$T = \frac{24EI}{\ell^2} \tan \alpha \tag{4.4}$$

For small values of α, this relationship is plotted in Figs. 3.2 to 3.11 as a linear between T and α up to the load $T=T_p$ that causes yielding through the cross section where the moments are at maximum. The line lies close to the experimental results for low values of load, but the experimental curves diverge from the straight line at loads much less than T_p as would result from the effect of gradually yielding of the cross section and exaggerated by residual stresses.

4.2.1.2 Combined Flexural and Membrane Analysis

When both tensile forces and moments act on a section, and when the section is stressed throughout to a maximum stress σ, either in tension or compression, the stress

distribution across the cross section is as shown in Fig. 4.3.

The moment acting on the section is given by

$$M = \sigma b \left(\frac{t^2}{4} - c^2\right) \tag{4.5}$$

where

t = the thickness of the plate.

c = half the thickness of the tensile zone

b = the width of the plate, and

σ = the maximum stress

The tensile force on the section is

$$P = 2\sigma bc \tag{4.6}$$

The maximum moment resistance of the section under pure moment is

$$M_u = \sigma b \frac{t^2}{4} \tag{4.7}$$

The maximum tensile resistance under axial tension only is

$$P_u = \sigma bt \tag{4.8}$$

Substituting Equation 4.7 in equation 4.5 gives

$$\frac{M}{M_u} = 1 - \frac{4c^2}{t^2} \tag{4.9}$$

From Equations 4.6, 4.8 and 4.9, the moment and tension acting on the section concurrently is given by

$$\frac{M}{M_u} + \frac{P^2}{P_u}_2 = 1 \qquad (4.10)$$

Fig . 4.4 shows a free body diagram for a deformed T-section tensile specimen. Summing forces in the Y-direction, the tensile force, T, is

$$T = 2P \sin \alpha + 2V \cos \alpha \qquad (4.11)$$

where P and V are the tensile and shear forces respectively in the plate.

Fig. 4.5 shows a free body diagram for the portion of the plate between the toe of the fillet weld and the edge of the bolt hole, from which the shear force is

$$V = \frac{2M}{\ell} \cos \alpha \qquad (4.12)$$

Combining Equations 4.11 and 4.12, the tensile force in the web, T, is expressed in terms of the moment and tensile force in the plate as

$$T = 2P \sin \alpha + 4 \frac{M}{\ell} \cos^2 \alpha \qquad (4.13)$$

Substituting for the value of M from Equation 4.10 into Equation 4.13 the tensile force T is given by

$$T = 2P \sin \alpha + 4 \cos^2 \alpha \frac{M_u}{\ell} - 4 \cos^2 \alpha \frac{M_u}{\ell} \left(\frac{P}{P_u}\right)^2 \qquad (4.14)$$

Setting the partial derivative of T with respect to P equal to zero gives

$$\frac{\partial T}{\partial P} = 2 \sin \alpha - 8 \cos^2 \alpha \frac{M_u}{\ell} \frac{P}{P_u^2} = 0 \qquad (4.15)$$

and hence

$$P = \frac{\ell P_u^2 \sin \alpha}{4 \cos^2 \alpha M_u} \qquad (4.16)$$

The maximization is physically equivalent to stating the force T will be carried in the most direct manner. Substituting this value of P in Equation 4.14 gives T in terms of ultimate moment and ultimate tension in the end plate as

$$T = \frac{\ell \tan^2 \alpha}{4M_u} P_u^2 + 4 \cos^2 \alpha \frac{M_u}{\ell} \qquad (4.17)$$

An examination of the specimens indicated that the strains at hinge locations are extremely large suggesting that the moment capacity be based on the ultimate stress σ_u, while between the hinges the strains are less suggesting that the tensile force developed be based on the yield stress σ_y. Thus for these conditions Equation 4.17 is written

$$T = \frac{\ell \tan^2 \alpha}{4M_u} P_y^2 + 4 \cos^2 \alpha \frac{M_u}{\ell} \qquad (4.18)$$

This analytical equation is plotted together with the experimental results on Figs. 3.2 to Fig. 3.11.

The analytical expression for combined flexural and membrane action lies close to the experimental curves for values of α above about 0.1 radians. For lower values the analytical expression, in general, lies considerably above the experimental curves. This is attributed to the fact that yielding occurs gradually through the thickness of the plate whereas the analytical expression is based on a maximum stress, whether in tension or compression through the total plate thickness.

4.3 Compression Tests on T-Sections

4.3.1 Investigation of Area Subjected to Compression

The web plate adjacent to the end plate (over the length located below the neutral axis) is subject to direct compressive forces. Directly below the end of the end plate, compressive forces will exist in the web plate due to the compressive load spreading out. This force should be considered when calculating the total compressive force accommodated by the connection due to an applied end moment.

Fig. 4.6 shows a T-section compression specimen simulating part of the end plate connection below the neutral axis. When subject to load, the compressive force is assumed to spread out beyond the ends of the flange of the T-section.

At the location where the deformation was measured (one inch (25 mm) from the flange toe), the length over

which spreading out has occurred is denoted by 's'.

For a uniform compressive stress σ', the total compressive force is

$$C = \sigma' wd' + 2\sigma' ws \qquad (4.19)$$

where

C = the applied compression force

σ' = the average compressive stress at one inch (25.4 mm) from the flange face

w = the web thickness

d' = the length of the flange of the T, and

s = the length over which spreading out occurs.

By rearranging Equation 4.19

$$s = \frac{C}{2\sigma' w} - \frac{d'}{2} \qquad (4.20)$$

To study the variaion of 's', a statistical study of the experimental results of the compression tests was carried out.

4.3.2 Statistical Study of the Length of Spread Out

Equation 4.20 was used to determine the experimental values of 's' for different T-section compression tests, as follows:

For all tests the value of C was found corresponding to several constant values of displacements such as 0.22

inches (5.6 mm), 0.24 inches (6.1 mm) displacement, and the maximum displacement. At these displacements the compressive stress would be relatively large. The length d' was chosen as either the length of the flange plate or out to out of weld returns as measured for the test.

Using a consistent value of σ' of 64.1 ksi (443 MPa), the ultimate strength of the 1/2 inch plate used in the tests, the least variation in 's' was obtained by using d' equal to the length of the flange plate. On this basis the mean value of 's' was found to be 1.11 inches (28.2 mm) when the maximum load C was applied and 0.934 inches (23.7 mm) for applied load causing a 0.2 inches (5.1 mm) deflection. Because these measurements were at distances of one inch (25.4 mm) from the flange plate, an angle of the spread-out of the compression force beyond the end of the plate of 45° appears reasonable.

4.3.3 Stress Displacement Relationships

By considering the force to spread out at an angle of 45° beyond the ends of the flange plate, the results of all the compression tests, irrespective of the length of the flange plate can be represented on one graph of stress versus displacement as shown in Fig. 4.7. On the same graph the mean curve for all results is plotted. The relatively narrow band of test results indicates that the use of a spread-out angle of 45° is appropriate.

From the mean curve, it is seen that first an elastic behaviour exists followed by inelastic behaviour which may be represented by a polynomial.

For the elastic portion, applicable up to a stress of 24 ksi (165.5 MPa) the expression

$$\sigma_c = 2000\Delta \qquad (4.21)$$

where

σ_c = the applied compressive stress, ksi, and

Δ = the corresponding displacement, inches fits the mean curve well.

Above a stress of 24 Ksi (165.5 MPa) the expression

$$\sigma_c = -21.2 + 45.4\Delta - 241.0\Delta^{1/2} + 310.0\Delta^{1/3} \qquad (4.22)$$

is valid.

These curves, also shown on Fig. 4.7, are in good agreement with the mean curves for all the tests.

4.4 Prediction of Moment Rotation Relationship for End Plate Connections

When an end plate connection is subjected to a moment, the resulting deformation varies along its depth. While the extreme end in tension may have developed plastic hinges, the material near centre of rotation behaves elastically. Therefore, no single stiffness can be used over the full depth of the connection nor for changing moments to predict the moment rotation relationship.

For any of the end plate connections tested, the first portion of the experimental M-θ curve indicates a certain stiffness of the connection; the slope of the M-θ is relatively steep and little deformation of the plate occurs. The yielding of the connection in tension at the upper end, with plastic hinges forming, and in the beam web in compression at the lower end, causes the stiffness to decrease and the M-θ curve tends to flatten out. Eventually the beam flange comes into contact with the face of the supporting member and the stiffness is considerably increased once again.

Below the neutral axis, there are two distinct phases separated by the instant when the rotation of the connection causes the bottom flange of the beam to come in contact with the column. Prior to this, the end plate below the neutral axis is the only source of compressive resistance. It is pushed into the beam web indicating that the compressive force is developed by yielding of part of the cross sectional area of the beam web below the neutral axis.

After the bottom flange of the beam contacts the column, sufficient compressive force to balance the increasing tension developed by the top portion of the plate appears to be obtained by bearing, with little deformation of the beam flange occurring.

The analysis in this study is concerned only with the moment rotation relationship prior to the beam flange coming into contact with the column. In all tests, contact did not

occur until the rotation exceeded that corresponding to yielding of a simple beam of a span to depth ratio of 24 and a yield strength of 44.0 ksi (303.2 MPa).

4.4.1 Methodology

Given here is a method of predicting the moment-rotation behaviour of a single end plate connection based on the preceding analysis of the behaviour of the short T-sections in compression and tension.

The method begins with the input into the computer program described subsequently of the material and geometrical properties for T-sections simulating a unit length of the end plate where the flange of the T represents the end plate and the stem represents the web of the beam. Material properties required are the yield and ultimate strengths of the end plate and of the beam web. Geometrical properties required for the T-sections are the thickness of the end plate, the gage of the bolt holes, and the beam web thickness. As well the overall depth of the connection is required.

Fig. 1.1 illustrates how an end plate connection is assumed to be subdivided into a number of short lengths or segments whose combined resistance to compression or tension is considered equivalent to that of a single end plate of the same total length subject to moment.

With this approach it should be possible to predict the moment rotation characteristics of a flexible connec-

tion without dependence on laboratory tests results, knowing only the material and geometrical properties of the connection and the analytical expressions derived for the end plate segments in tension and compression and the location of centre of rotation.

4.4.2 Location of Centre of Rotation

Based on the analysis of T-section tension tests and T-section compression tests, as discussed in Sections 4.2 and 4.3, respectively, the theoretical location of the neutral axis for a certain rotation is obtained by knowing that the sum of horizontal forces $(T-C) = 0$.

The deformation along the depth of the connection is assumed to be linear as was found experimentally. For some given angle of rotation a preliminary position of the neutral axis is assumed. For this angle the tension and compression forces at incremental distances above and below the neutral axis respectively, are calculated based on the deformation at the distance as a function of the angle of rotation, according to the derived analytical relationships for tension and compression versus deformation.

If the tensile and compressive forces so calculated do not satisfy statical equilibrium, a new location is chosen for the same angle of rotation until statics is satisfied $(T-C=0)$.

A computer program has been developed to carry out this iterative procedure expeditiously.

4.4.3 Theoretical Moment Rotation Curve

Having established the position of the neutral axis for a given angle of rotation, the corresponding bending moment is determined by summing moments of the tension and compression forces to give one point on the moment rotation curve. The procedure is then repeated starting with another assumed value of the rotation.

The computer program that has been developed is given in Appendix II.

In the program the depth of the connection is sub-divided into elemental strips of one inch width measured both ways from the neutral axis.

A comparison between the experimental and analytical moment rotation curves for the beam tests is given in Figs. 4.8 to 4.13 for moments up to that corresponding to the rotation where the beam flange came into contact with the column flange. Also plotted on these figures are beam lines representing first yielding at the extreme fibre and complete yielding through the depth of the cross-section of the beam at the centre line for a WWF27x106 beam with yield strength of 44 ksi and length of 54 feet when uniformly loaded. The 54 foot length corresponds to a span to depth ratio of 24 which is not likely to be exceeded in

practice. The beam line for complete yielding through the depth, that is for the beam when it has reached the fully plastic moment, M_p, at the centre line has been drawn assuring elastic-plastic moment rotation behaviour of the cross-section.

In none of the tests did the beam flange contact the column until the beam line rotation was surpassed. Thus even for this large span to depth ratio the connections had adequate flexibility.

The analytical curves for the eight tests are in reasonable agreement with the experimental curves which represent a wide variety of end plate connections. The connections tested had end plate thickness of 1/4, 3/8 and 1/2 inches (6.3, 9.5, and 12.7 mm), gage of bolts of 4 and 5.5 inches (102 and 140 mm) and 4, 6, and 8 rows of bolts representing depths of plates of 12, 18 and 24 inches.

For small angles of rotation, say less than 0.01 radians, the theoretical curves lie above the experimental results. This is attributed to the fact that the theoretical relationship derived for the behaviour of the T-section in tension at low loads lies considerably above the experimental curve. This in turn is due to the fact that the behaviour of the cross-section was assumed to be elasto-plastic and the gradually yielding of the plate through its thickness was not taken into account.

Beyond this small angle of rotation the experimental and theoretical curves are in good agreement.

The analysis is valid only up to the moment at which the bottom flange of the beam contacts the column. After this, the additional compressive force developed between the beam flange and the column changes the behaviour and would make the analysis invalid.

The computer program developed for this study, for a given beam rotation, determines the centre of rotation and assesses geometrically whether or not the bottom flange has come in contact with the column and invalidates the results if this is so. From Fig. 4.16 contact is made when the bottom movement $\Delta_b = \ell_b \theta$, where ℓ_b is the distance to the bottom of the flange from the neutral axis and θ is the rotation, is equal to the end plate thickness.

In Table 4.1 are given for all tests (except test 8 in which welds cracked before the beam flange came in contact with the column) the ratios of the test to predicted moments and test to predicted rotations at the instant when contact of the beam flange with the column occurred.

The ratio of the test to predicted moment varies from 0.801 to 1.180 with a mean value of 1.013 and a coefficient of variation of 0.105. The relatively small coefficient is considered indicative of a narrow dispersion of the test results from the predicted value.

The ratio of the test to predicted rotation varies from 0.679 to 1.735 with a mean value of 1.113 and a coefficient of variation of 0.275. While the mean value is only 11% above that predicted the coefficient of variation is relatively large.

The analytical model defines the moment developed when the beam contacts the column more closely than the corresponding angle of rotation. It is postulated that considerable changes in the location of the centre of rotation do not change the moment appreciably but do affect the angle of rotation at contact considerably. Furthermore the model developed does not take into account the deformation of the bolts.

4.4.4 Determination of Moment and Rotation at Contact

In practical cases the designer may only be interested in determining the moment and rotation at the instant the beam flange contacts the column and thereby to ascertain that this occurs at a rotation beyond the beam line representing full plastification of the beam cross-section at the beam centre line.

To determine this set of values using the computer program a small angle of rotation is assumed (say 0.01 radians) and the position of the neutral axis is deter-

mined such that statics is satisfied. The movement at the bottom of the beam, Δb, is then found as $\ell_b \theta$. Successively larger angle of rotation are assumed until the value Δb calculated is just equal to the flange plate thickness and then the corresponding moment is determined.

In practice it is recommended that the moment at contact be calculated as described herein but to minimize the possibility of developing an excess moment when the beam contacts the column that the predicted rotation at contact be multiplied by 2/3 to allow for the variation of the analytical results from the experimental results. Thus, for a particular beam, considered simply supported, if the end rotation corresponding to attainment of maximum moment at the centre line is θ radians. Then 2/3 of the predicted rotation at contact should exceed θ radians, or the simple span rotation increased by 1.5 times should not exceed the predicted rotation.

4.4.5 Location of Point of Zero Moment Within Beam Span

When this type of end connection is used for framing a simple beam the bending moment changes from a negative value at the face of the support to zero and then to a positive value somewhere along the length of the beam. The test set-up have been based on the assumption that

the entire extent of the connection measured parallel to the beam axis is within the negative moment region, that is the point of zero moment occurs at a point remote from the end plate within the beam proper.

With the deepest connection tested, capable of developing the full factored shear capacity, a uniformly loaded beam with a span of 12.62 ft. (3847 mm) will reach the yield moment and the yield shear capacity simultaneously as given in Section 2.5.1. For this span, assuming elasto-plastic action, from the results of test E-7 the end rotation is found to be 0.0064 radians and the corresponding end moment 1100 inch kips. The distance from the face of the column to the point of zero moment is then 2.7 inches (68.6 mm) as compared to the end plate thickness of 0.375 inches (9.5 mm).

For the shallowest connection tested, again basing calculations for a beam span corresponding to reaching the yield moment when the connection shear capacity is attained, the beam span is found to be 24.5 feet as (7477 mm) as given in Section 2.5.1. This span, from the results of test E-4, corresponds to an end rotation of 0.0086 radians and an end moment of about 160 in kips. With this end moment the distance from the face of the column to the point of zero moment is then 0.8 inches (20.3 mm) as compared to the end plate thickness of 0.25 inches (6.3 mm).

Thus for the two extreme depths of connections tested and for the two extreme end moments developed uniformly loaded simple span would result in the point of zero moment laying beyond the extent of the connection within the beam.

CHAPTER V

SUMMARY AND CONCLUSIONS

5.1 Summary and Conclusions

1. An experimental and analytical study has been made into the behaviour of welded end plate connections.

2. The three main groups of tests conducted are:

   (i) 27 tension tests on T-sections simulating a segment of the end plate and web above the neutral axis,

   (ii) 15 compression tests on T-sections simulating a segment of the end plate and web below the neutral axis,

   (iii) 8 tests on the end plate connection themselves where the end plate connections are used to fasten a beam to a column and subjected to shear and moment.

3. In the main group of tests on the end plate connections one beam size, WWF 27x106 (WWF 690x158),* was used. Geometrical parameters studied were:

   (i) end plate thickness of 1/4, 3/8 and 1/2 inches (6.3, 9.5, 12.7 mm),

   (ii) gage of bolts, 4 and 5.5 inches (102 and 140 mm),

*Not available in SI units

(iii) number of rows of bolts, 4, 6 and 8,

(iv) depth of end plate, 12, 18 and 24 inches (305, 457 and 610 mm).

4. The general behaviour of the T-section specimens in tension led to an analysis in which the flanges are first considered to act as flexural members eventually developing yield moments at the toes of the flange-stem welds and at the fasteners and then subsequently a combined flexural membrane analysis when more and more of the load with continued loading is carried by membrane action. This analysis gave results in good agreement with experimental value.

5. The behaviour of the T-sections in compression is first elastic followed by inelastic deformations. An analysis was developed to determine the angle - 45° - at which the load spreads out at the end of the connection and to describe the stress-displacement curve in compression. The analytical curve obtained by curve fitting agreed well with experiments.

6. The end plate connections tested exhibited a wide range of connection flexibility depending on the geometrical parameters used in test.

7. An analytical relationship between moment and rotations for the end plate connections was derived on the basis of the behaviour in the simulated T-section tension and compression tests by considering the connection to be

divided into a number of short segments and integrating the contribution of the elemental lengths of the T-sections in tension and compression over the full end plate depth.

The analytical curves are in relatively good agreement with the experimental results.

8. It is recommended that the moment developed when the beam comes in contact with the column be determined on the basis of the analytical procedures developed herein.

9. Because of the dispersion of test results from predicted values it is recommended that the rotation in the connection be taken as 2/3 the value predicted to ensure that premature contact with the column does not occur in practice.

10. Contact of the test beam with column occurred at rotations which usually exceeded the yield beam lines confirming that end plate connections have adequate rotational capacity to provide the flexibility for normal structural applications.

11. An analysis of the two extreme depths of connections tested as would be used for simple framing of beams and corresponding to the extreme range of end moments developed confirmed that the entire connection would be in a region of negative moment and thus validated the test procedure of testing the connections under shear and cantilever moment.

5.2 Further Areas of Research

Areas where further study would be valuable are:

1. An analytical study of moment rotation behaviour of end plate connections beyond the point where the beam flange contacts the column,

2. The behaviour of the T-section compression specimens was derived in this thesis by curve fitting. An analytical relationship, as derived for the T-sections in tension, based on material and geometrical properties would be a useful extension to this work,

3. An experimental investigation of skewed end connections would confirm whether or not the analytical procedures developed here could be applied to such connections and if not could lead to modifications of these procedures.

4. The analytical procedure developed herein, probably with some modifications, could be applied to connection formed with two angles fastened to the beam web. An experimental and analytical study of such end connections would be of value.

TABLES

TABLE 2.1

Matrix of Tension Tests on T-Sections

Test No.	Plate Thickness Inches (mm)			Gage Inches (mm)	
Test No.	1/4 (6.3)	3/8 (9.5)	1/2 (12.7)	4 (102)	5.5 (140)
1	x				x
2			x		x
3		x			x
4	x				x
5			x		x
6		x			x
7		x			x
8		x		x	
9		x		x	
10		x		x	
11	x			x	
12	x			x	
13		x		x	
14	x			x	
15	x				x
16		x			x
17			x		x
18			x		x
19			x		x
20		x			x
21		x			x
22	x				x
23	x				x
24		x		x	
25		x		x	
26	x			x	
27	x			x	

TABLE 2.2

Matrix of Compression Tests on T-Sections

Test No.	Length of Web Plate inches (mm)			Length of End Plate inches (mm)			Location* of Gages		
	7 (178)	8 (203)	9 (229)	1 (25)	2 (51)	3 (76)	2.51	2.52	2.53
1			x			x	x		
2		x			x		x		
3	x			x			x		
4			x			x		x	
5		x			x			x	
6	x			x				x	
7			x			x			x
8		x			x				x
9	x			x					x
10		x			x				x
11			x			x			x
12	x			x					x

*See Section 2.4.1 for description.

TABLE 2.3

Matrix of End Plate Tests

Test No.	End Plate Thickness inches, (mm)			Gage inches (mm)		No. of rows of bolts		
	1/4 (6.3)	3/8 (9.5)	1/2 (12.7)	4 (102)	5.5 (140)	4	6	8
1		x		x			x	
2	x			x			x	
3		x			x		x	
4	x				x	x		
5		x			x	x		
6			x		x	x		
7		x			x			x
8	x				x			x

TABLE 3.1

Static Tension Test Results

A. Tests on End Plate

Plate Thickness inches	Yield Stress σ_y ksi	Ultimate Strength σ_u ksi	Elongation in 2-inch. in/in
1/4	52.0	79.2	0.31
	52.2	78.0	0.29
	53.2	78.4	0.29
Average	52.5	78.5	0.30
3/8	42.3	65.1	0.40
	42.1	65.8	0.42
	42.2	65.5	0.42
Average	42.2	65.5	0.41
1/2	41.0	64.0	0.44
	42.1	64.0	0.44
	43.7	64.3	0.42
Average	42.2	64.1	0.43

B. Tests on Beam Web

Yield Stress σ_y ksi	Ultimate Strength σ_u ksi
49.0	77.2
46.5	76.7
48.7	76.6
48.3	76.7
45.7	75.8
46.0	75.8
Average 47.4	76.5

TABLE 3.2

Data for Test E-1-6-3/8-4

Obs. No.	Load kips	Rotation rad. $x10^{-2}$	Experimental Moment inch. kips	Theoretical Moment inch. kips
1	5.0	0.063	192.5	361.0
2	11.0	0.156	423.5	642.3
3	17.0	0.330	654.5	825.4
4	23.0	0.606	885.5	1002.7
5	29.0	1.210	1116.5	1130.1
6	32.0	2.050	1232.0	1212.1
7	33.0	2.720	1270.5	1223.0
8	39.0	2.910	1501.5	-
9	45.0	3.011	1732.5	-
10	50.0	3.320	1925.0	-
11	60.0	3.640	2310.0	-
12	67.0	3.870	2579.5	-
13	71.0	4.080	2733.5	-
14	74.2	4.222	2856.7	-
15	76.0	4.302	2926.0	-

TABLE 3.3

Data for Test E-2-6-1/2-4

Obs. No.	Load kips	Rotation rad. $x10^{-2}$	Experimental Moment inch. kips	Theoretical Moment inch. kips
1	6.0	0.126	231.0	419.0
2	9.0	0.221	346.5	480.0
3	13.0	0.434	500.5	588.5
4	17.5	0.666	673.7	658.7
5	20.0	1.215	770.0	755.2
6	22.0	1.830	847.0	807.8
7	23.0	2.170	885.5	839.6
8	24.0	2.960	924.0	918.3
9	27.0	2.990	1039.5	921.7
10	32.0	3.180	1232.0	-
11	36.7	4.100	1412.9	-
12	27.0	4,500	1039.0	-

TABLE 3.4

Data for Test E-3-6-3/8-5.5

Obs. No.	Load kips	Rotation rad. $x10^{-2}$	Experimental Moment inch. kips	Theoretical Moment inch. kips
1	5.0	0.065	192.5	274.1
2	10.0	0.153	385.0	424.0
3	14.0	0.448	539.0	551.7
4	19.0	1.550	731.5	746.1
5	27.0	3.320	847.0	881.8
6	24.0	3.970	924.0	930.5
7	29.0	4.090	1116.5	941.4
8	34.0	4.250	1309.0	-
9	39.0	4.250	1501.5	-
10	44.0	4.430	1694.0	-
11	50.0	4.620	1925.0	-
12	60.0	5.420	2310.0	-
13	65.0	5.690	2502.5	-

TABLE 3.5

Data for Test E-4-4-1/4-5.5

Obs. No.	Load ips	Rotation rad. $x10^{-2}$	Experimental Moment inch. kips	Theoretical Moment inch. kips
1	2.0	0.257	77.0	124.7
2	4.0	0.736	154.0	176.5
3	5.0	1.81	192.5	219.0
4	6.0	2.68	231.0	241.5
5	6.5	3.16	250.25	253.9
6	7.0	3.23	269.5	255.7
7	8.0	3.29	308.0	257.2
8	10.0	3.33	385.0	-
9	12.0	3.37	462.0	-
10	15.0	3.43	577.5	-
11	17.0	3.46	654.5	-
12	20.0	3.53	770.0	-
13	24.0	3.91	924.0	-
14	25.0	4.16	962.5	-
15	26.0	4.49	1001.0	-
16	28.0	5.29	1078.0	-

TABLE 3.6
Data for Test E-5-4-3/8-5.5

Obs. No.	Load kips	Rotation rad. $x10^{-2}$	Experimental Moment inch. kips	Theoretical Moment inch. kips
1	2.0	0.089	77.0	123.1
2	4.0	0.178	154.0	182.9
3	6.0	0.402	231.0	240.7
4	7.5	1.200	288.7	298.5
5	8.0	1.920	308.0	342.6
6	9.0	2.850	346.5	369.3
7	10.0	3.100	385.0	376.9
8	14.0	3.180	539.0	378.7
9	16.0	3.210	616.0	-
10	18.0	3.240	693.0	-
11	20.0	3.270	770.0	-
12	25.0	3.360	962.5	-
13	30.0	3.450	1155.0	-
14	35.0	3.620	1347.5	-
15	40.0	4.200	1540.0	-
16	45.0	5.010	1732.5	-

TABLE 3.7

Data for Test E-6-4-1/2-5.5

Obs. No.	Load kips	Rotation rad. $x10^{-2}$	Experimental Moment inch. kips	Theoretical Moment inch. kips
1	2.0	0.072	77.0	136.2
2	5.0	0.16	192.5	243.5
3	9.0	0.719	346.5	368.5
4	10.0	2.42	385.0	468.0
5	12.0	3.11	462.0	500.3
6	13.0	3.35	500.5	516.3
7	19.0	3.54	731.5	521.7
8	25.0	3.71	962.5	-
9	30.0	3.81	1155.0	-
10	35.0	3.92	1347.5	-
11	40.0	4.02	1540.0	-
12	50.0	4.30	1925.0	-
13	55.0	4.73	2117.5	-
14	57.0	5.05	2194.5	-
15	60.0	5.31	2310.0	-
16	64.0	5.86	2464.0	-
17	68.0	6.45	2618.0	-
18	72.0	6.95	2772.0	-

65

TABLE 3.8

Data for Test E-7-8-3/8-5.5

Obs. No.	Load. kips	Rotation rad. $x10^{-2}$	Experimental Moment inch. kips	Theoretical Moment inch. kips
1	4.0	0.011	154.0	110.9
2	9.0	0.061	346.5	564.1
3	14.0	0.102	539.5	706.9
4	18.0	0.174	693.0	834.3
5	22.5	0.291	866.2	928.9
6	27.0	0.488	1039.5	1041.5
7	31.5	0.838	1212.1	1191.5
8	35.0	1.450	1347.5	1360.1
9	37.0	1.900	1424.5	1435.7
10	40.0	2.510	1540.0	1528.8
11	42.0	2.960	1617.0	1606.13
12	45.0	3.580	1732.0	1720.0
13	50.0	4.110	1925.0	1830.0
14	55.0	4.400	2117.5	1902.0
15	60.0	4.680	2310.0	-
16	65.0	5.010	2502.5	-
17	70.0	5.330	2695.0	-
18	76.0	5.830	2926.0	-

TABLE 3.9

Data for Test E-8-8-1/4-5.5

Obs. No.	Load kips	Rotation rad. $x10^{-2}$	Experimental Moment inch. kips	Theoretical Moment inch. kips
1	4.0	0.050	154.0	226.9
2	8.0	0.147	308.0	477.5
3	12.0	0.345	462.0	622.7
4	16.0	0.574	616.0	728.6
5	20.0	0.843	770.0	794.3
6	24.0	1.220	924.0	858.3
7	28.0	1.960	1078.0	986.9
8	30.0	2.710	1155.0	1153.3
9	26.0	4.120	1001.0	-

TABLE 3.10

Location of Centre of Rotation Expressed as a Percentage of Connection Depth from top

Test No.	End Plate Connection Rotation (Rad.)					
	0.005	0.01	0.015	0.02	0.025	0.03
E-1-6-3/8-4	89	90	91	93	-	-
E-2-6-1/4-4	88	87	90	92	93	-
E-3-6-3/8-5.5	60	61	61	65	68	72
E-4-4-1/4-5.5	33	54	62	67	68	78
E-5-4-3/8-5.5	54	60	63	65	66	68
E-6-4-1/2-5.5	67	70	68	65	63	64
E-7-8-3/8-5.5	74	78	80	81	82	-
E-8-8-1/4-5.5	60	77	80	83	84	-

TABLE 4.1

Comparison of Test and Predicted Moments and Rotation When Beam Came Into Contact With Column

Test No.	TEST		PREDICTED		RATIO	
	M_t inch.kips	θ_t radians	M_{pr} inch. kips	θ_{pr} radians	$\frac{M_t}{M_{pr}}$	$\frac{\theta_t}{\theta_{pr}}$
1	1260	0.0272	1241	0.0326	1.015	0.850
2	940	0.0296	863	0.0247	1.089	1.198
3	900	0.0395	903	0.0369	0.996	1.070
4	255	0.0321	217	0.0185	1.180	1.735
5	365	0.0290	357	0.0250	1.022	1.155
6	490	0.0335	495	0.0303	0.989	1.105
7	1780	0.0394	2221	0.0580	0.801	0.679
8*	-	-	1724	0.046	-	-
				Mean Value	1.013	1.113
				Standard Deviation	.107	.306
				Coeffient of Variation	.105	.275

*In this test the connection failed before the beam came into contact with the column but after the beam line was reached.

FIGURES

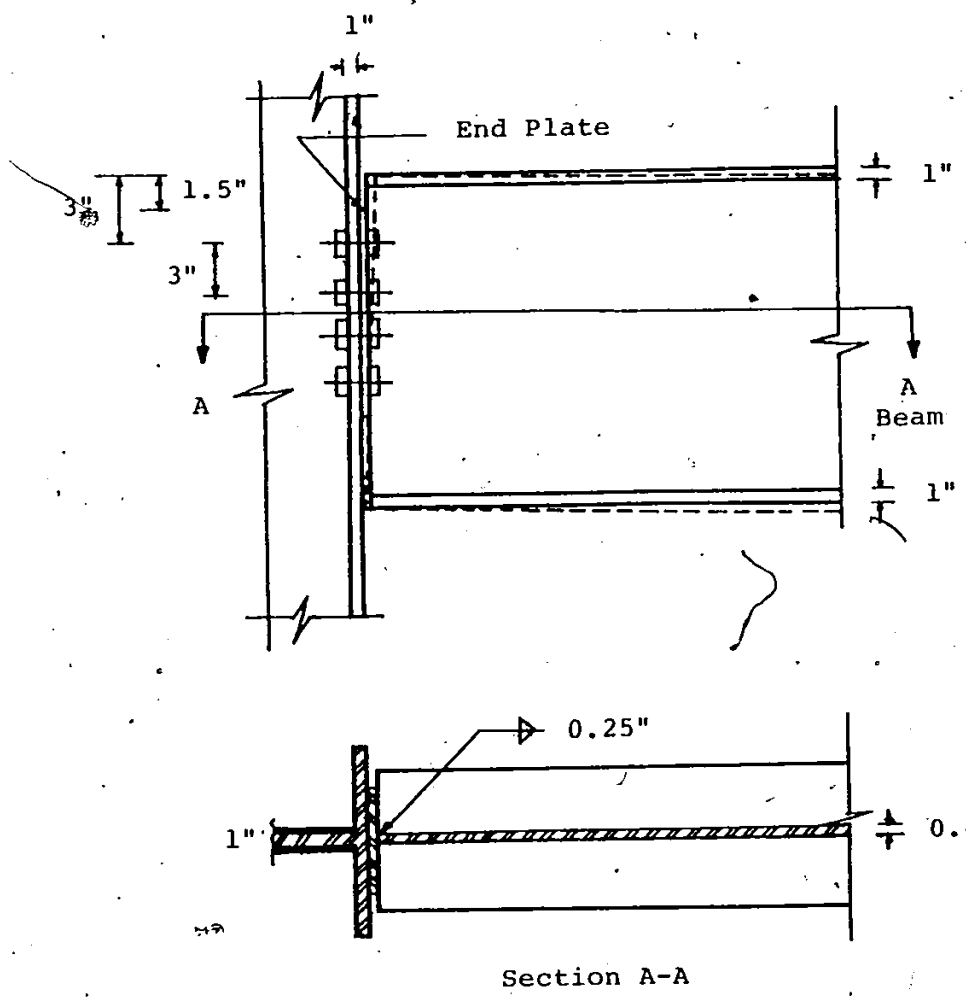

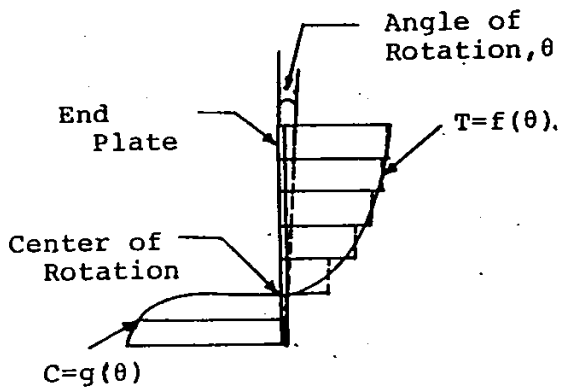

Fig. 1.1 End Plate Connection and Forces Developed in Constituent T-Sections.

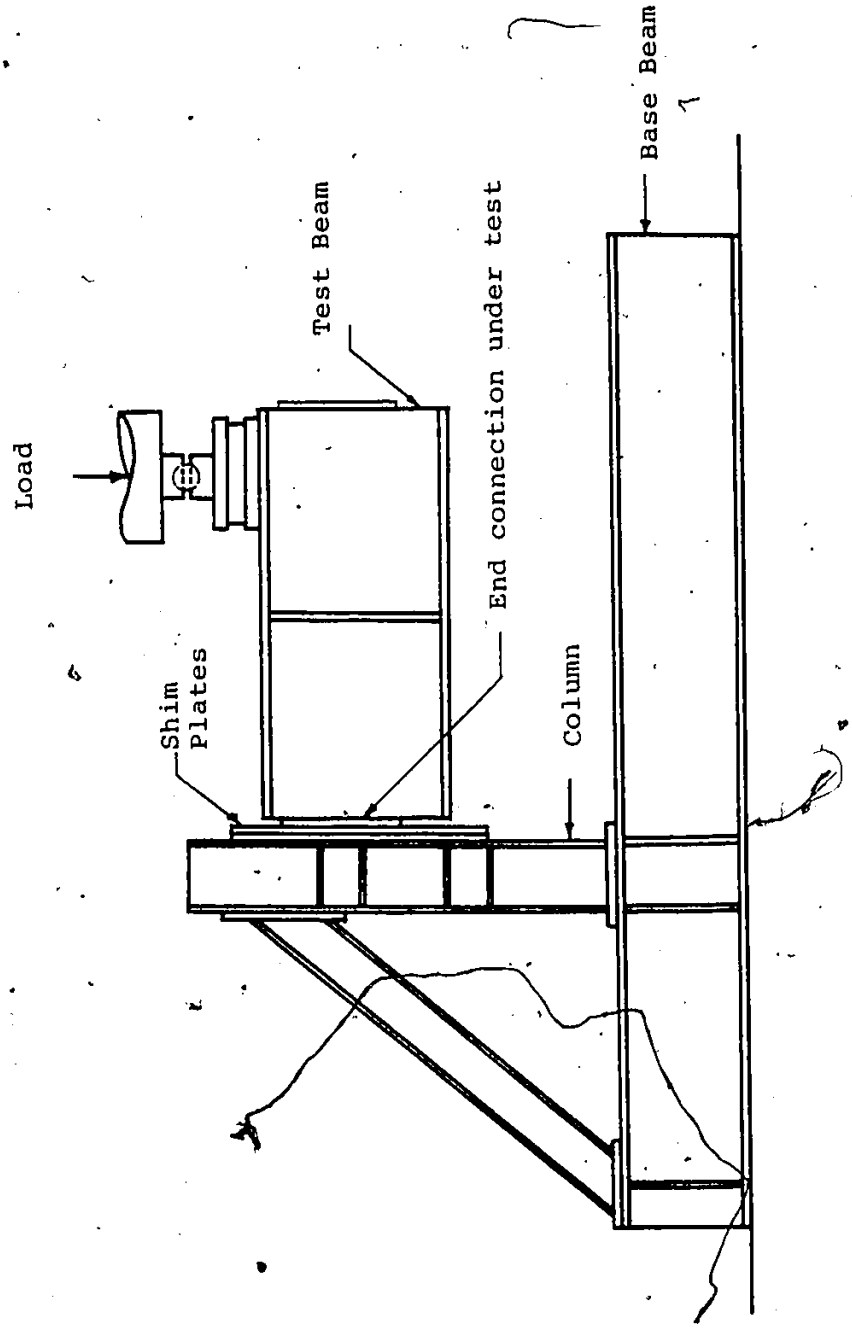

Fig. 2.1 Test Frame

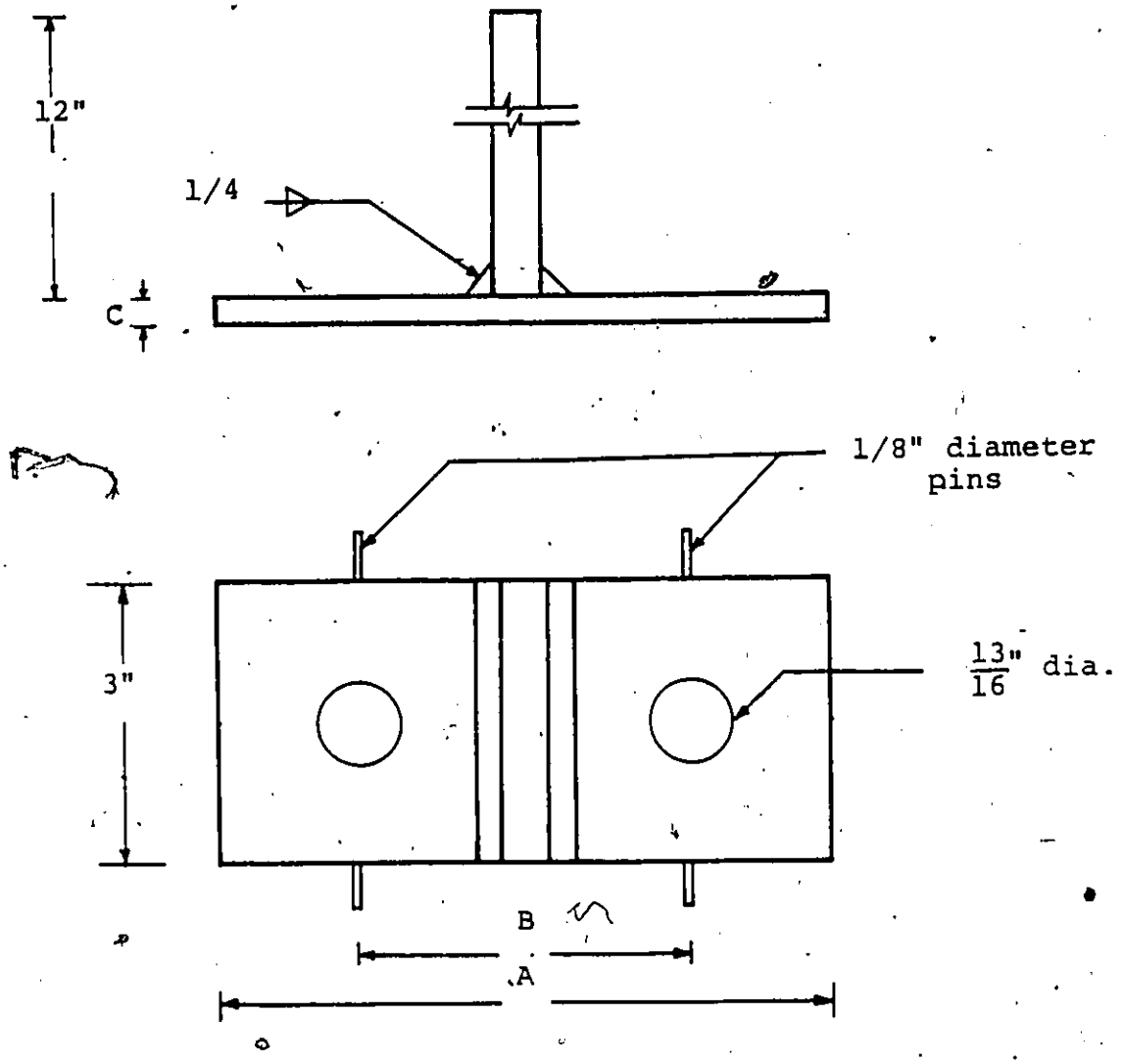

A = $6\frac{1}{2}$" or 8"

B = 4" or $5\frac{1}{2}$"

C = $\frac{1}{4}$" or $\frac{3}{8}$" or $\frac{1}{2}$"

Fig. 2.2 Tensile Specimen.

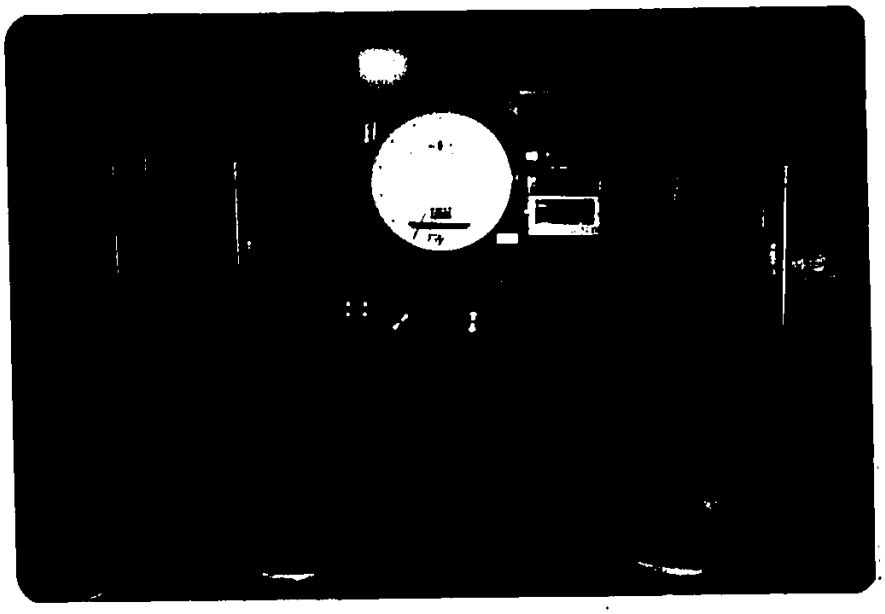

Fig. 2.3. Universal testing machine.

Fig. 2.4. T-Section tension specimen in UTM during testing.

Fig. 2.5 Compression Specimens

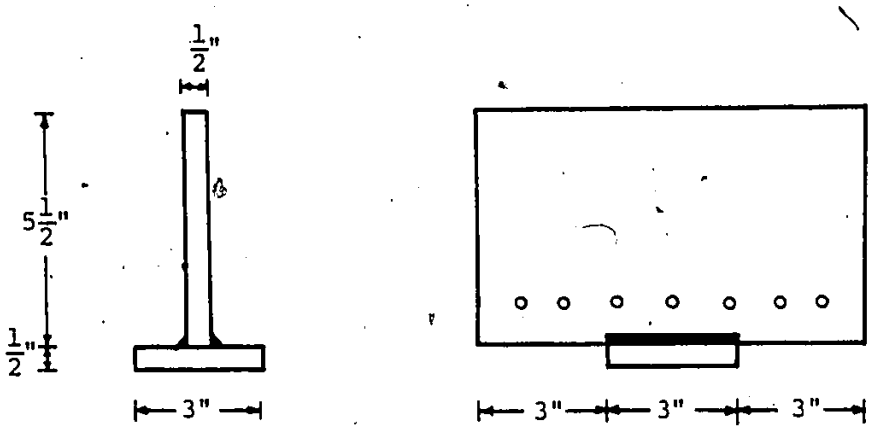

Fig. 2.5.1 Group 1, Pattern 3.

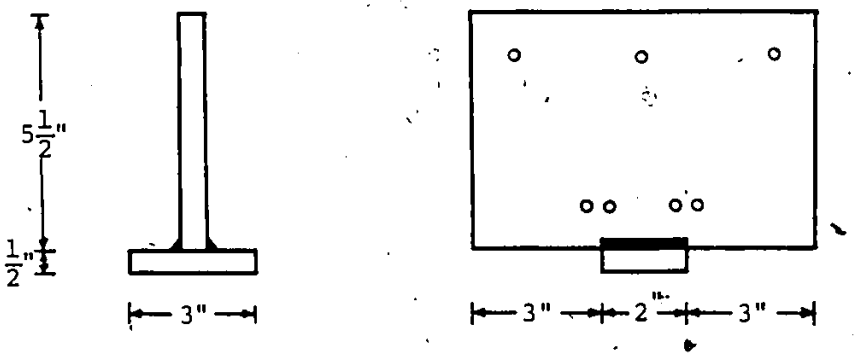

Fig. 2.5.2 Group 2, Pattern 2.

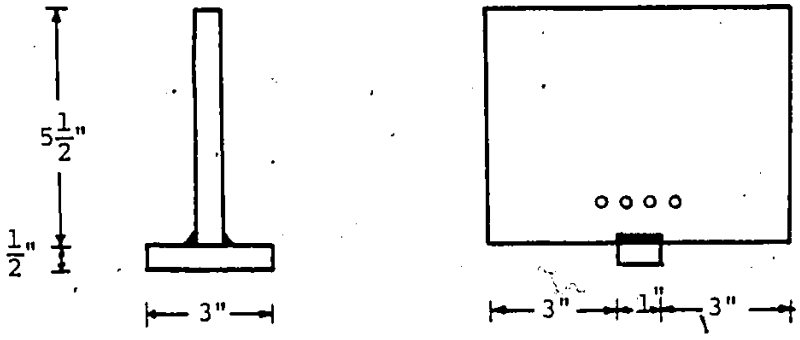

Fig. 2.5.3 Group 3, Pattern 1

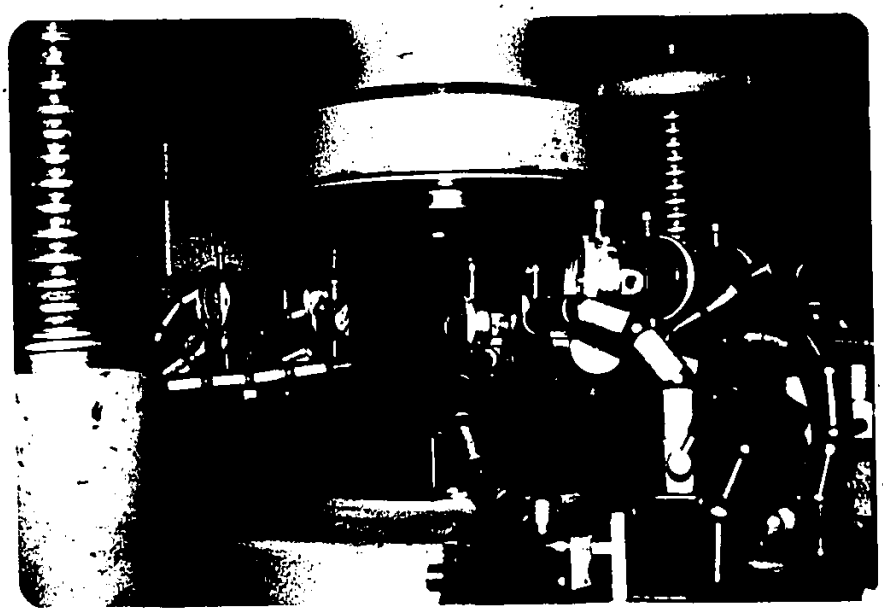

Fig. 2.6. T-Section compression specimen in testing machine.

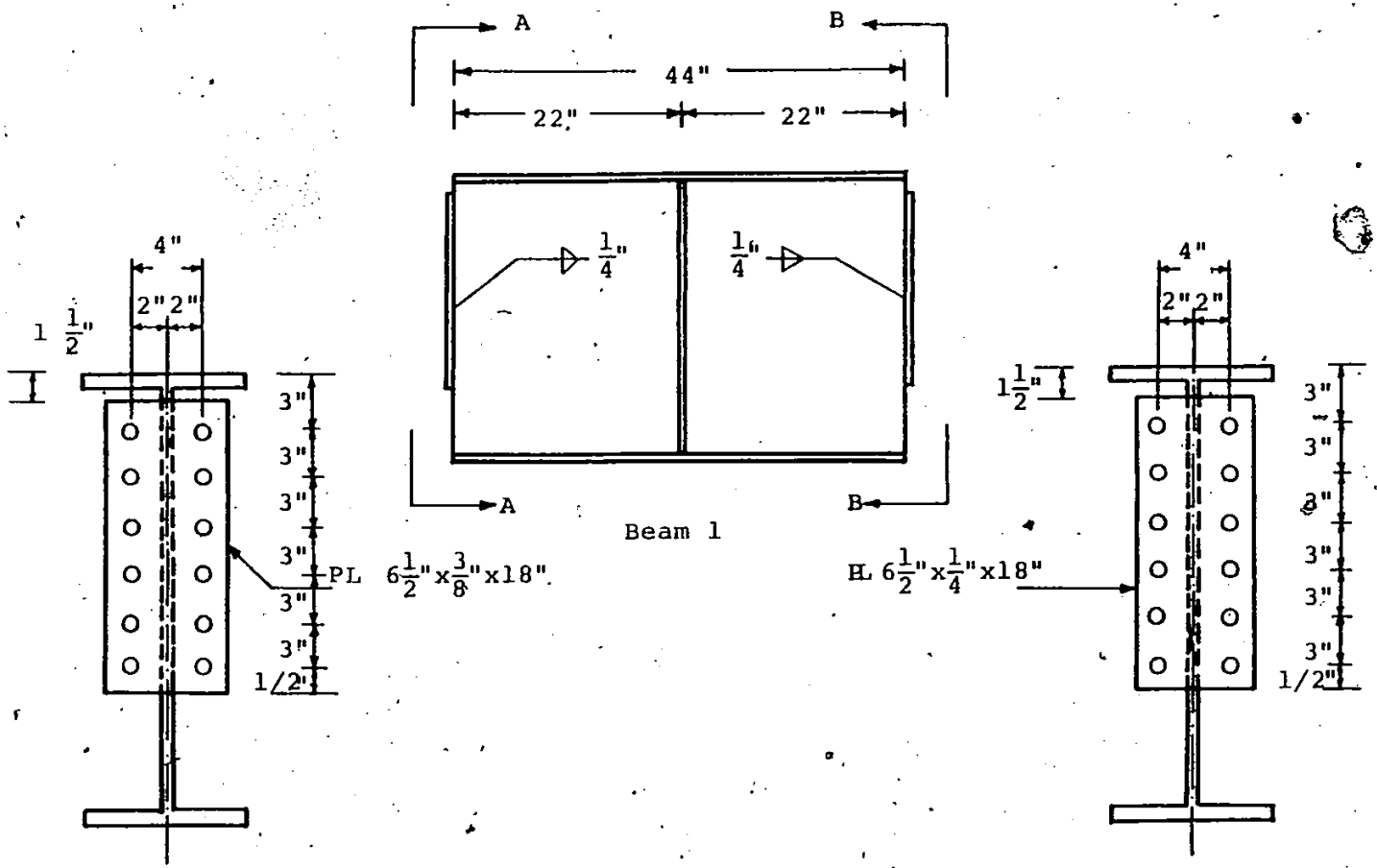

Fig. 2.7 Details of Beam 1.

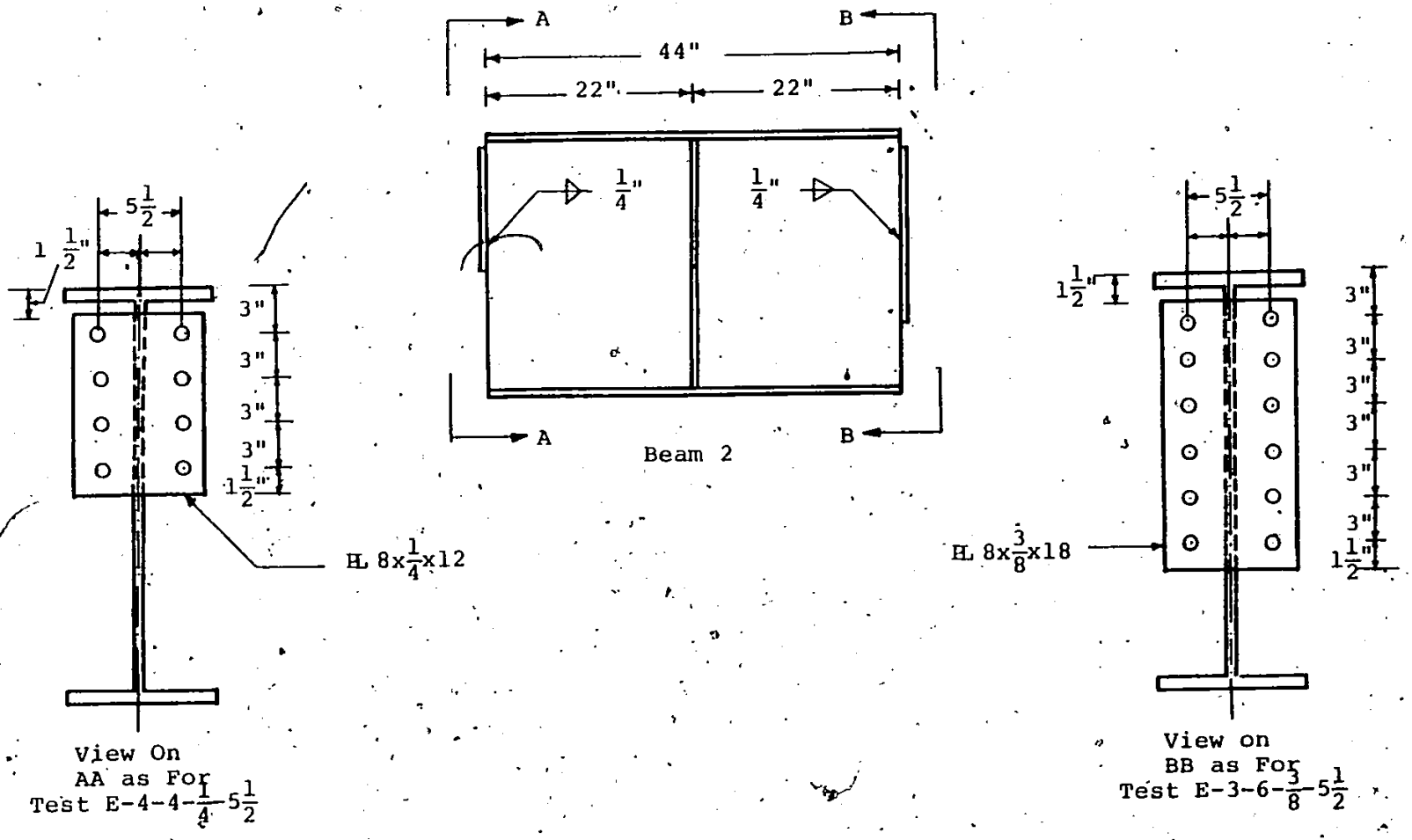

Fig. 2.8 Details of Beam 2.

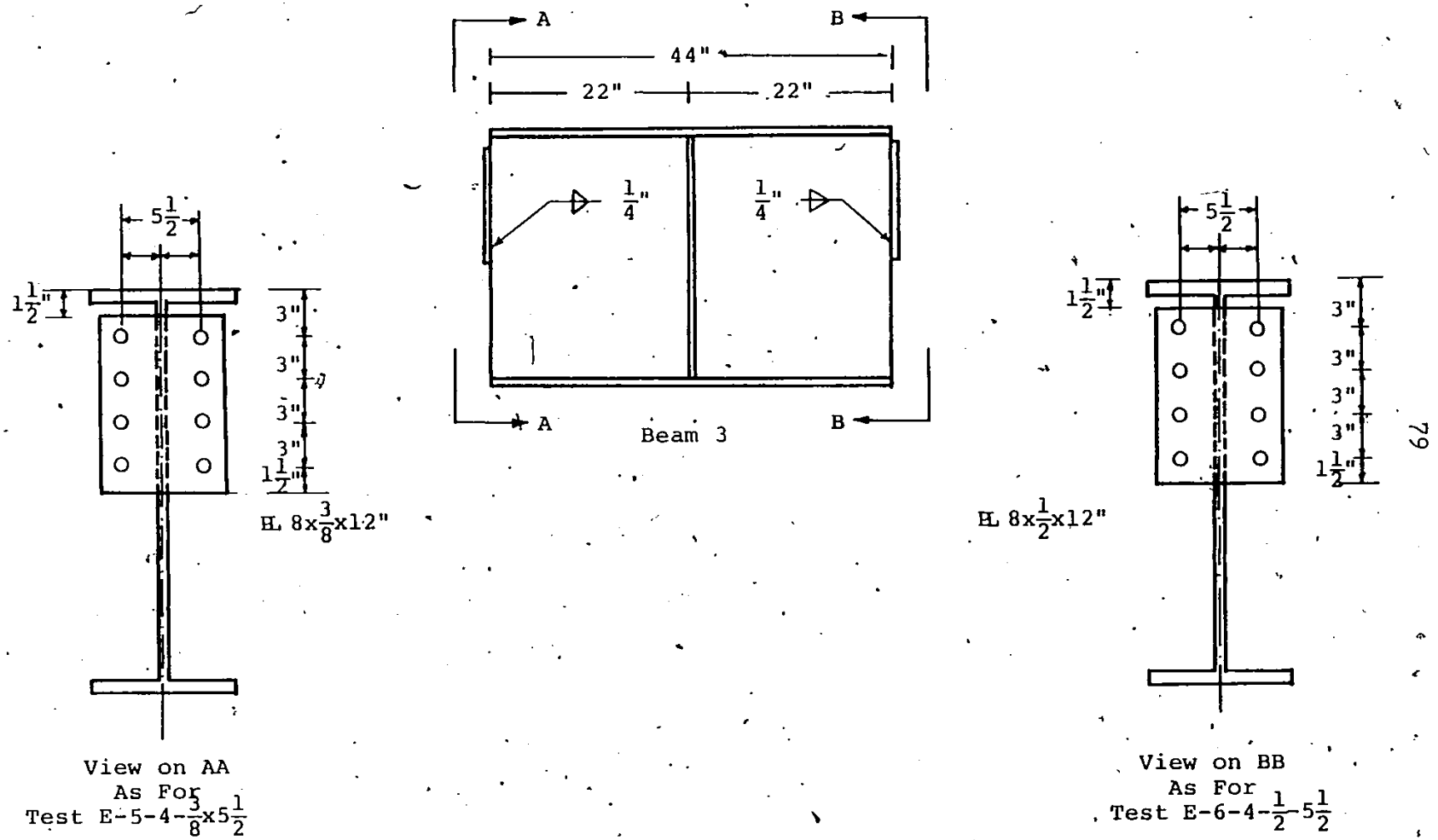

Fig. 2.9 Details of Beam 3.

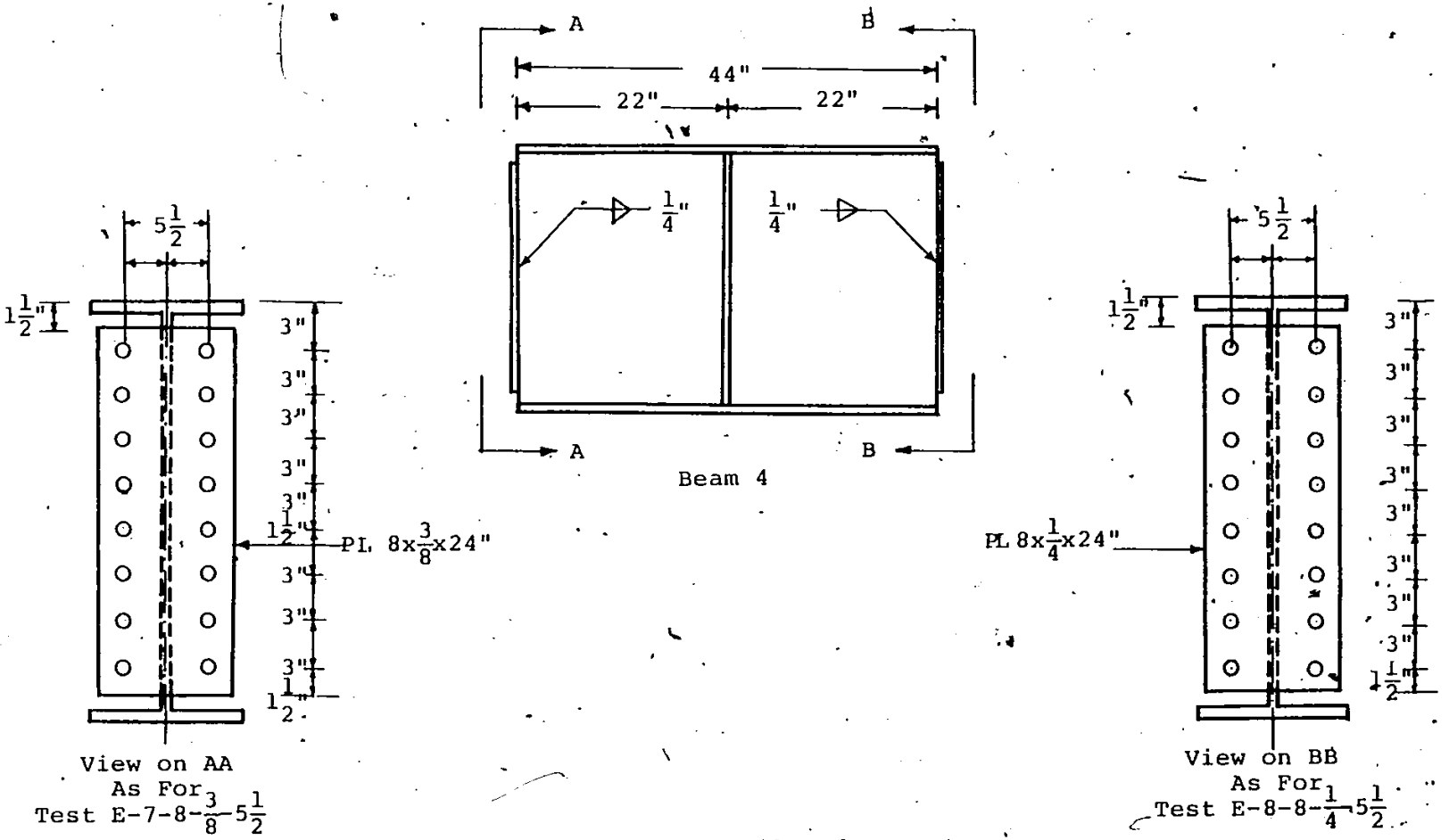

Fig. 2.10 Details of Beam 4.

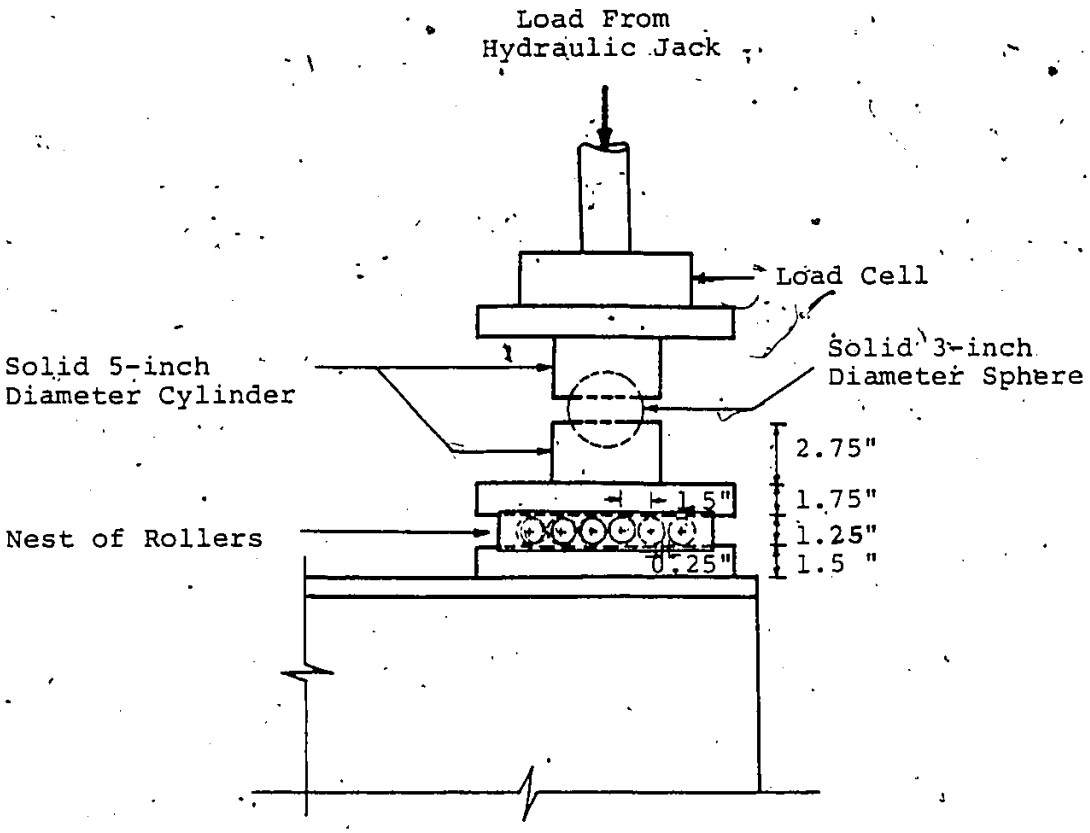

Fig. 2.11 Loading Assembly

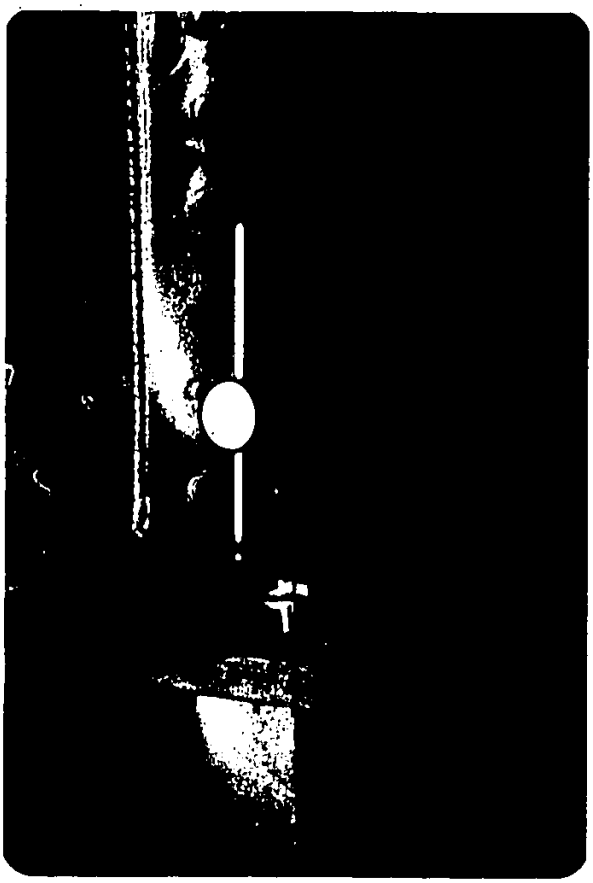

Fig. 2.12. Dial gage for measurement of beam deflection.

Fig. 2.13. Dial gages for measurements at end plate connection.

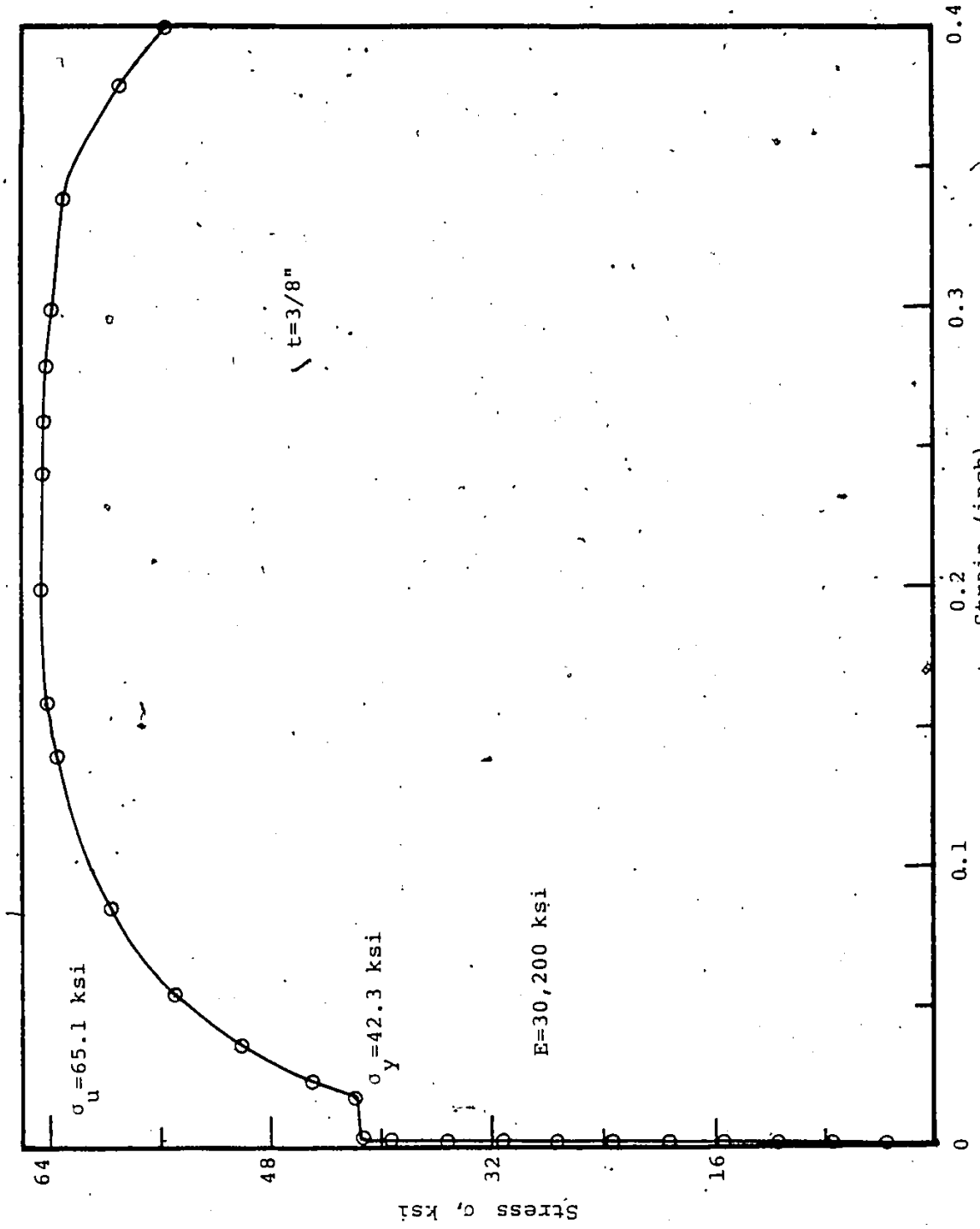

Fig. 3.1 Typical Stress Strain Curve.

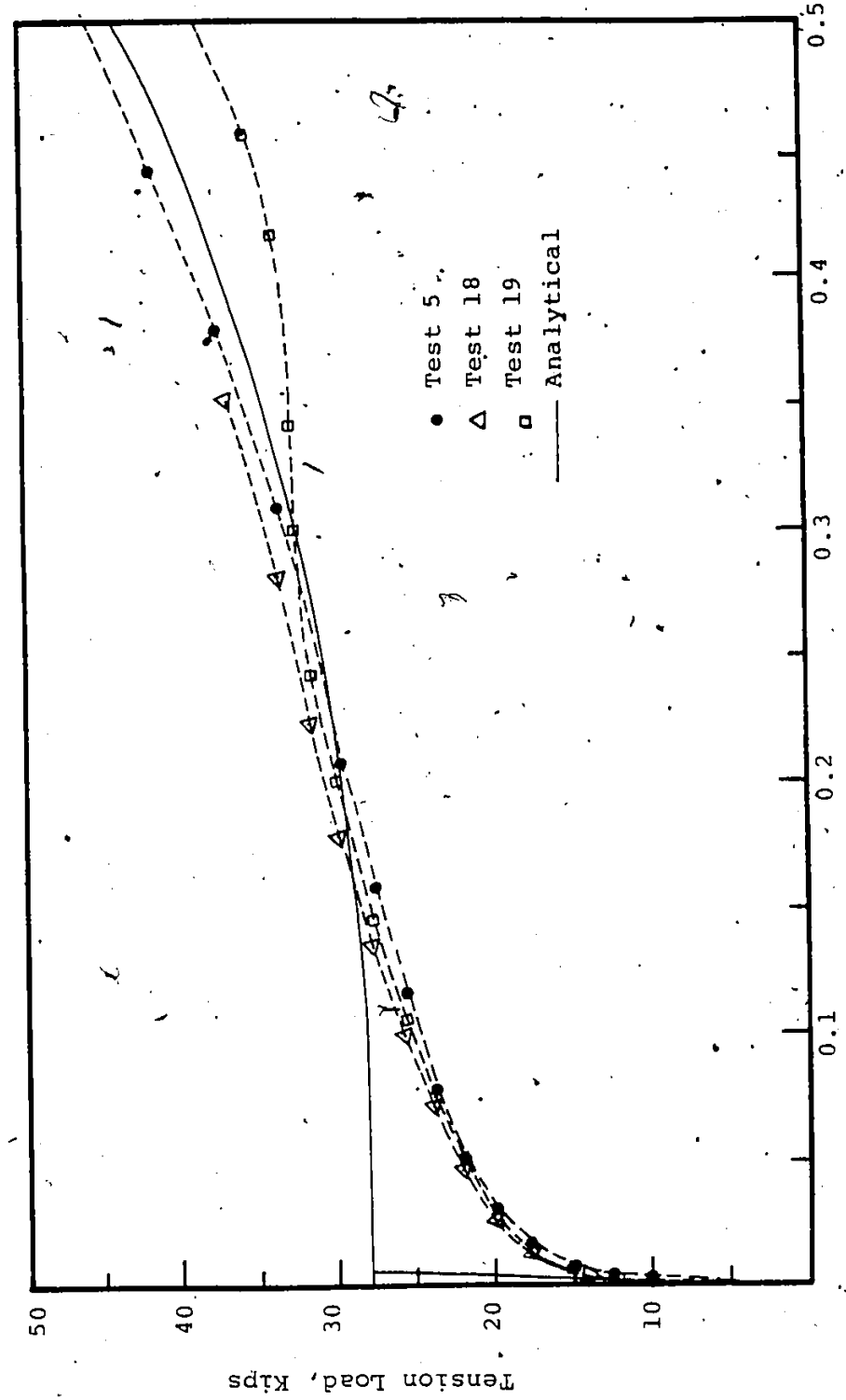

Fig. 3.2. Load versus angle of deformation for T-section tension specimens of 1/2" plate and 5.5" gage.

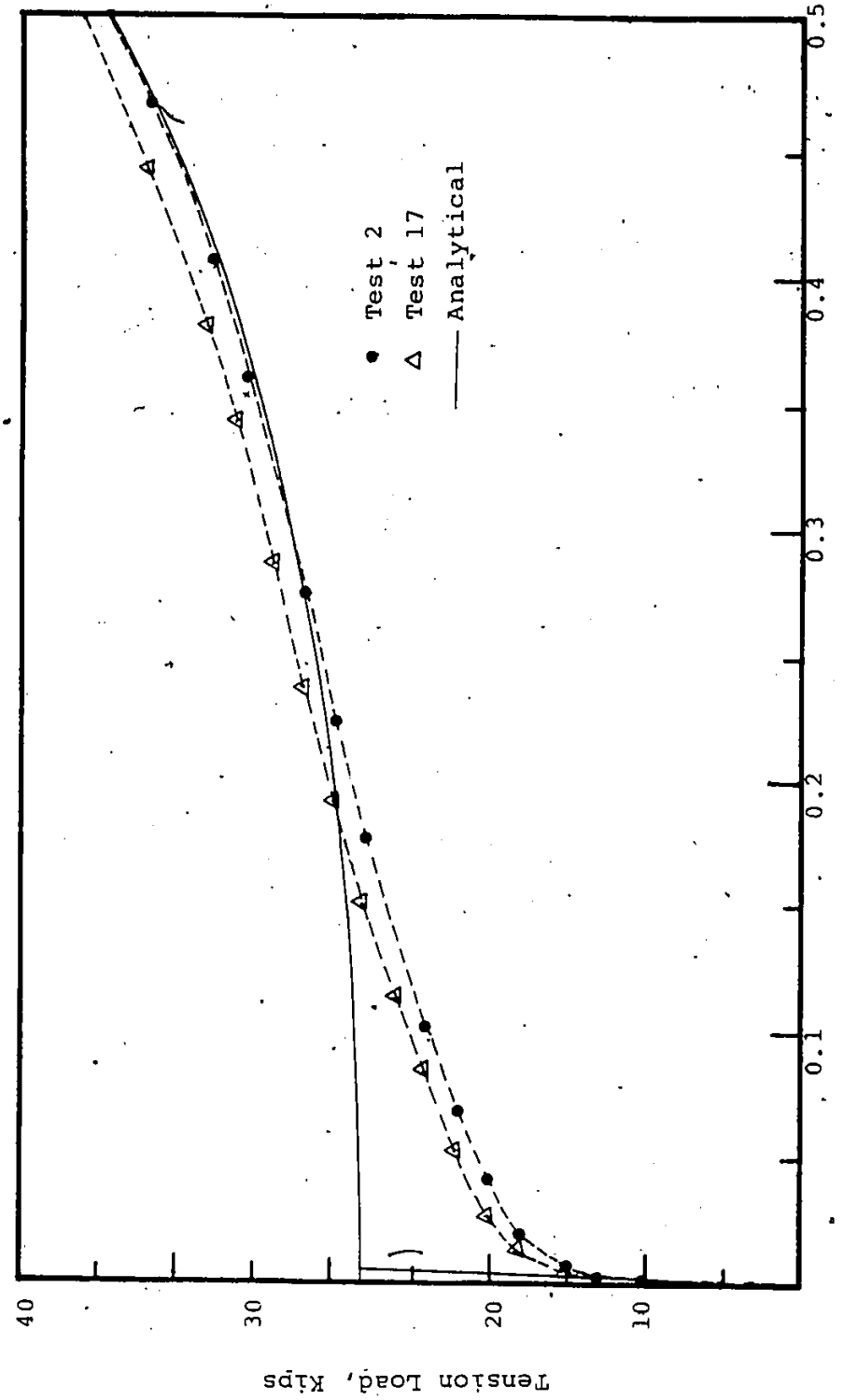

Fig. 3.3. Load versus angle of deformation for T-section tension specimens of 1/2" plate and 5.5" gage.

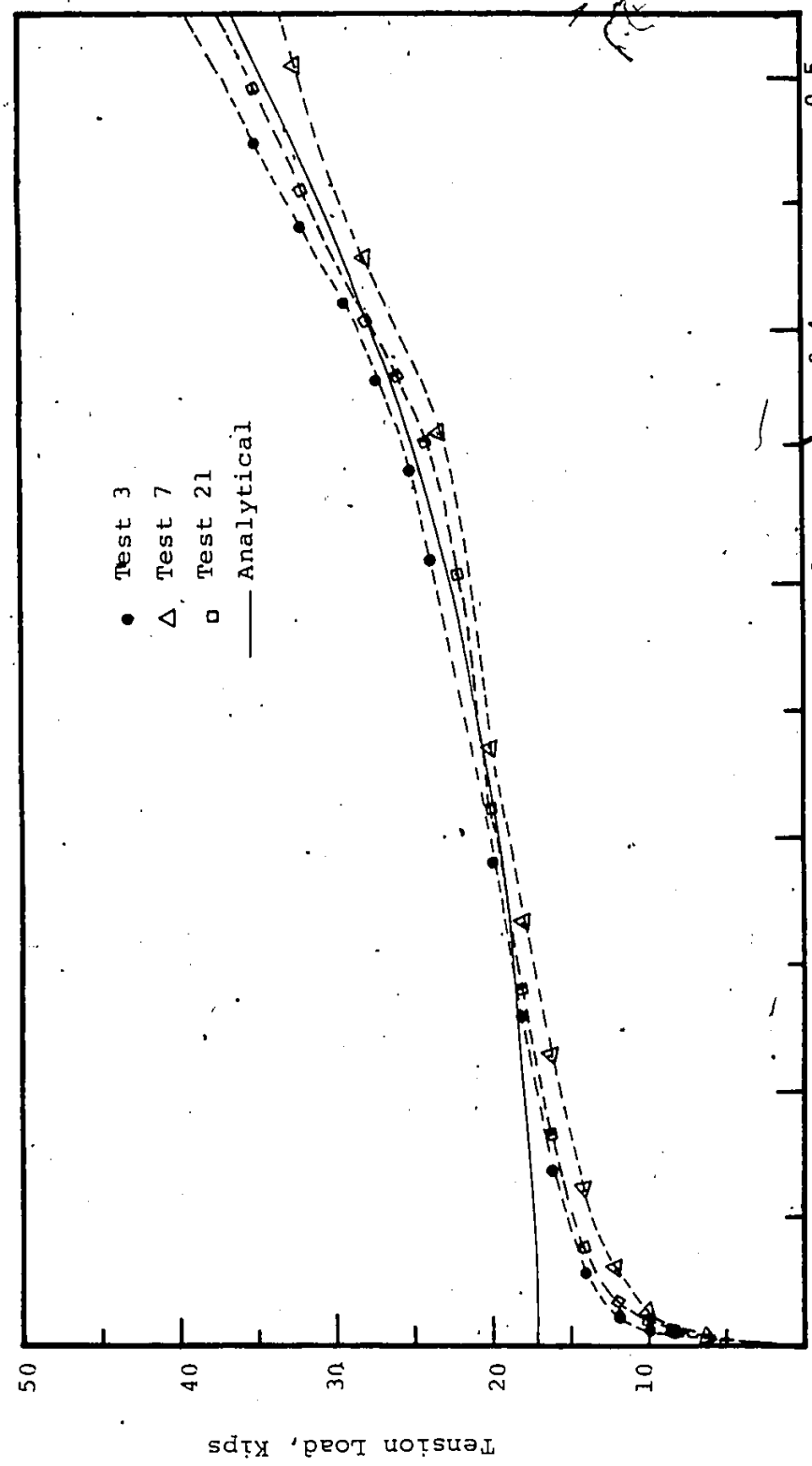

Fig. 3.4. Load versus angle of deformation for T-section tension specimens of 3/8" plate and 5.5" gage.

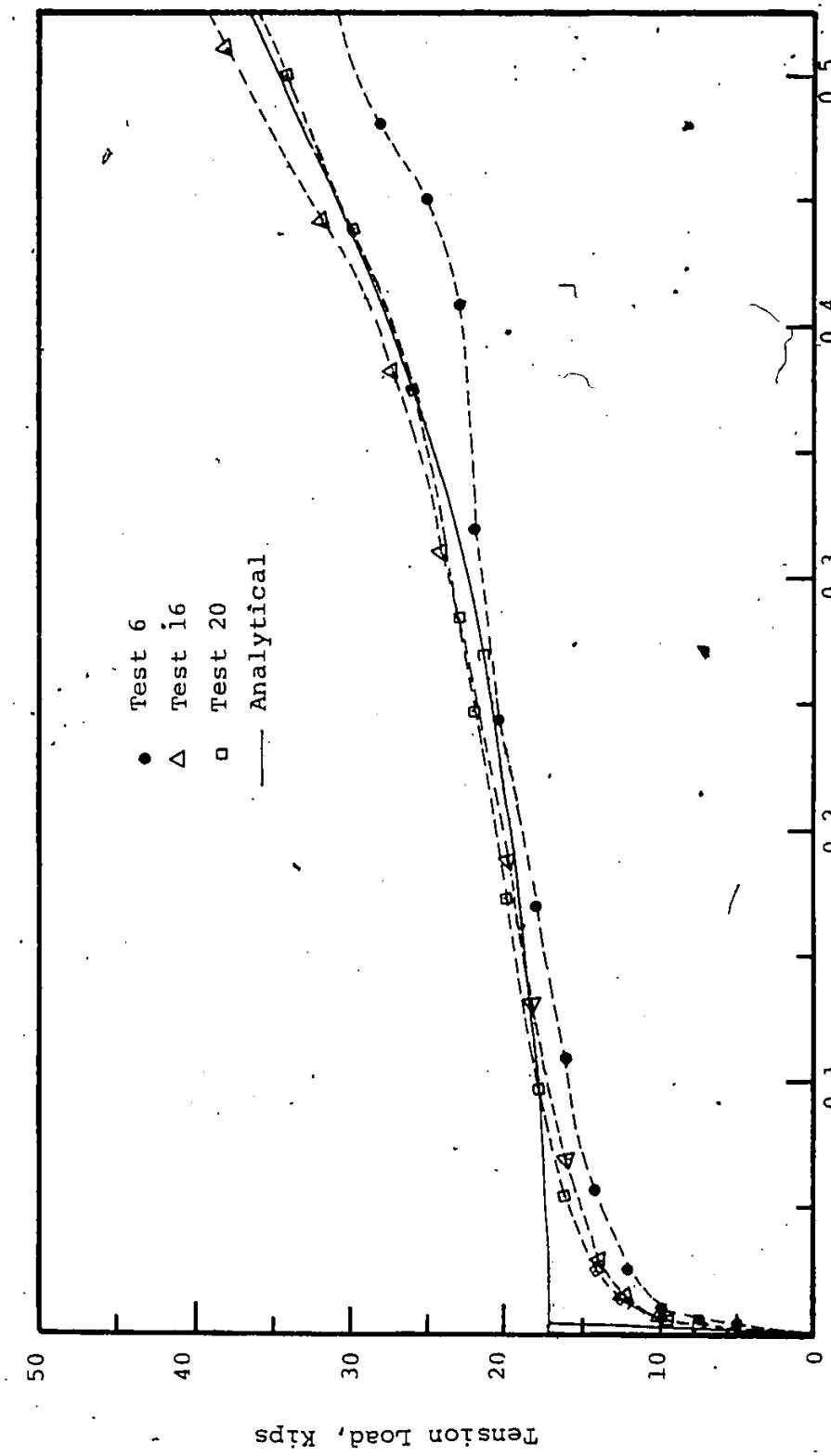

Fig. 3.5. Load versus angle of deformation for T-section tension specimens of 3/8" plate and 5.5" gage.

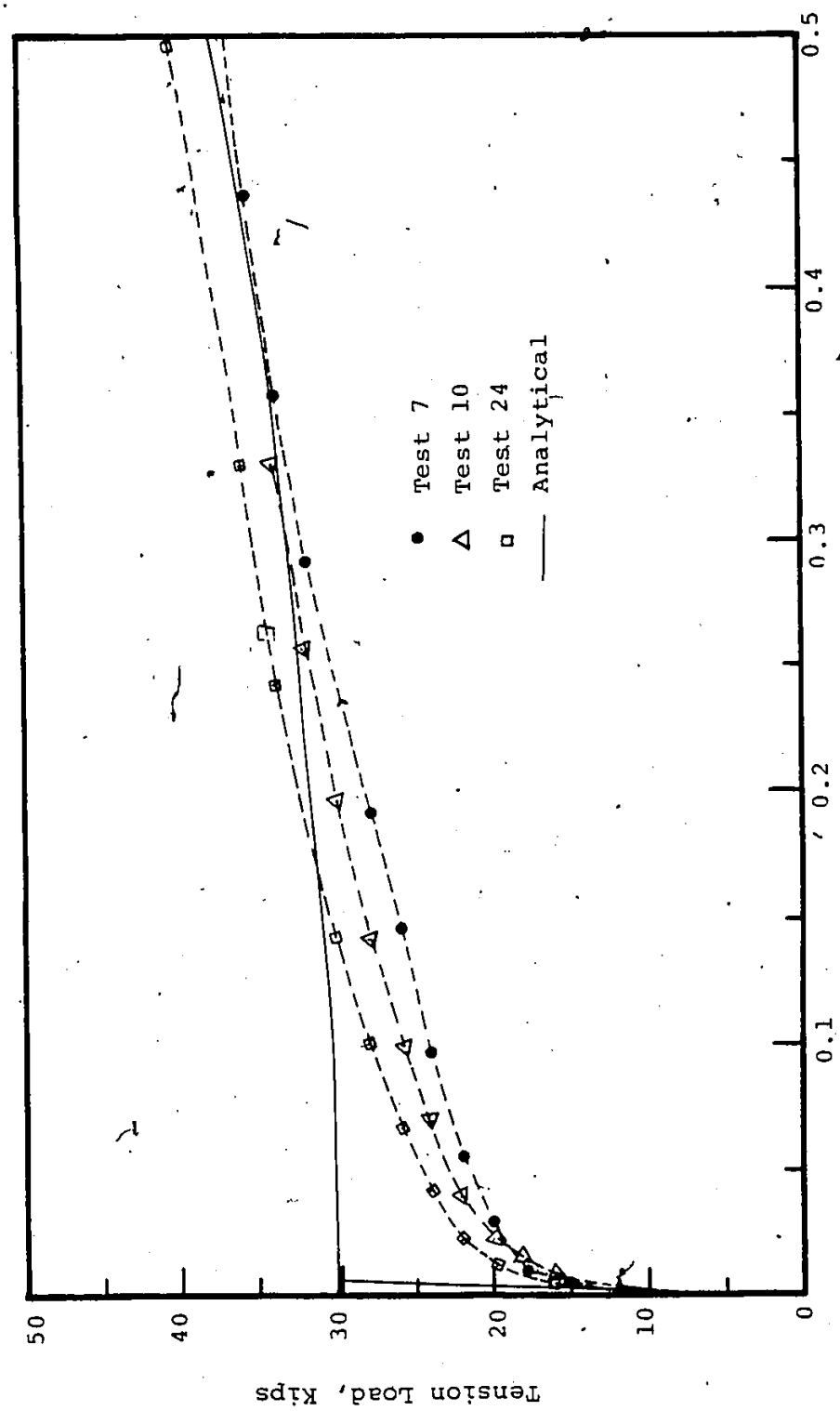

Fig. 3.6. Load versus angle of deformation for T-section tension specimens of 3/8" plate and 4" gage.

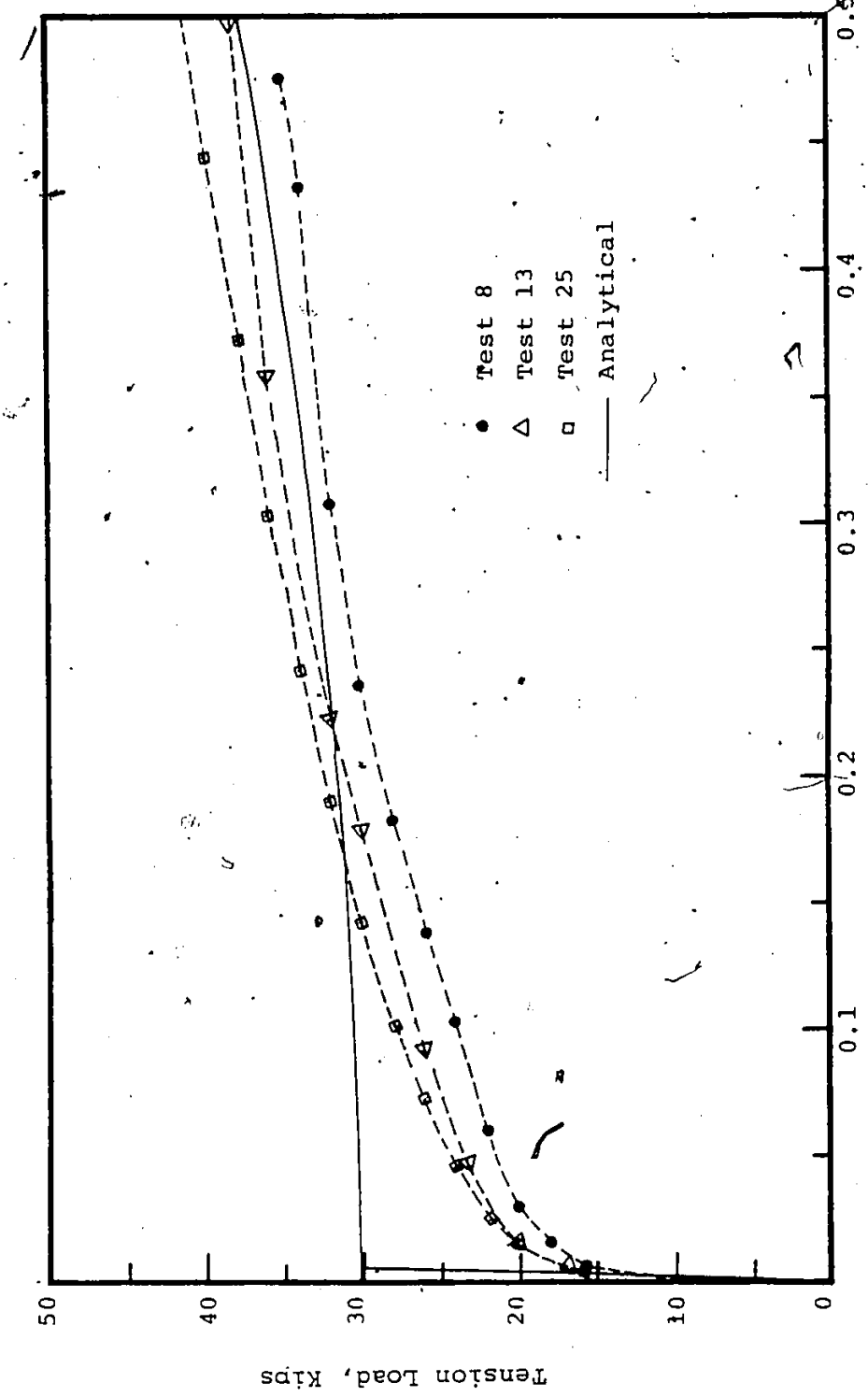

Fig. 3.7. Load versus angle of deformation for T-section tension specimens of 3/8" plate and 4" gage.

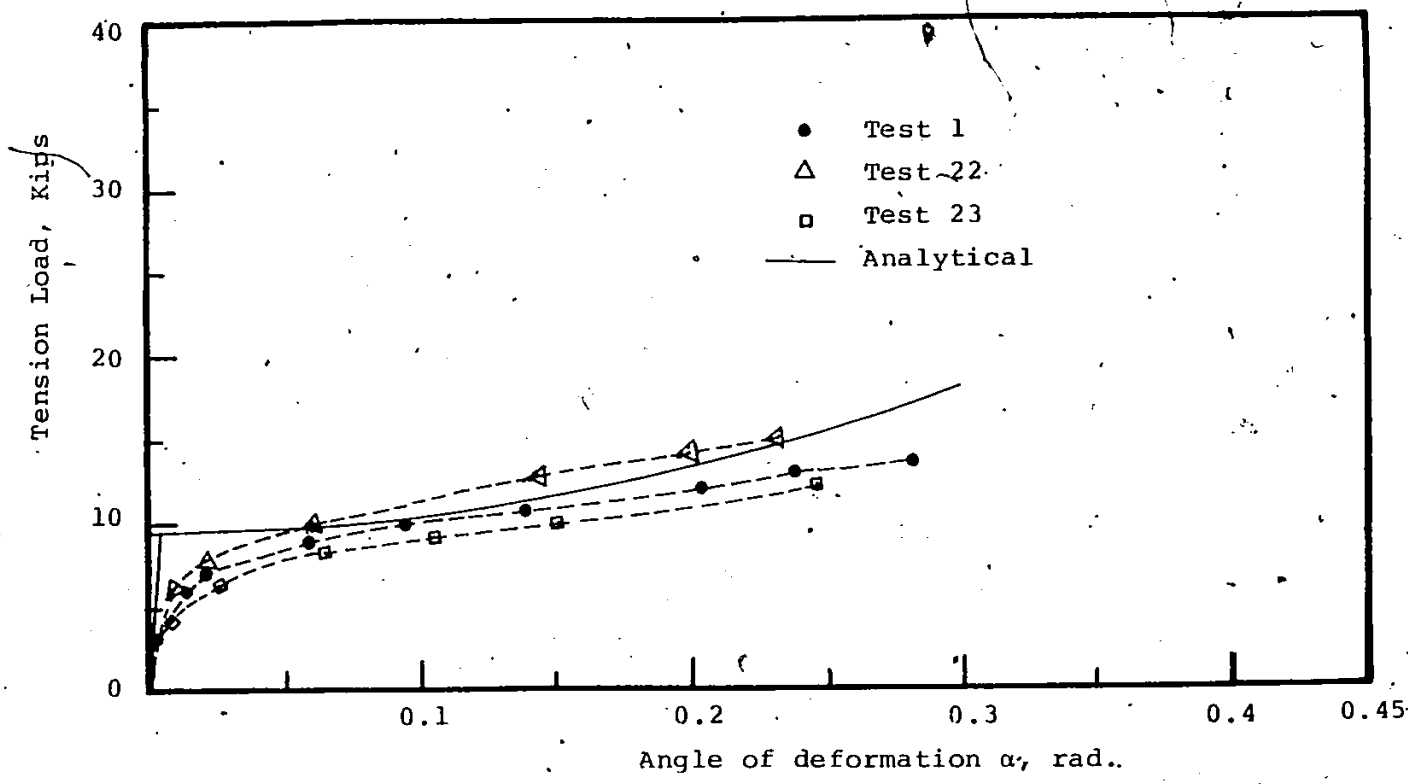

Fig. 3.8. Load versus angle of deformation for T-section tension specimens of 1/4" plate and 5.5" gage.

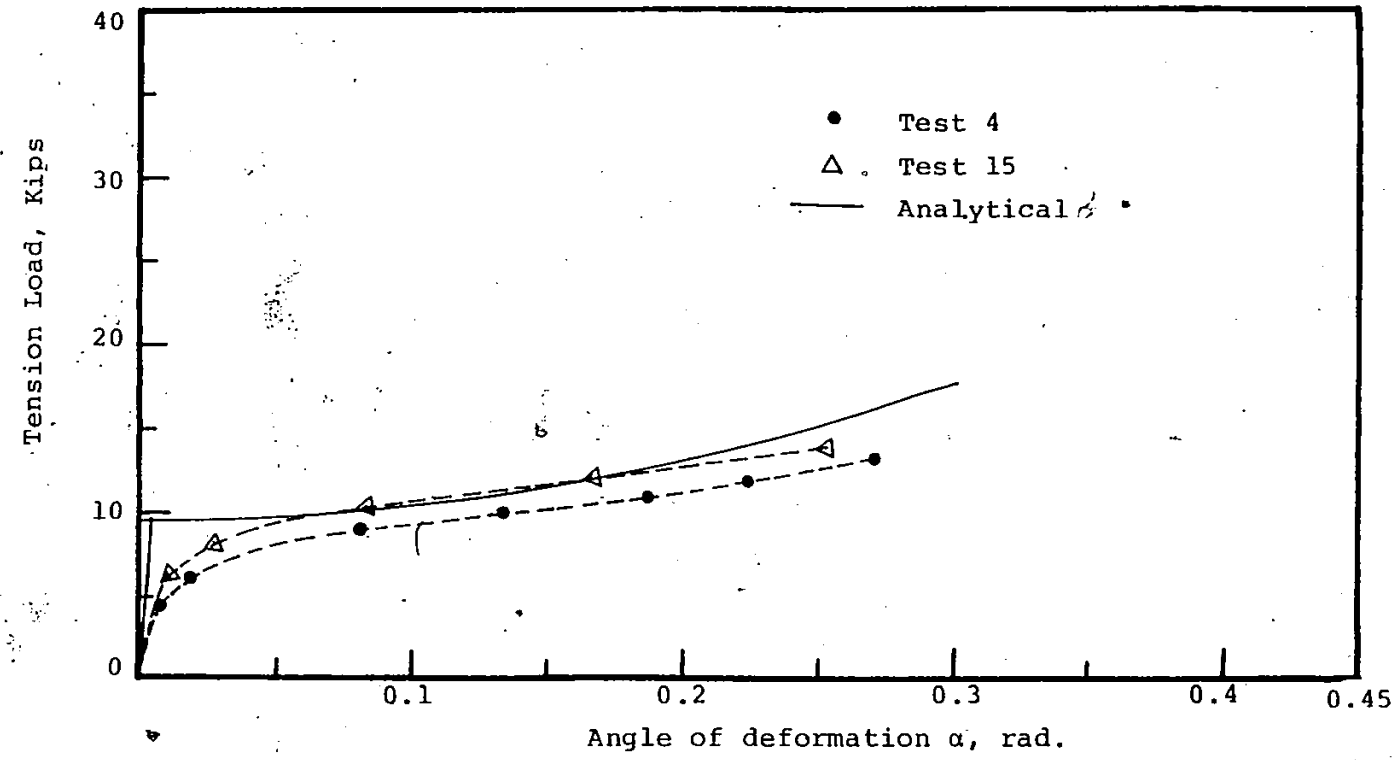

Fig. 3.9. Load versus angle of deformation for T-section tension specimens of 1/4" plate and 5.5" gage.

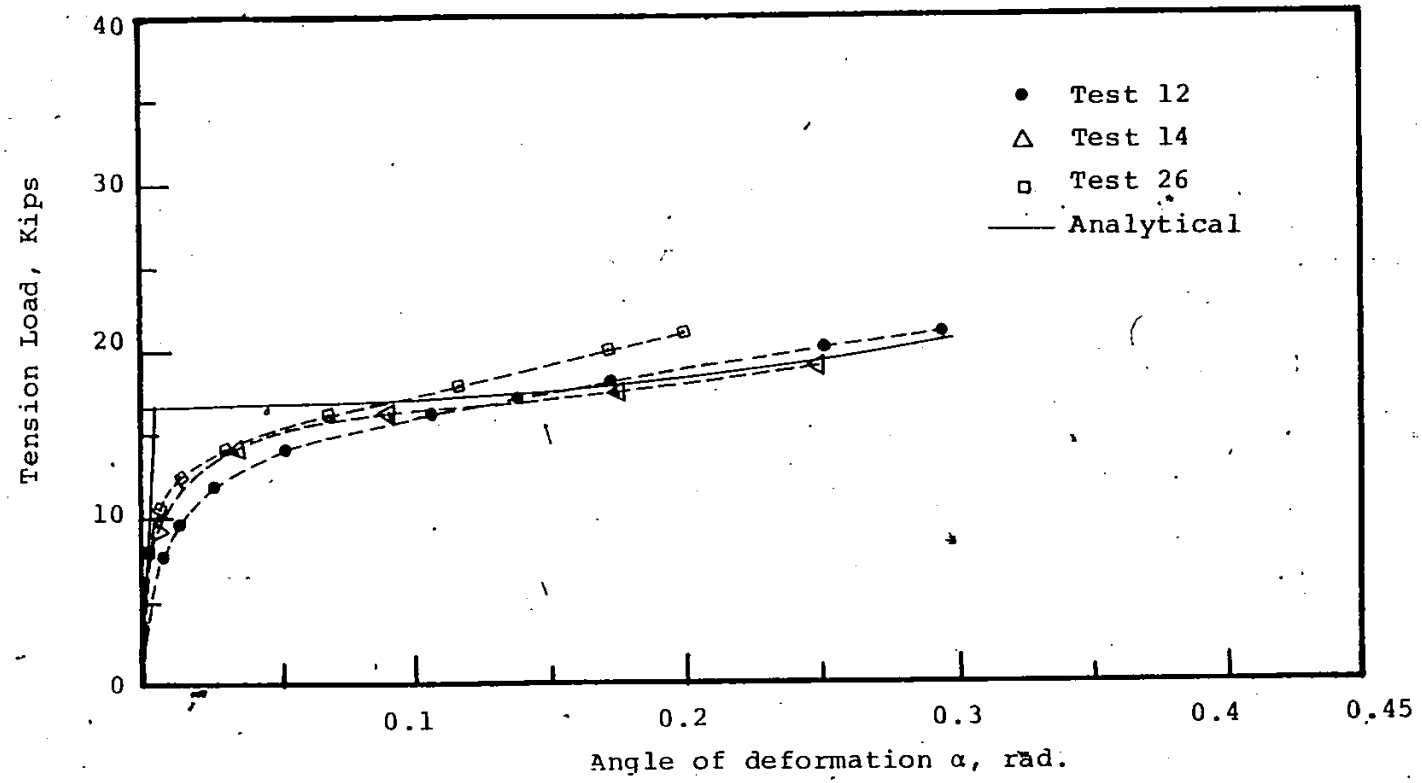

Fig. 3.10 Load versus angle of deformation for T-section tension specimens of 1/4" plate and 4" gage.

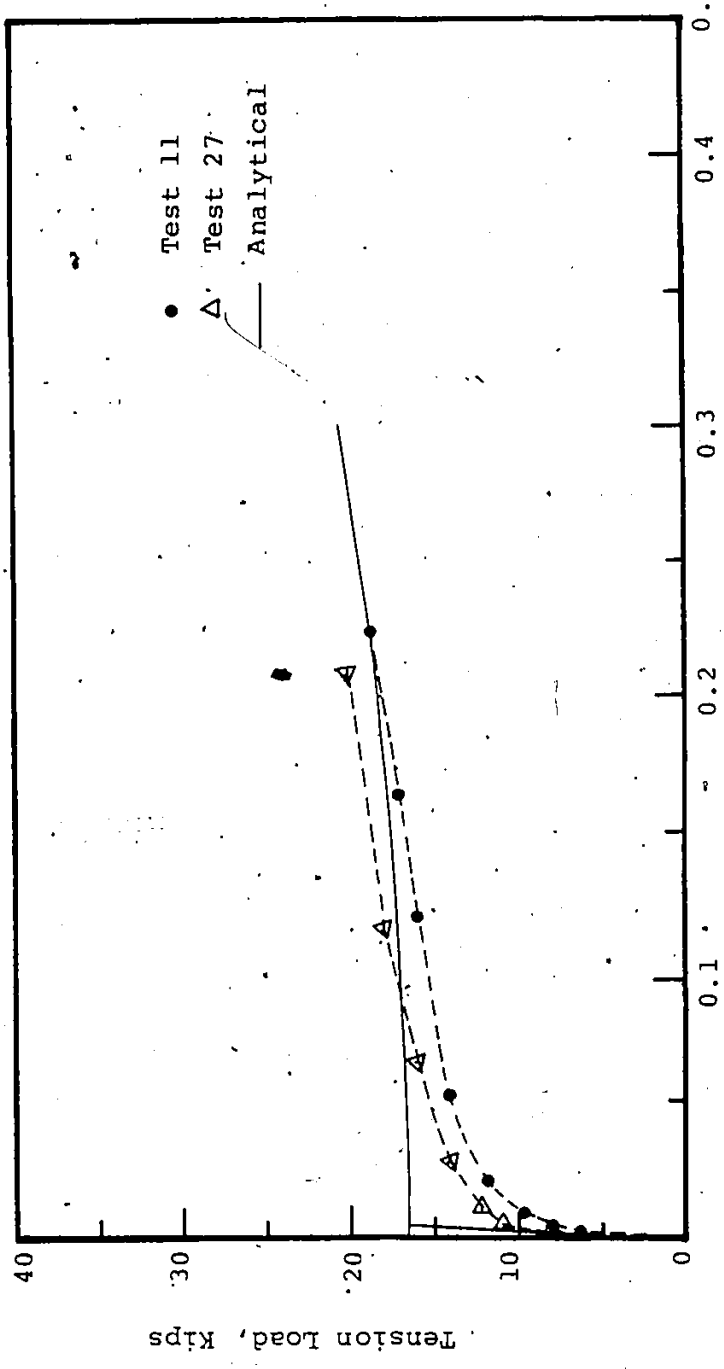

Fig. 3.11. Load versus angle of deformation for T-section tension specimens of 1/4" plate and 4" gage.

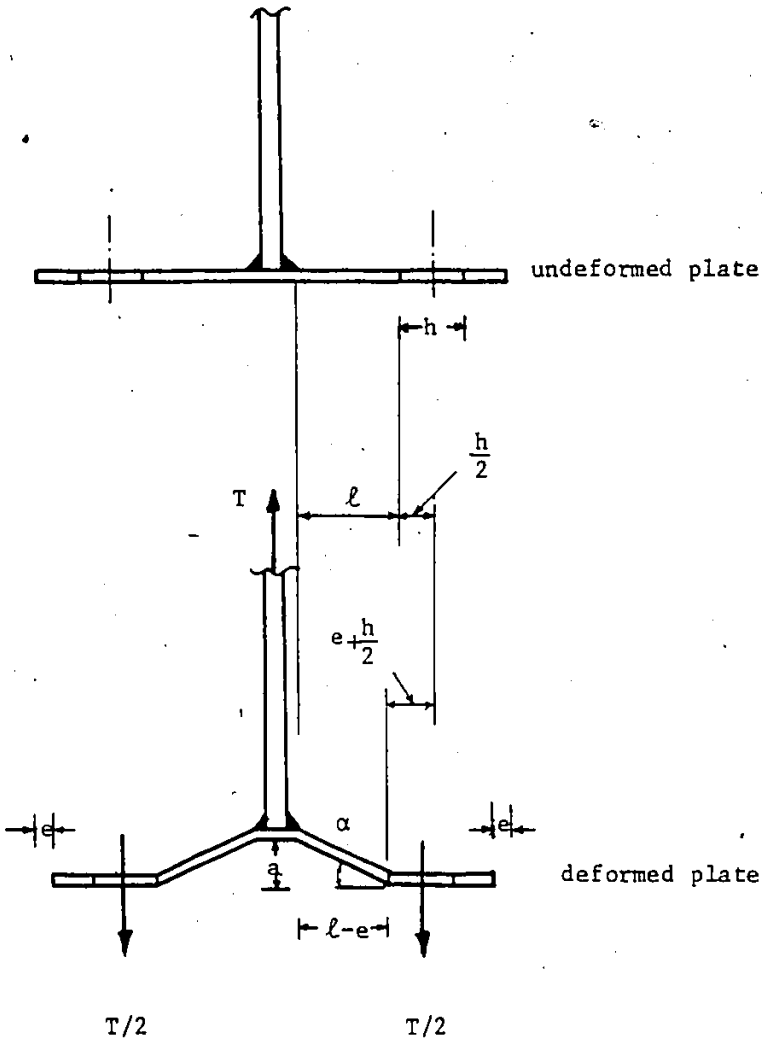

Fig. 3.12. Deformation of T-section.

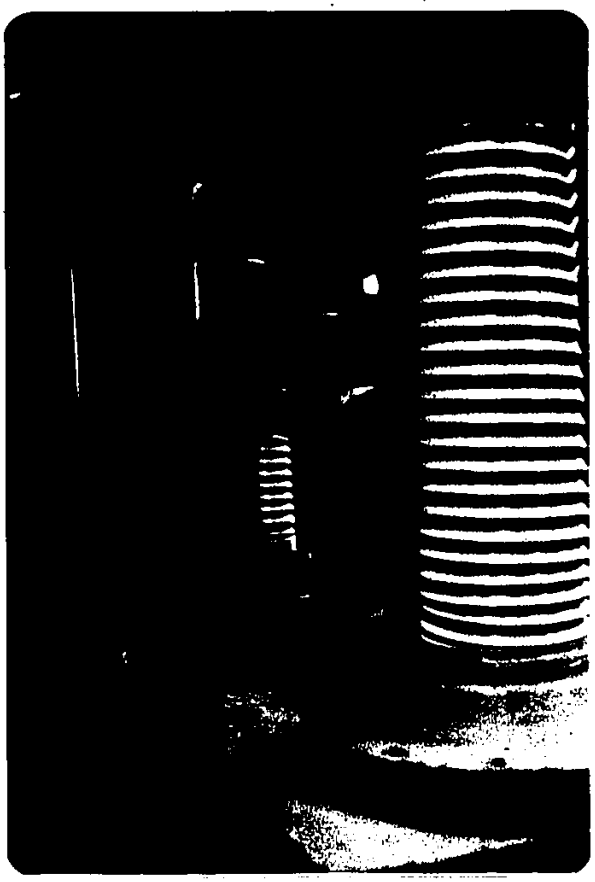

Fig. 3.13. T-Section tension test specimen after testing.

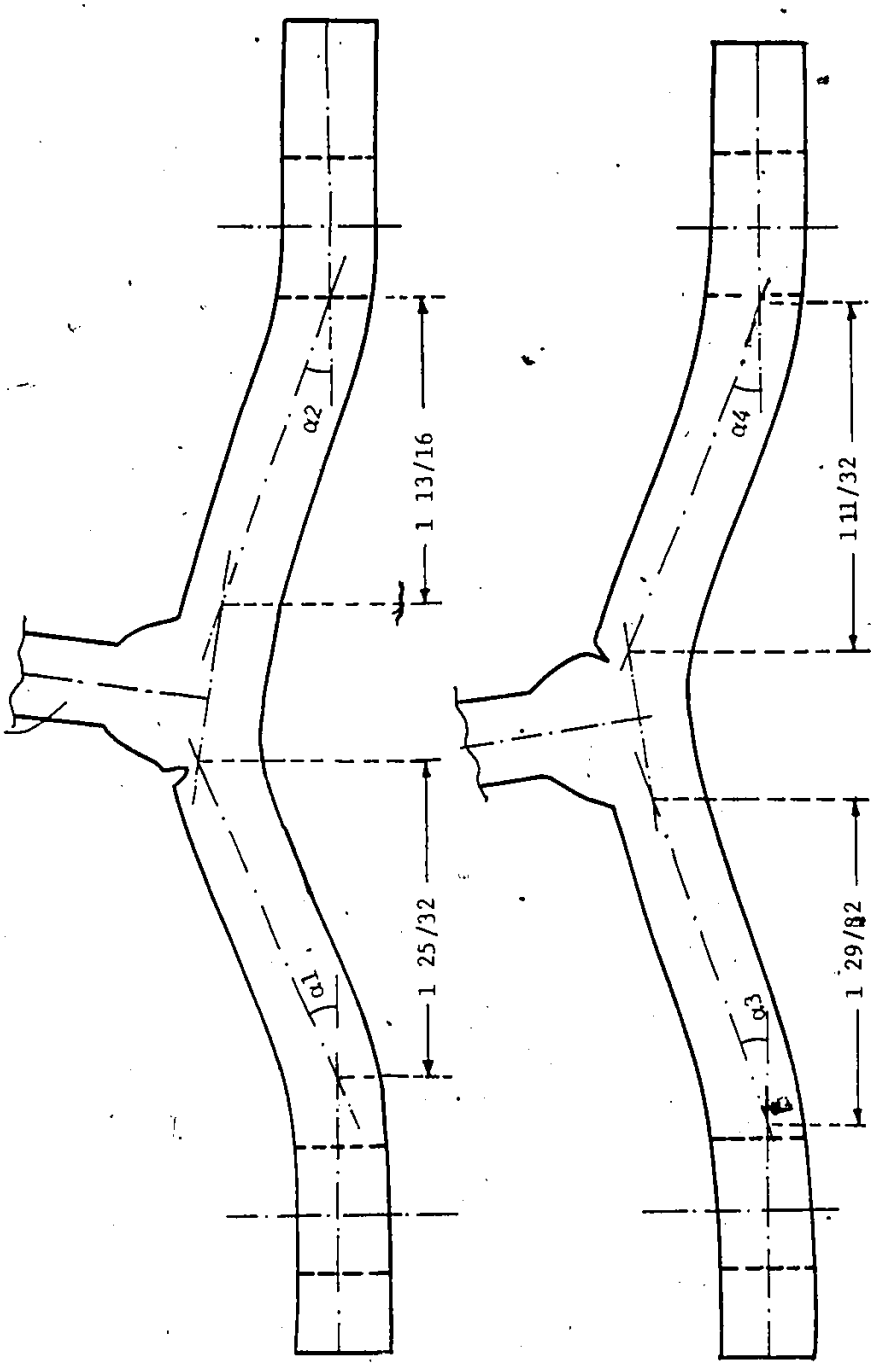

Fig. 3.14. Cross-section of deformed T-section.

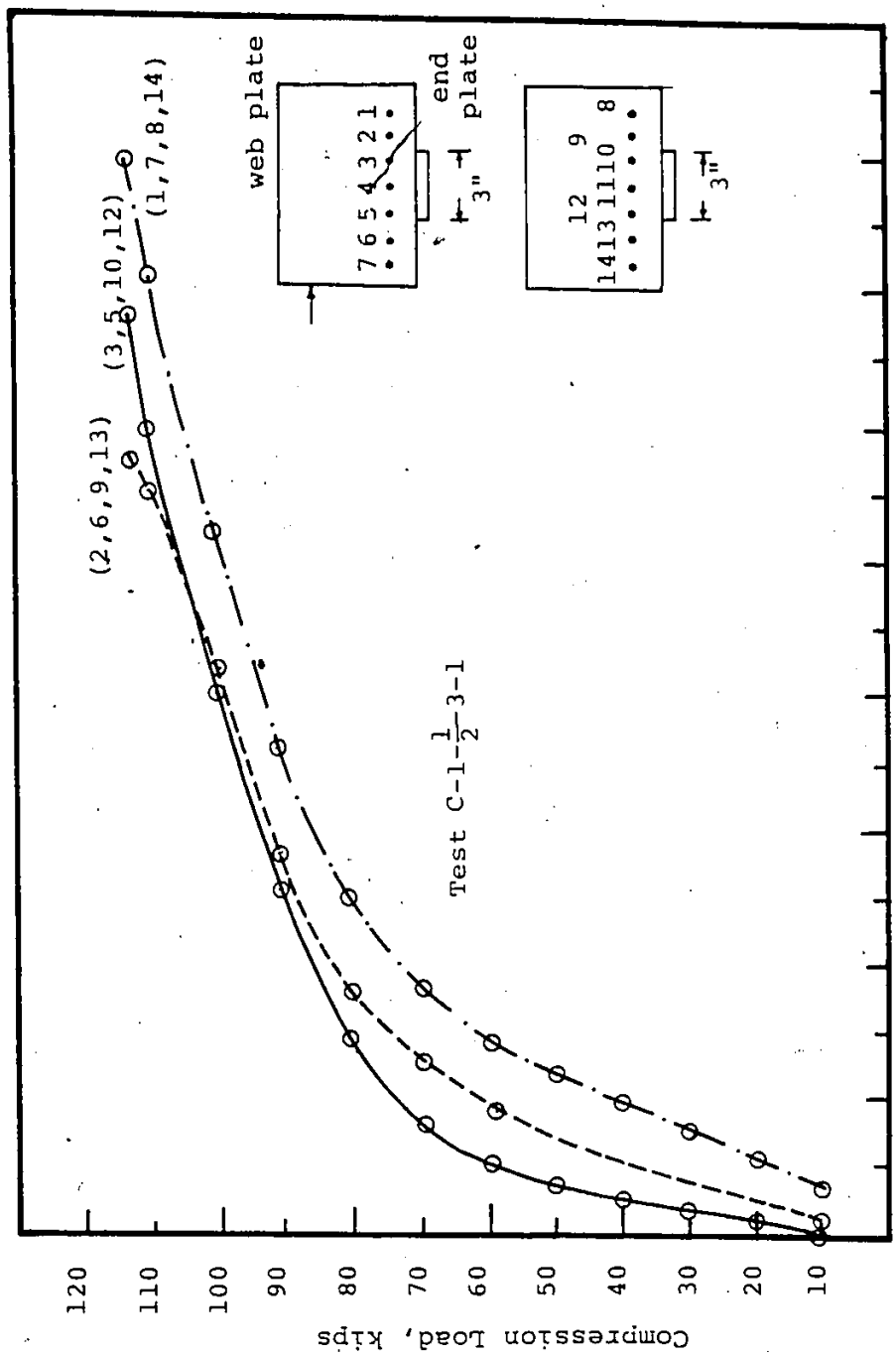

Fig. 3.15 Compression tests on T-sections, end plate length of 3 inches.

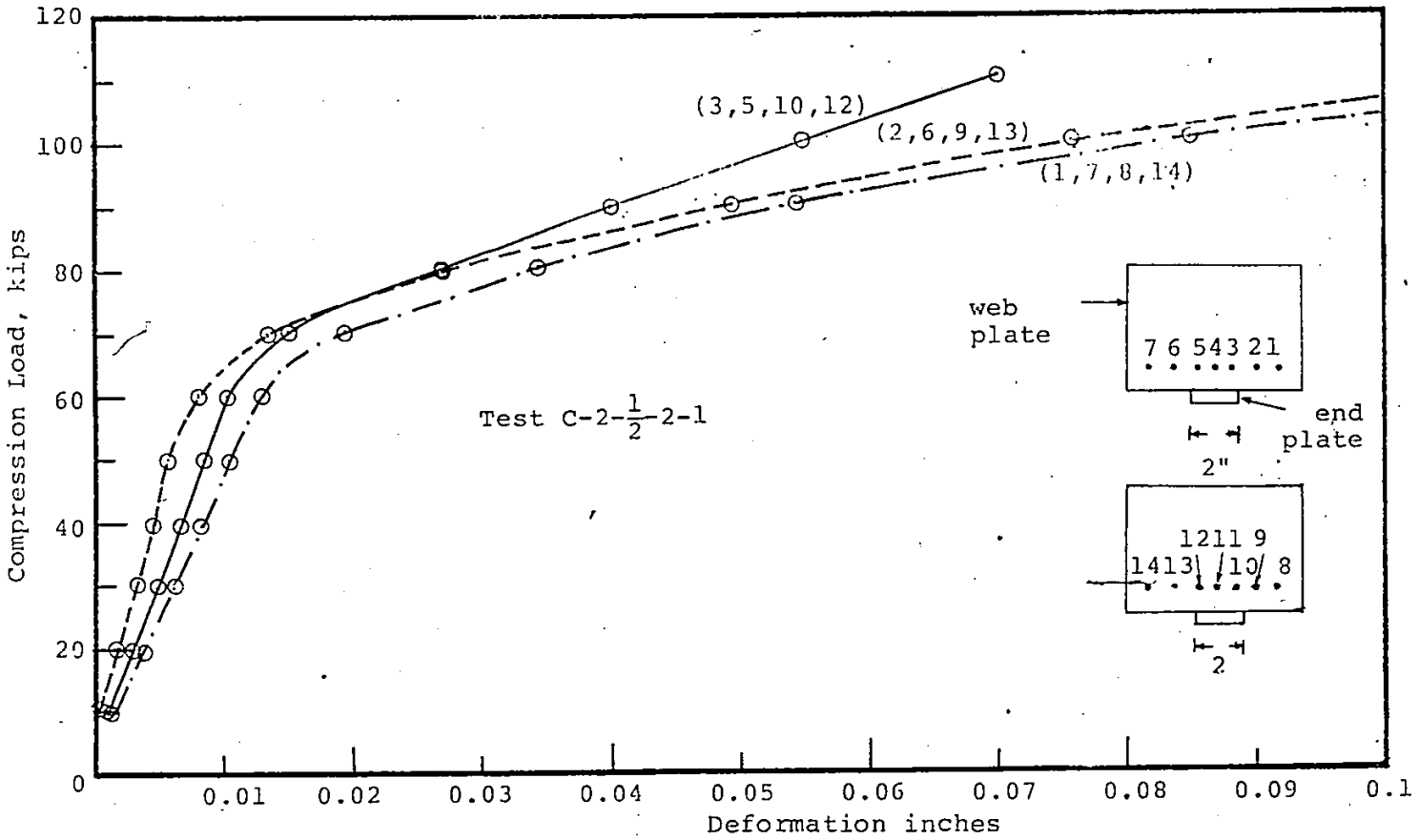

Fig. 3.16 Compression tests on T-section, end plate length of 2 inches.

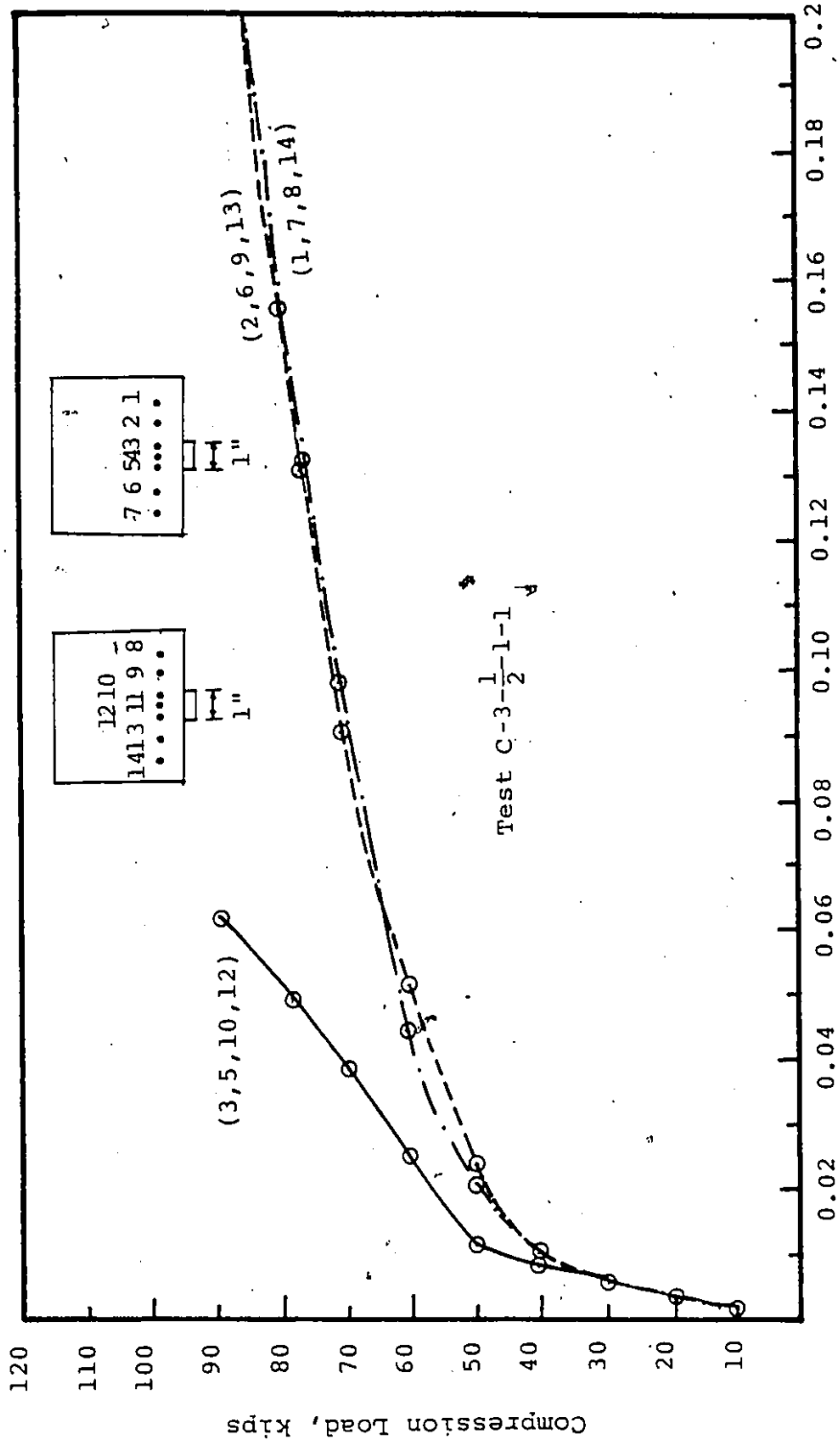

Fig. 3.17 Compression tests on T-sections, end plate length of 1 inch.

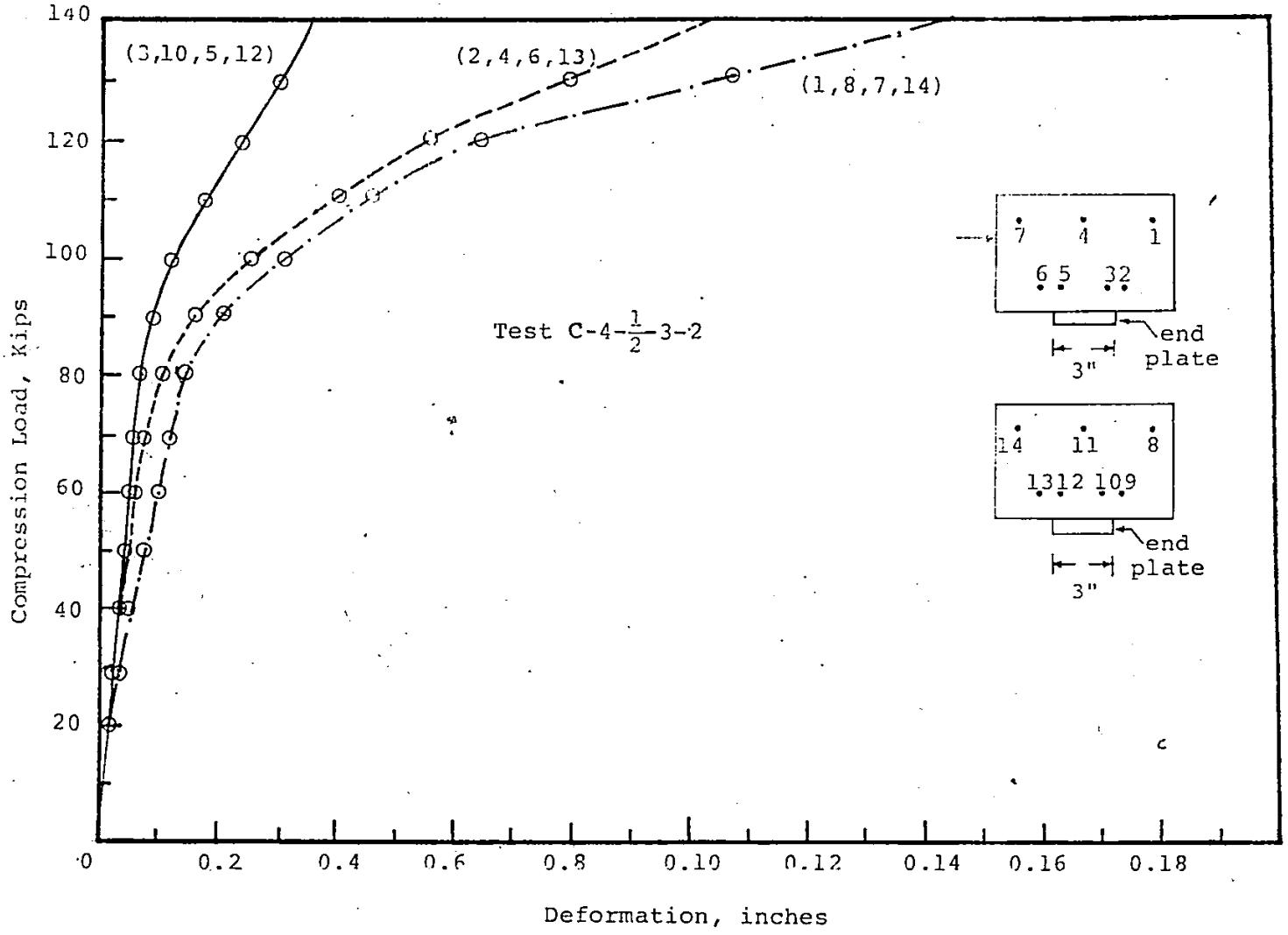

Fig. 3.18 Compression Test on T-Sections, end plate length 3 inches.

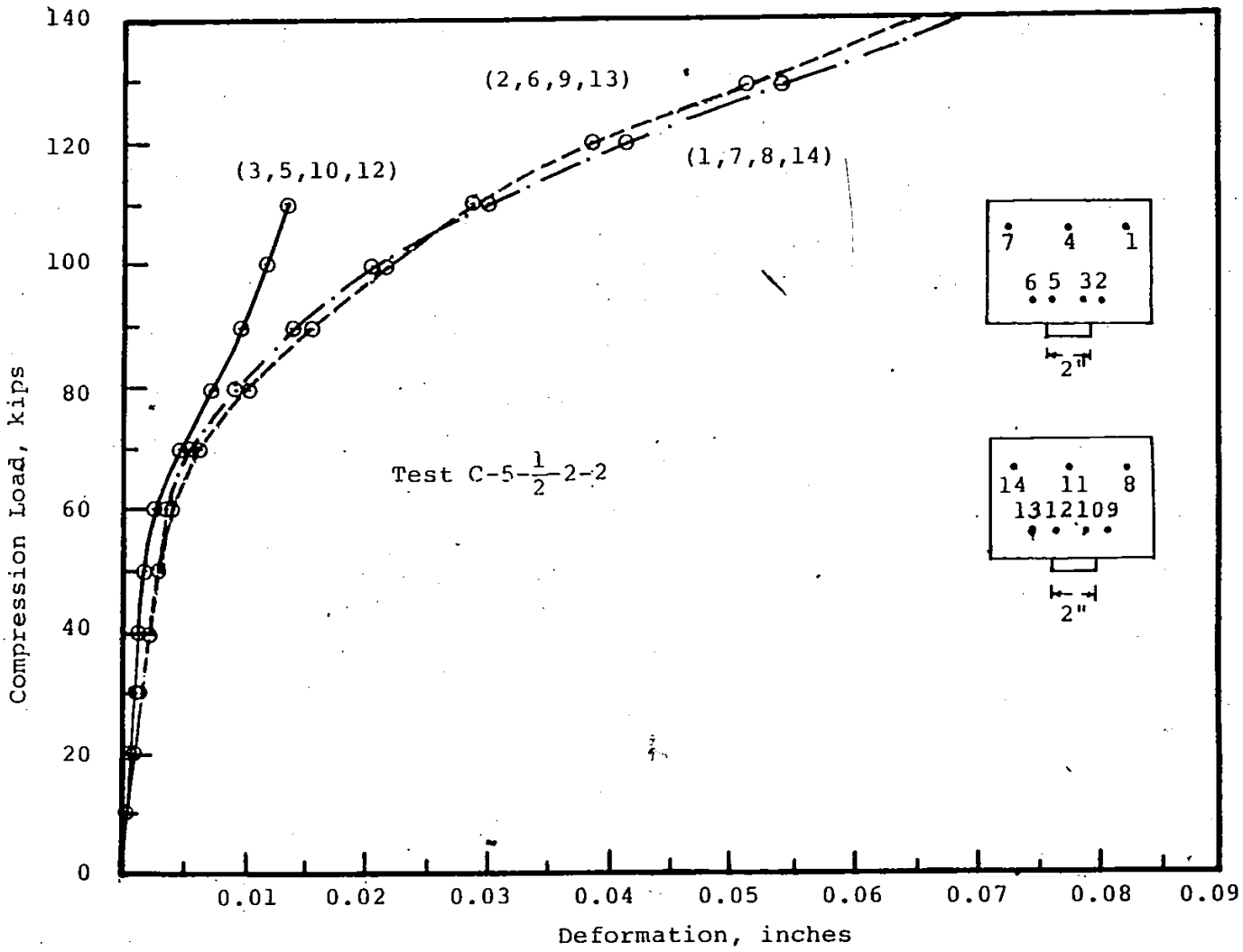

Fig. 3.19 Compression tests on T-sections, end plate length of 2 inches.

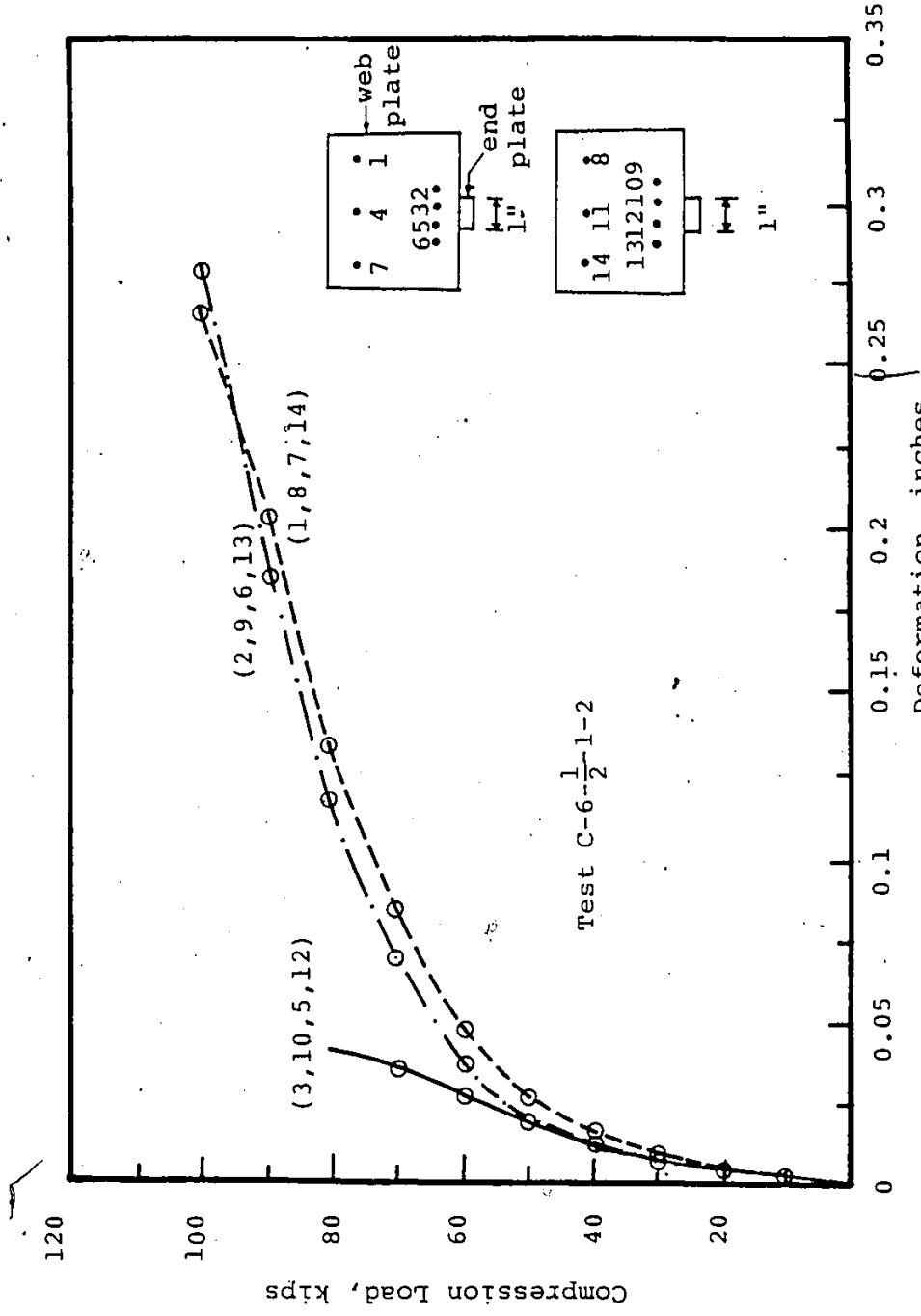

Fig. 3.20 Compression tests on T-sections, end plate length of 1 inch.

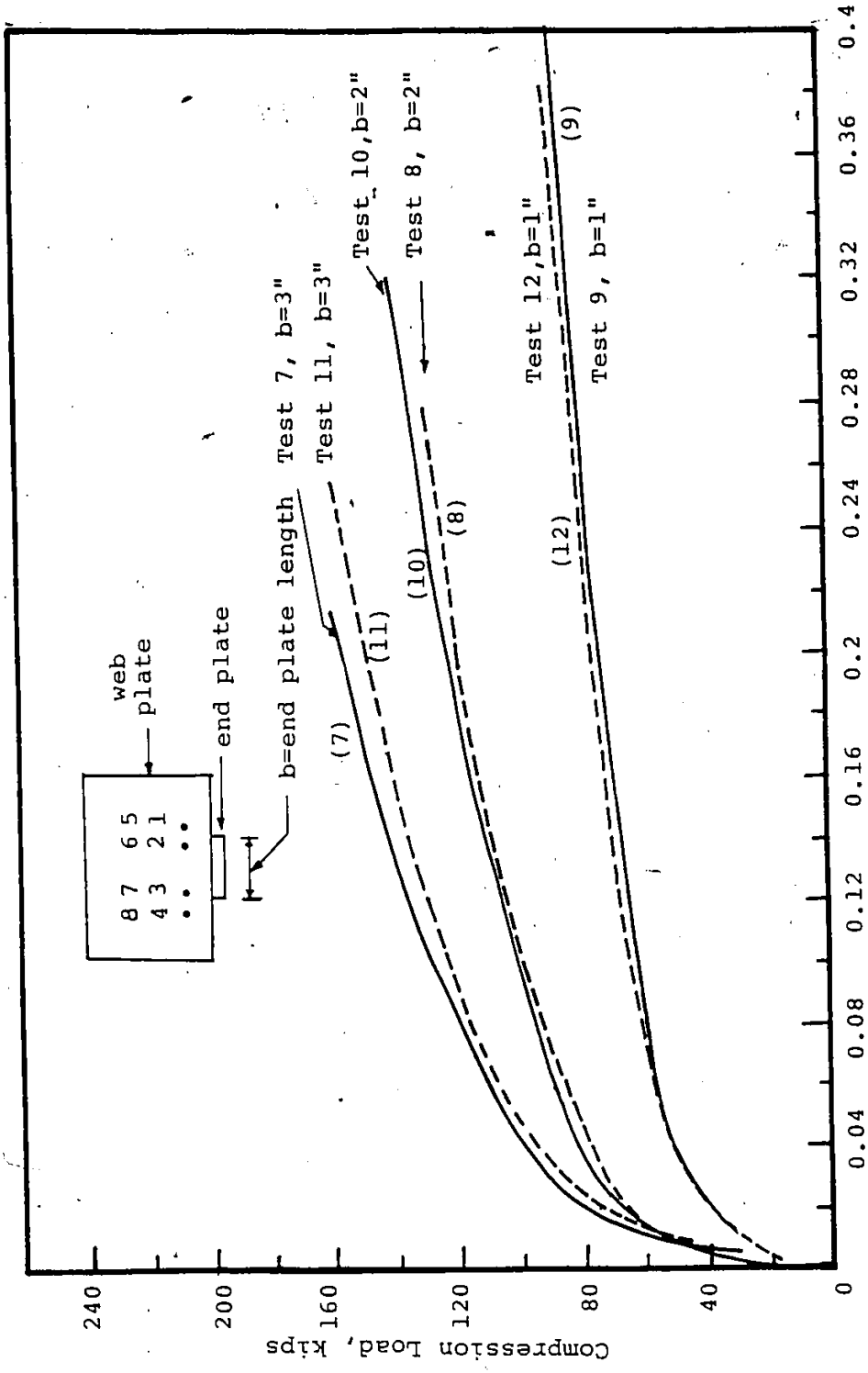

Fig. 3.21 Compression tests on T-sections, end plate lengths as noted.

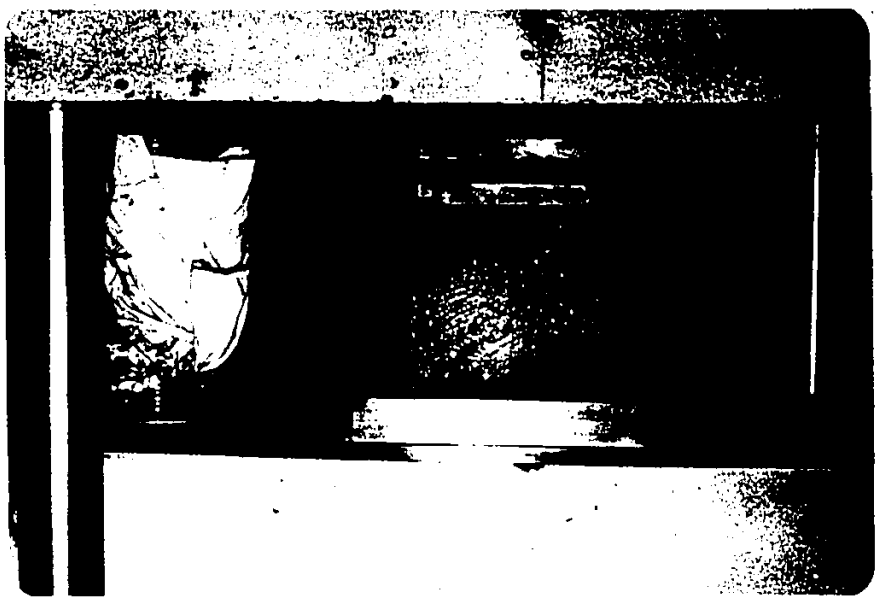

Fig. 3.22. Compression test specimen on completion of test.

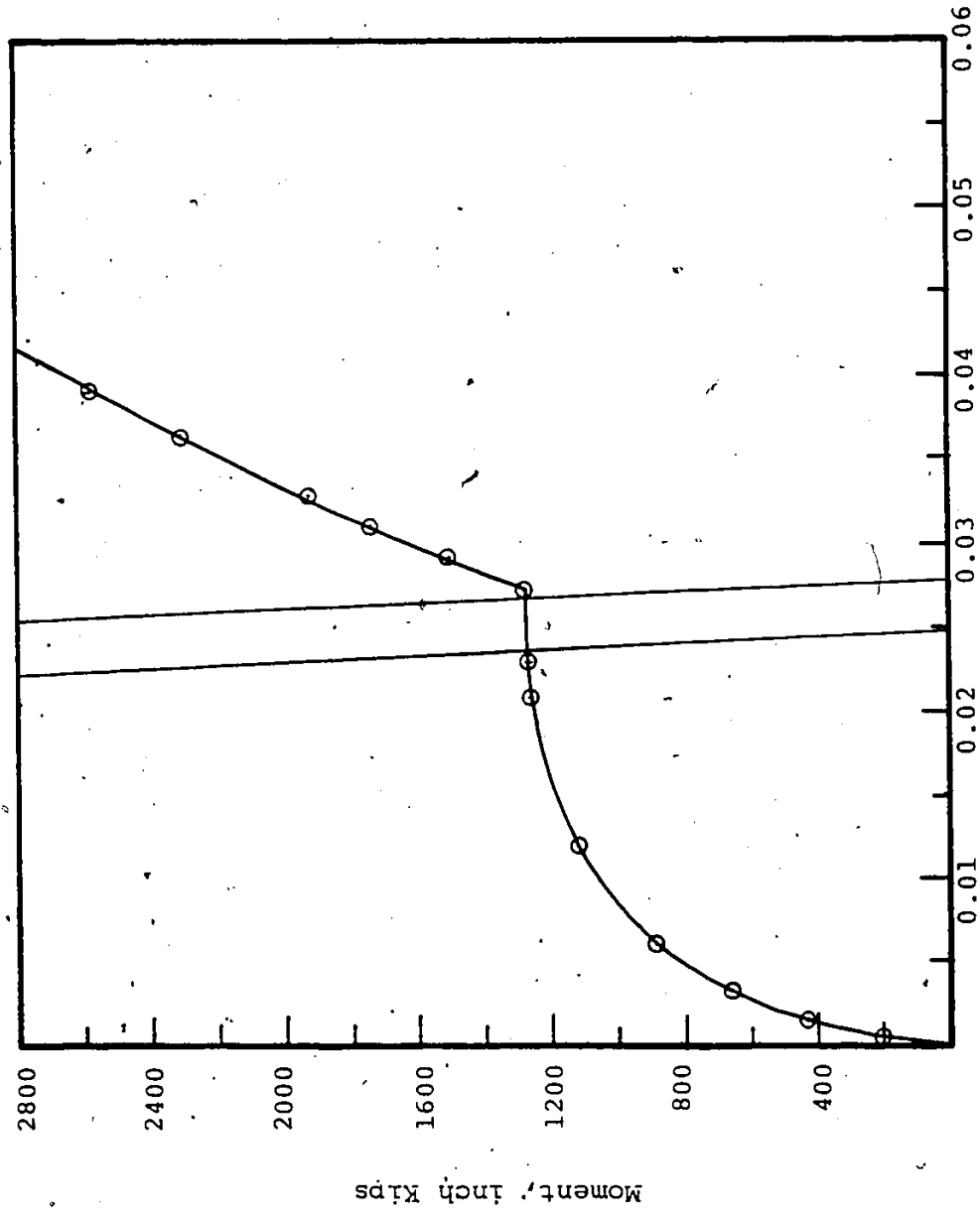

Fig. 3.23. Moment rotation curves for Test E-1-6-3/8-4

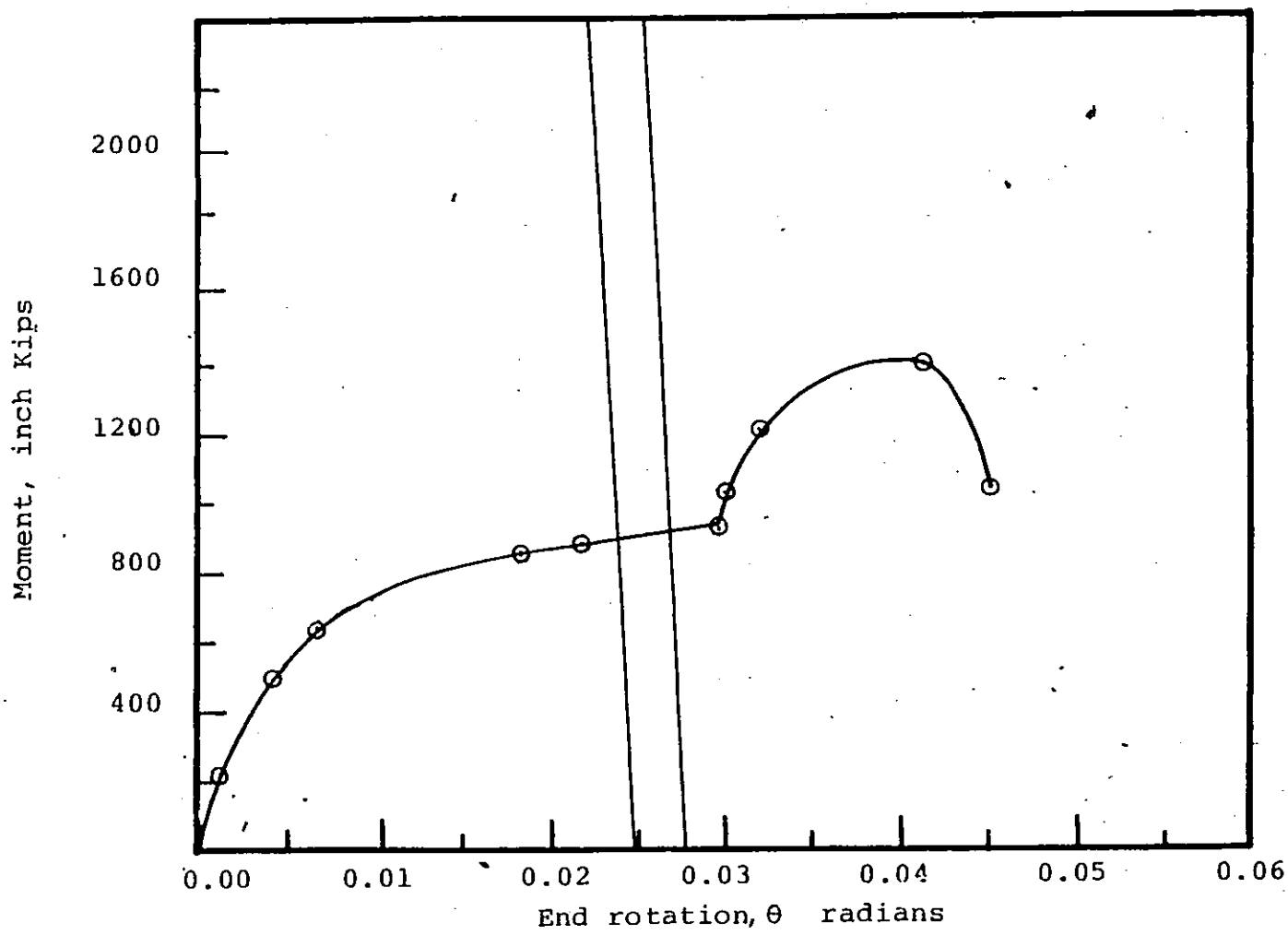

Fig. 3.24. Moment-Rotation curve for Test E-2-6-1/4-4.

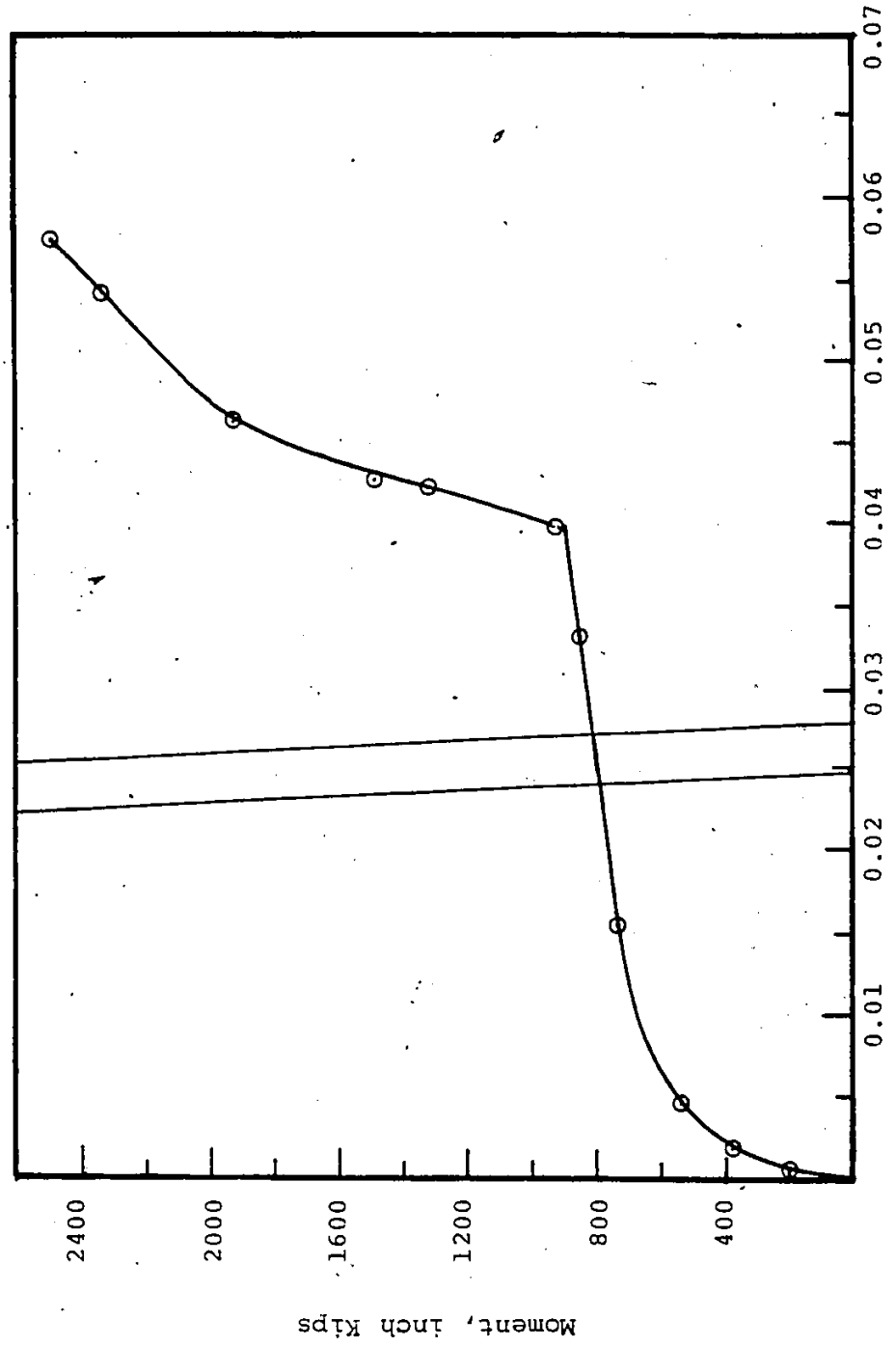

Fig. 3.25. Moment rotation curves for Test E-3-6-3/8-5.5.

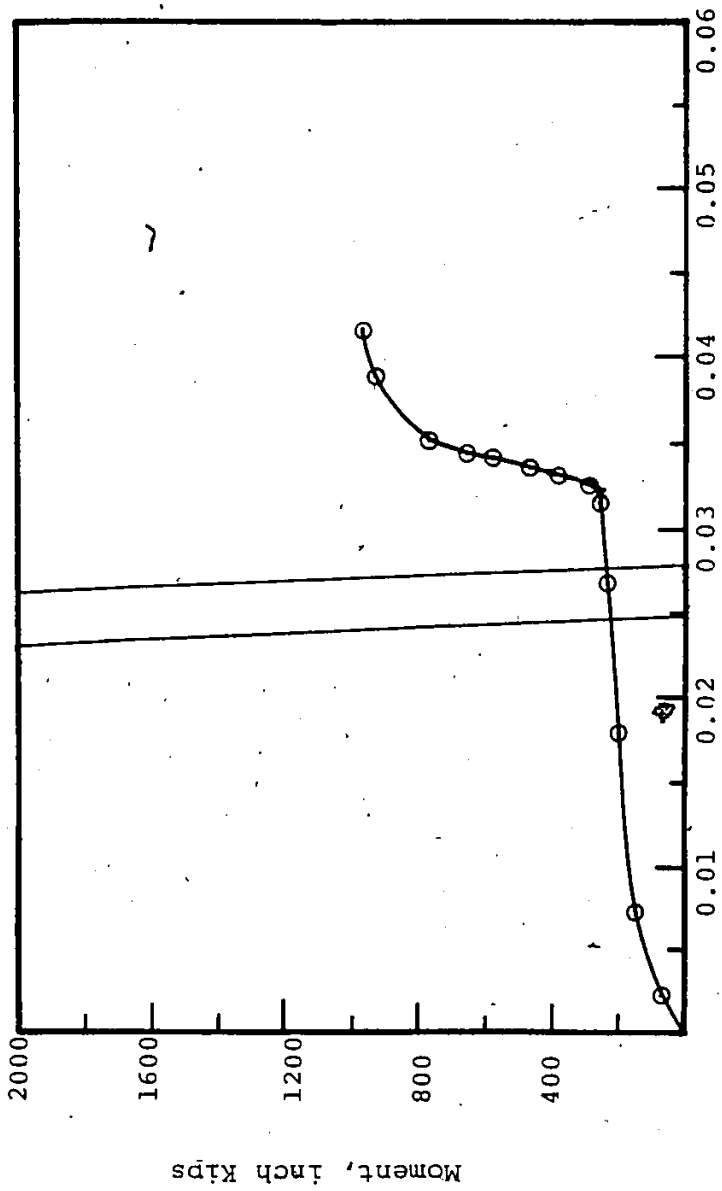

Fig. 3.26. Moment rotation curve for Test E-4-4-1/4-5.5.

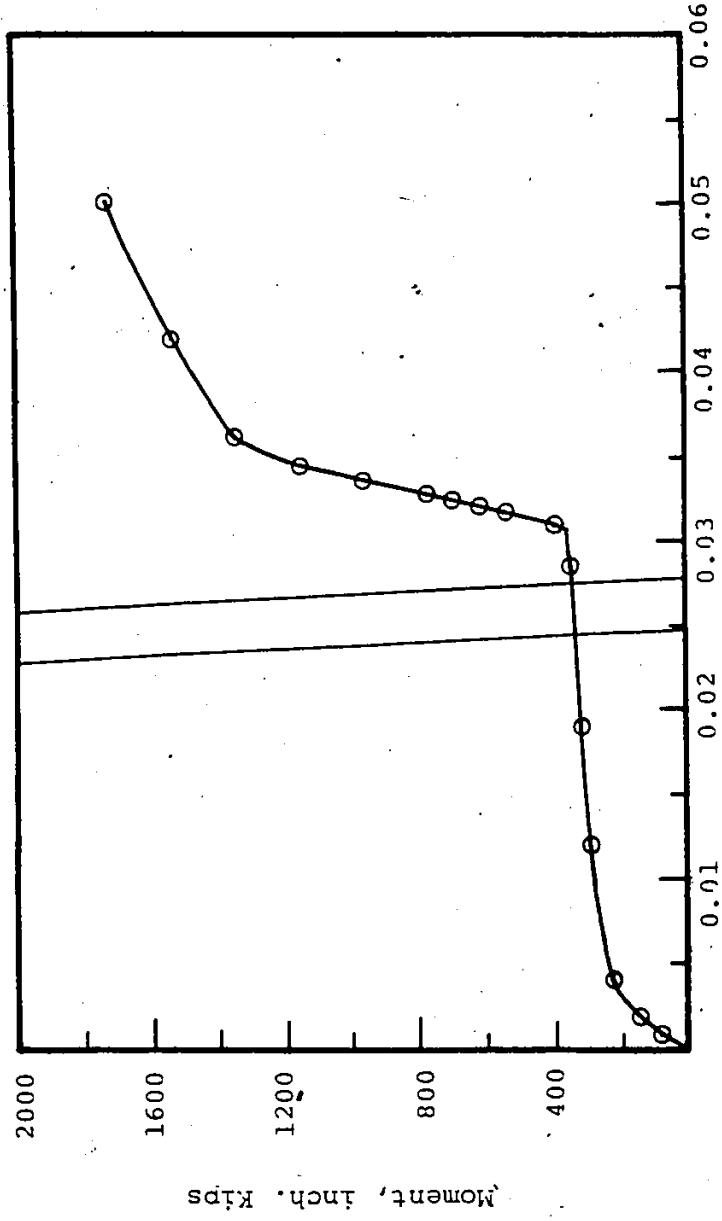

Fig. 3.27. Moment rotation curve for Test E-5-6-3/8-5.5

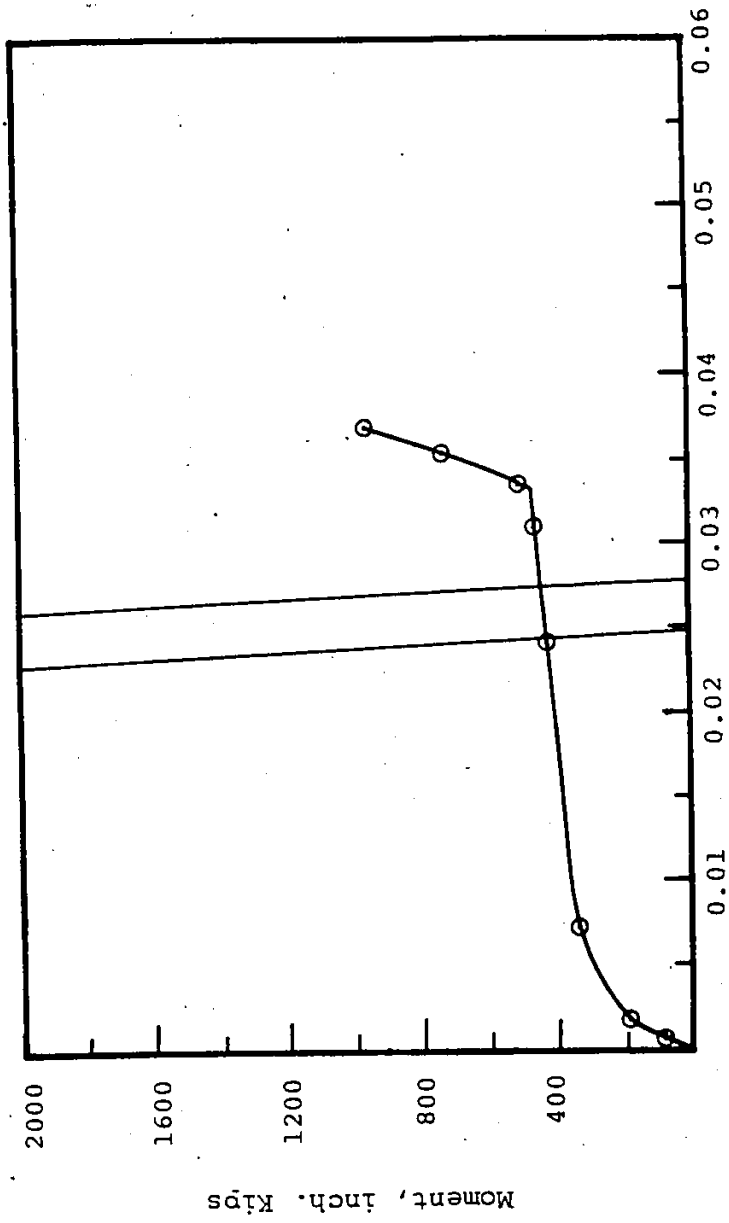

Fig. 3.28. Moment Rotation curve for Test E-6-4-1/2-5.5

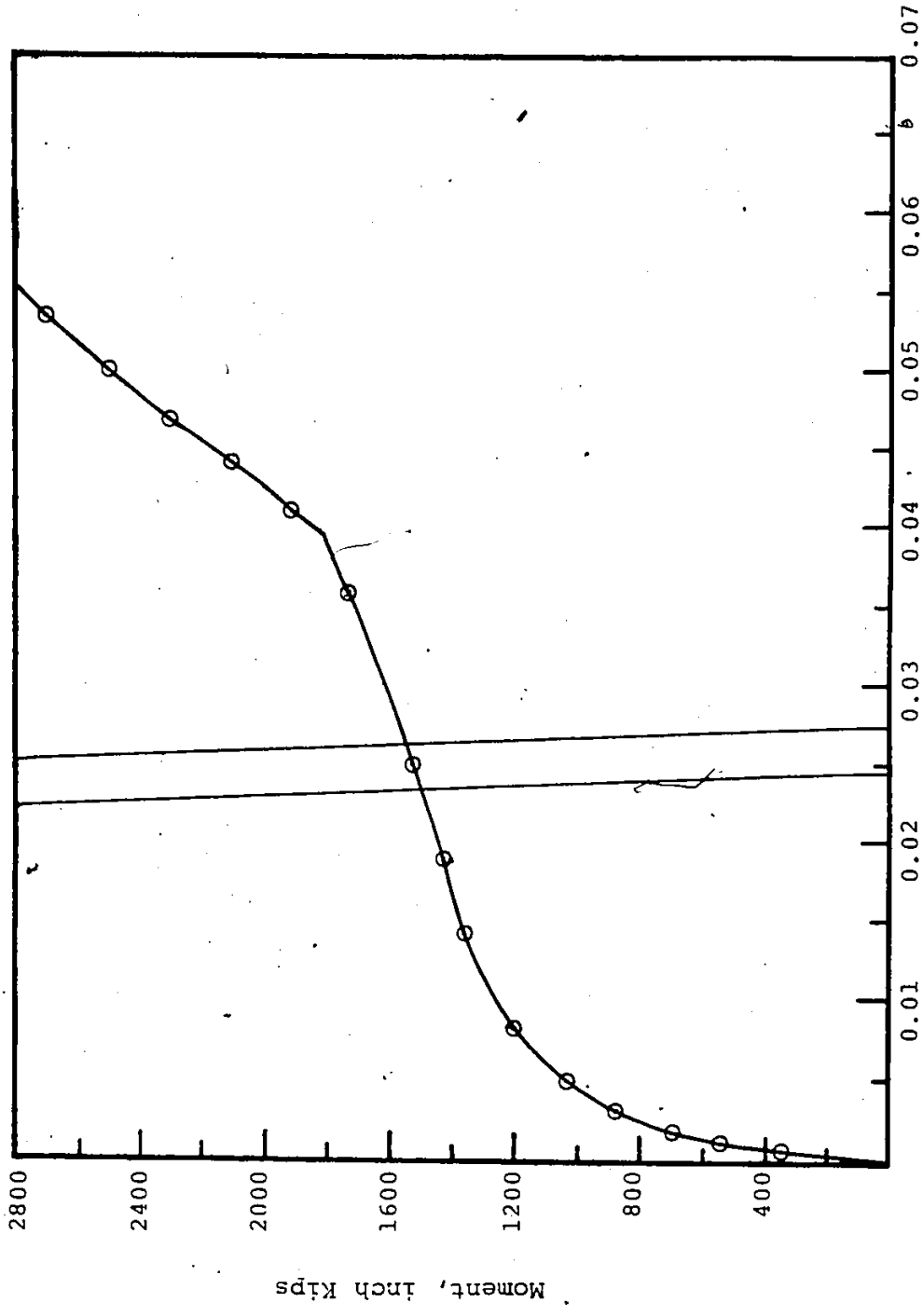

Fig. 3.29. Moment rotation curve for Test E-7-8-3/8-5.5

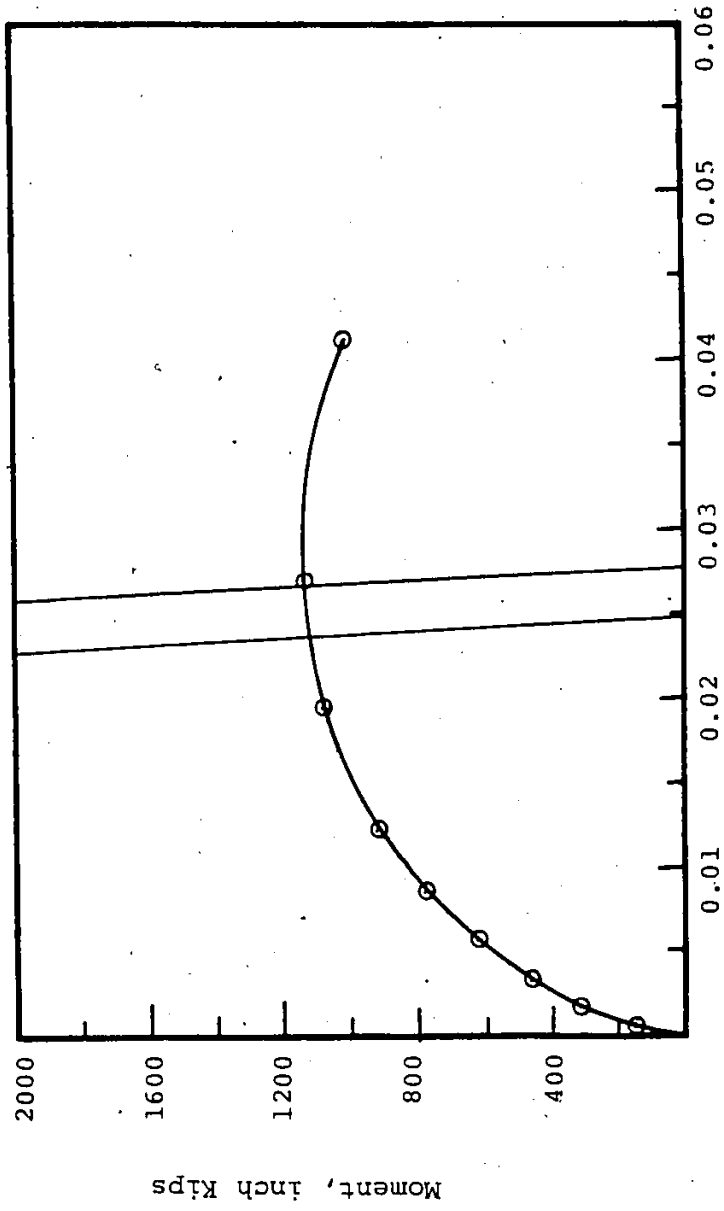

Fig. 3.30. Moment rotation curve for Test E-8-8-1/4-5.5

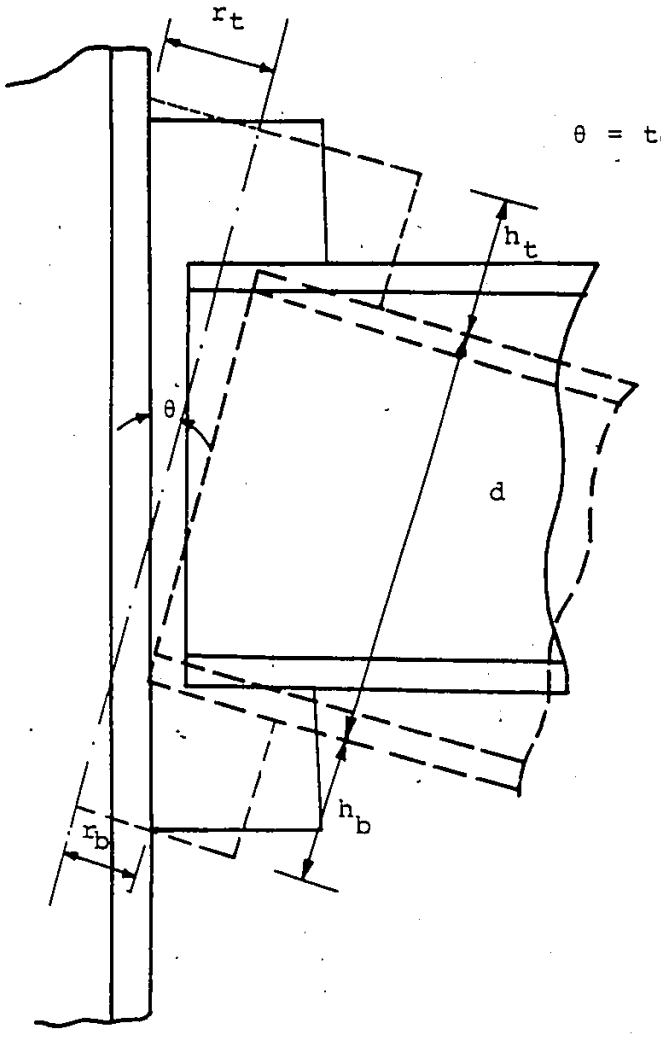

$$\theta = \tan^{-1} \frac{r_t + r_b}{d + h_t + h_b}$$

Fig. 3.31 Rotation of Beam.

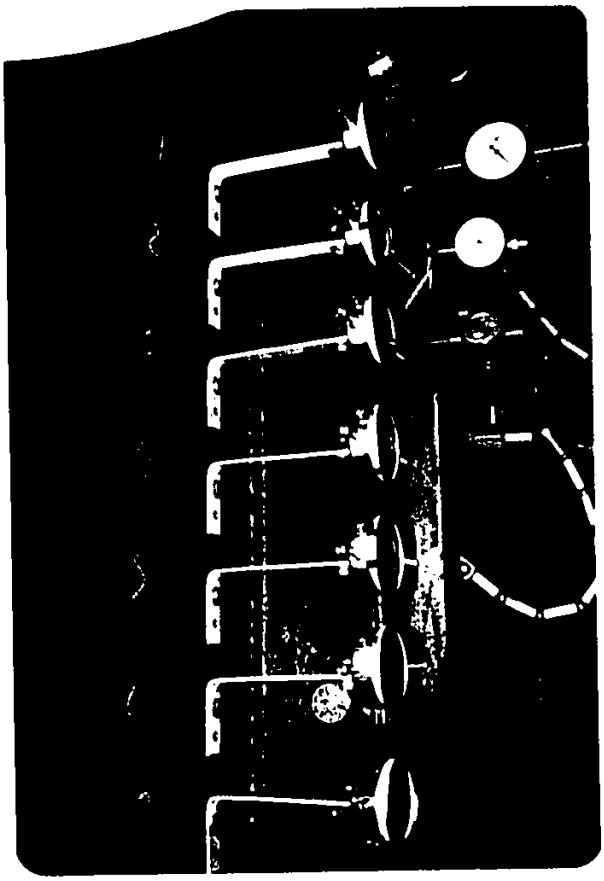

Fig. 3.32. Yield lines for Test E-7-8-3/8-5.50.

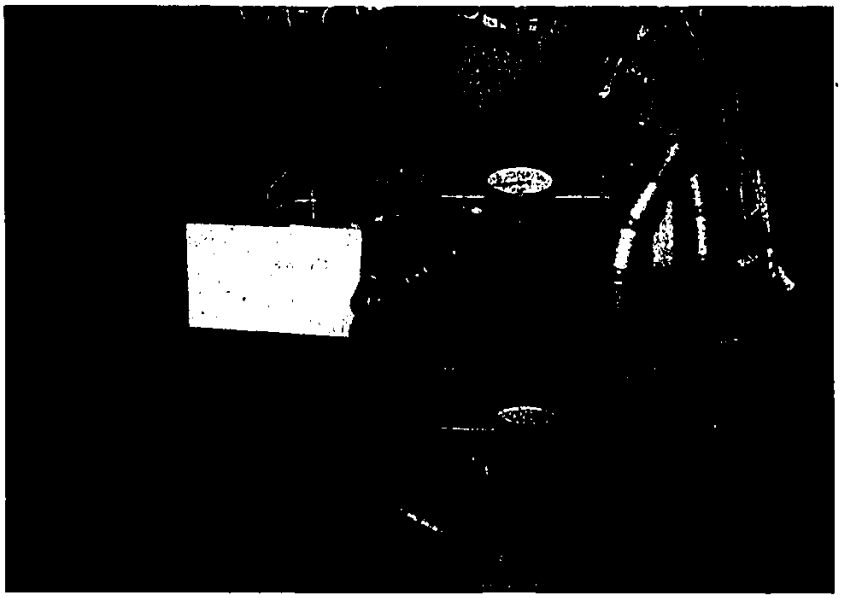

Fig. 3.33. Yielding of the beam web around the lower portion of the end plate.

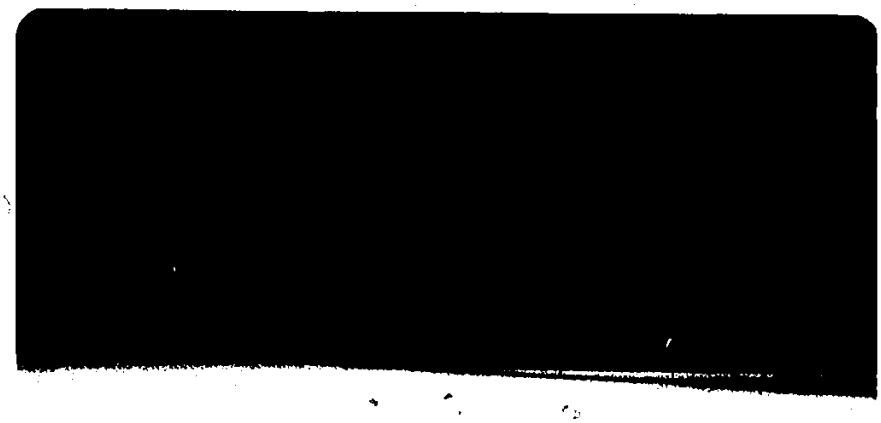

Fig. 3.34. Deformed bolts after beam Test E-6-4.5-5.5.

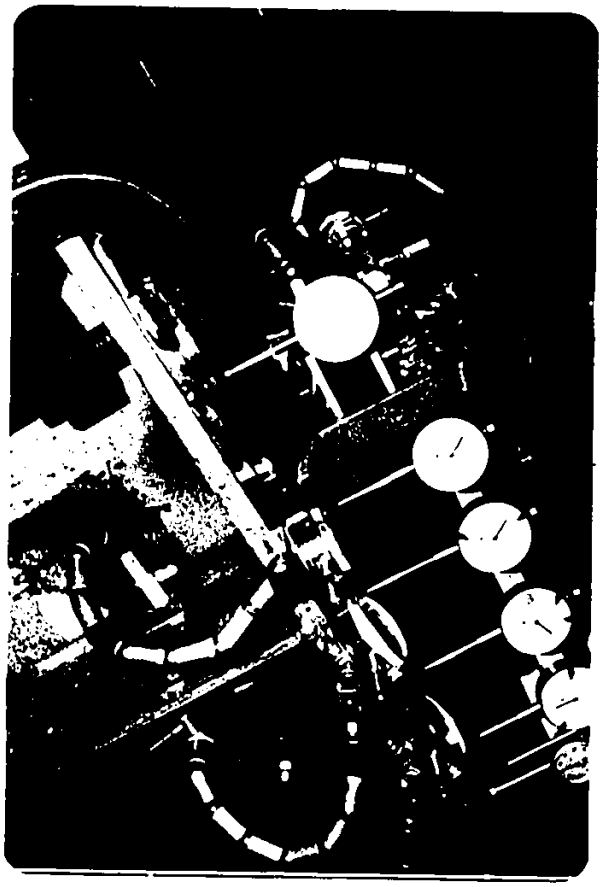

Fig. 3.35. Outward movement of top beam from column.

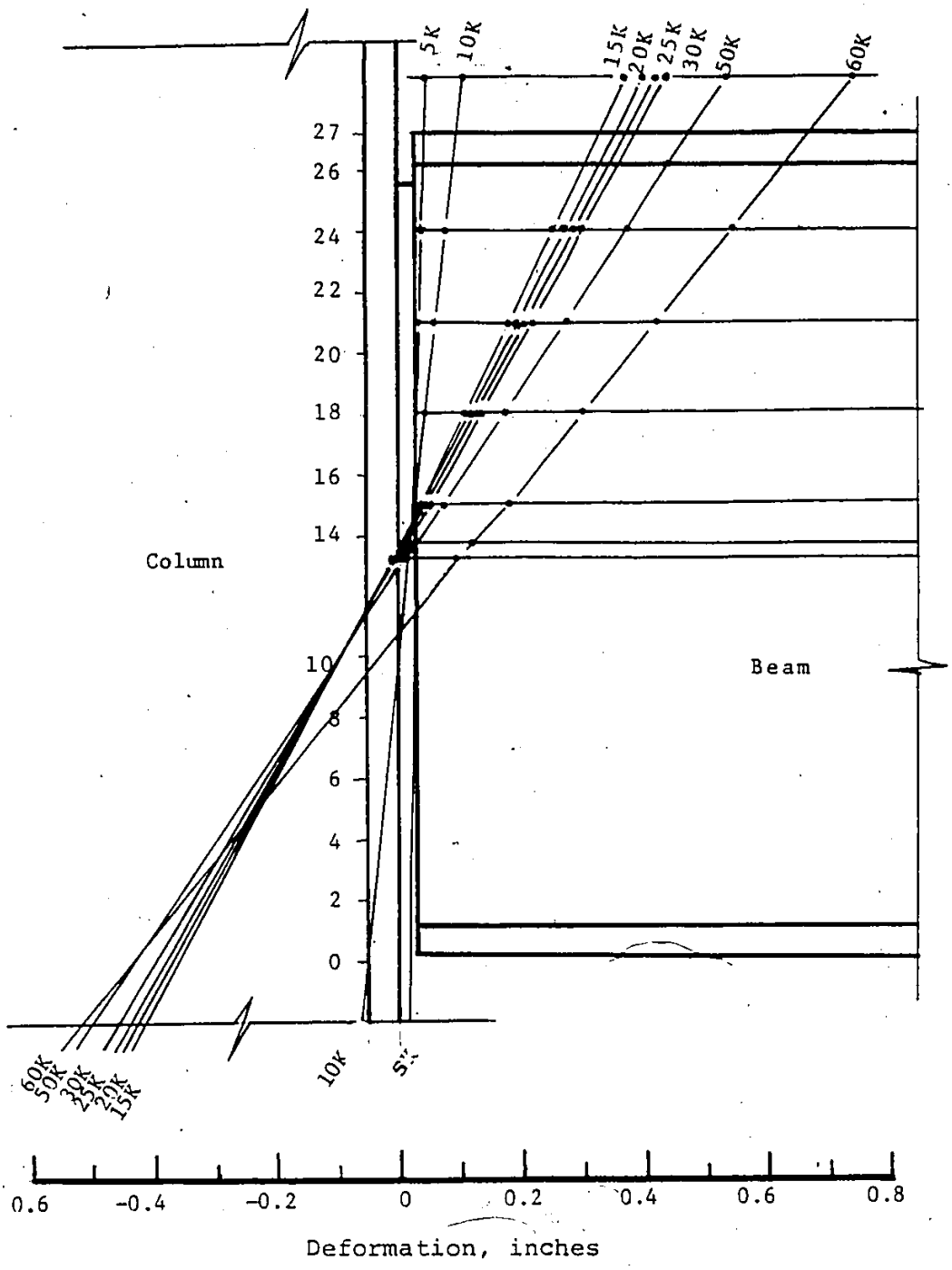

Fig. 3.36. Web deformation near end plate for Test E-6-4-1/2-5.5 at different loads.

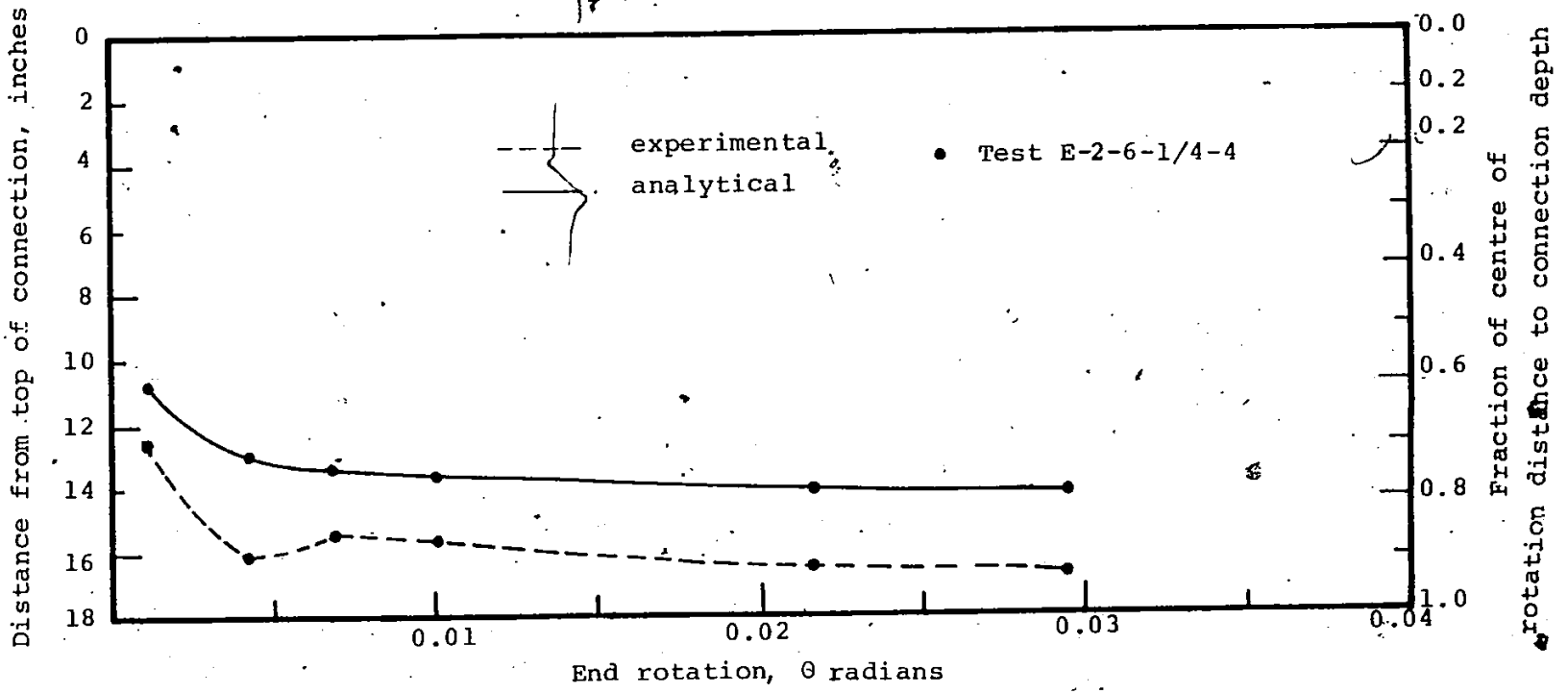

Fig. 3.37 Location of centre of rotation

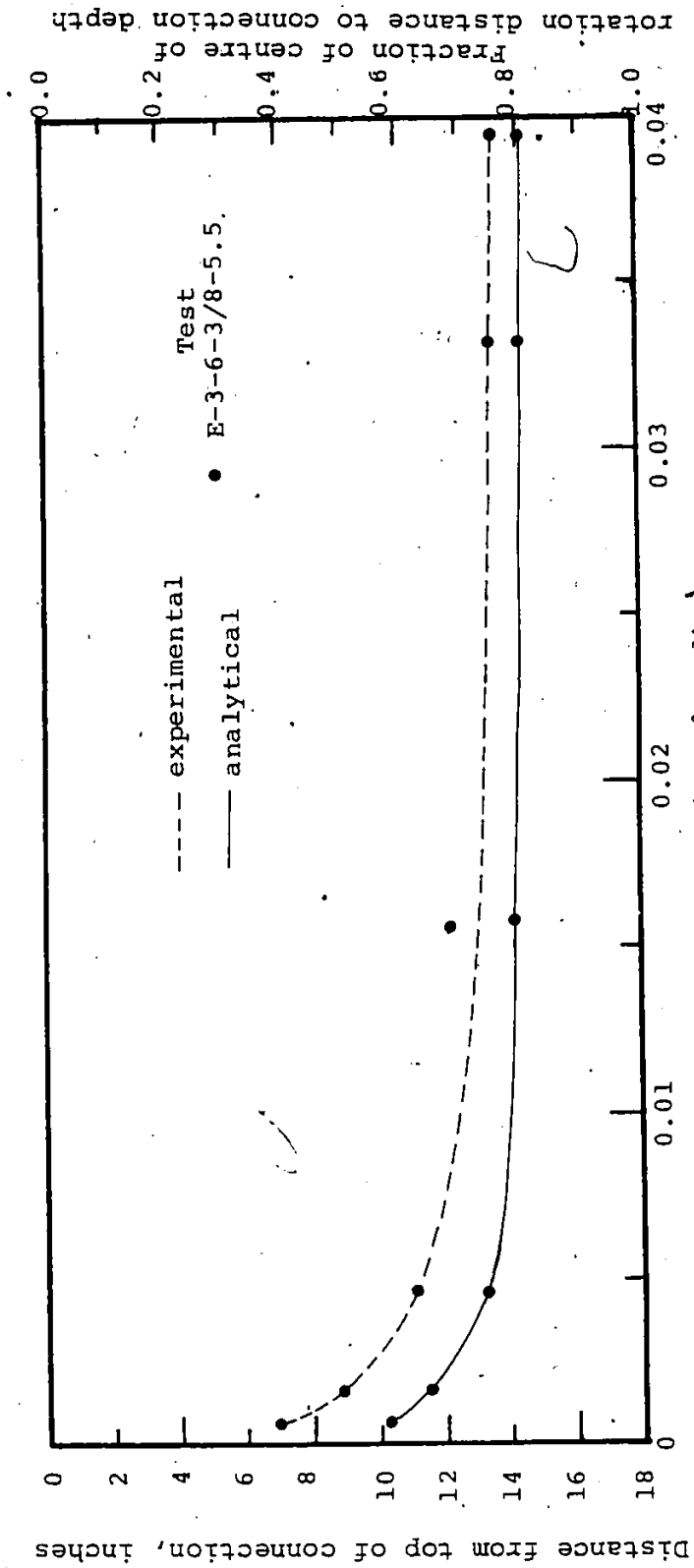

Fig. 3.38. Location of centre of rotation.

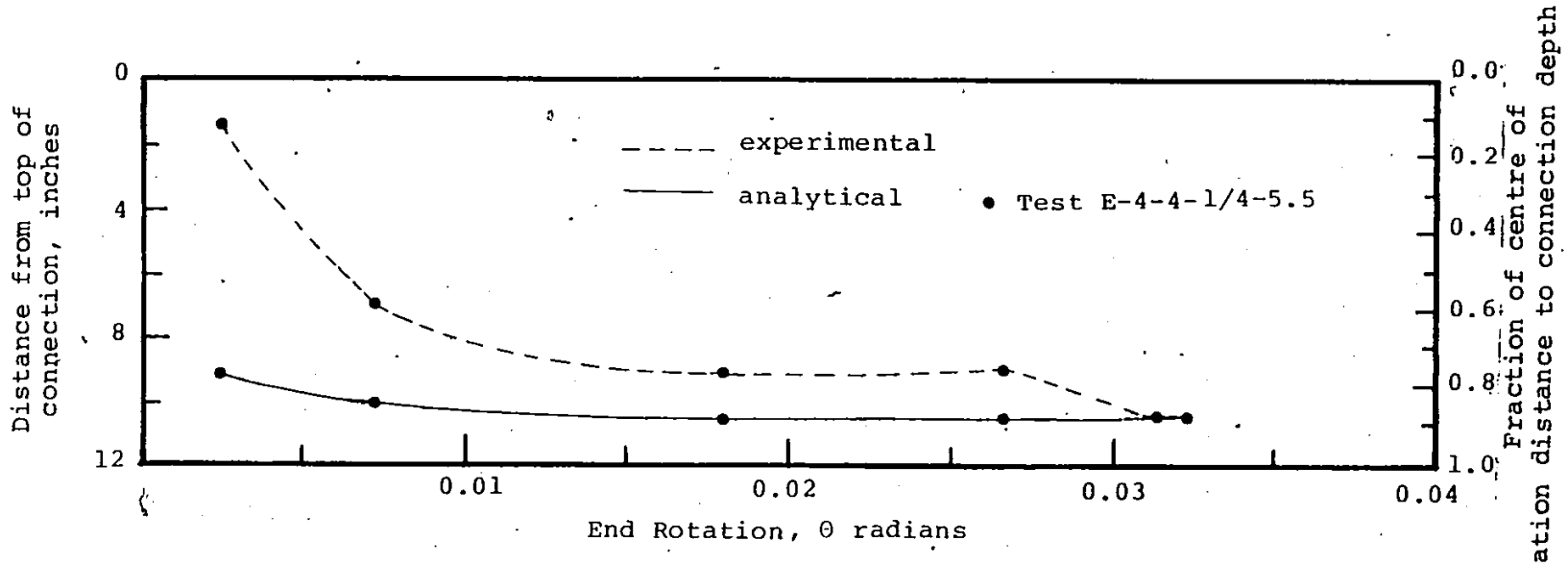

Fig. 3.39. Location of centre of rotation.

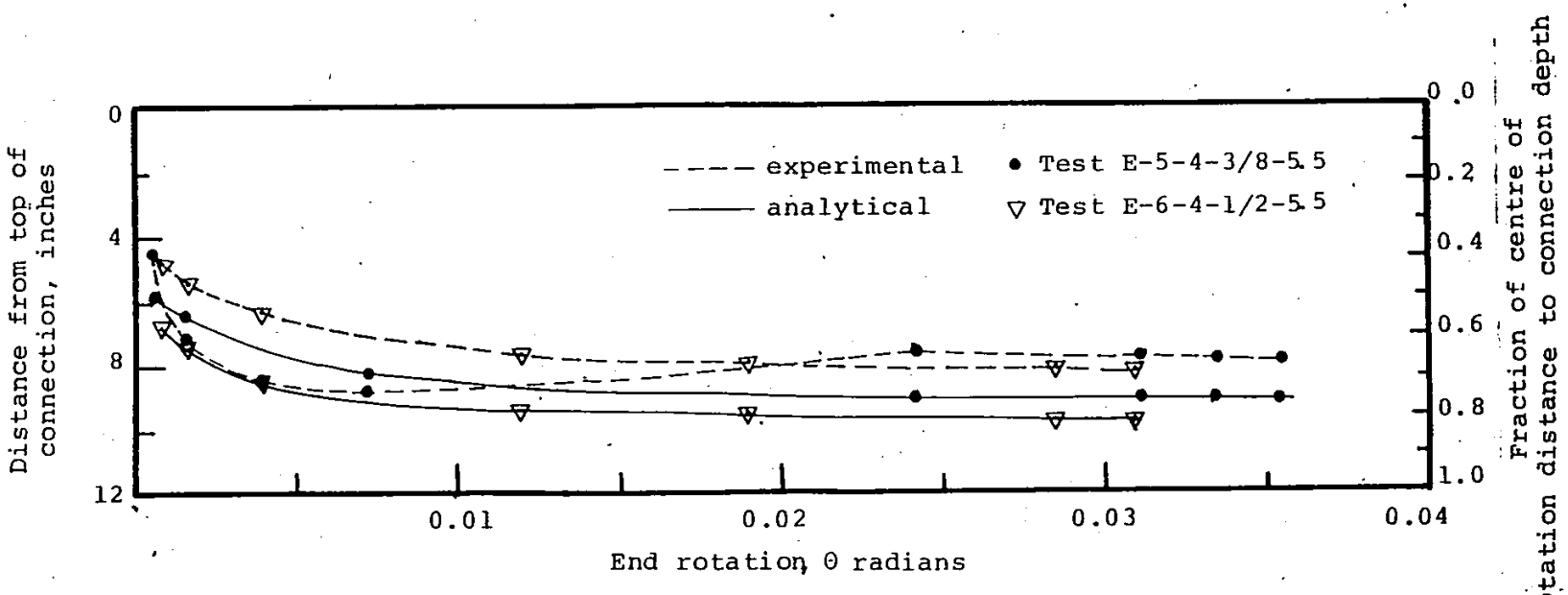

Fig. 3.40. Location of centre of rotation.

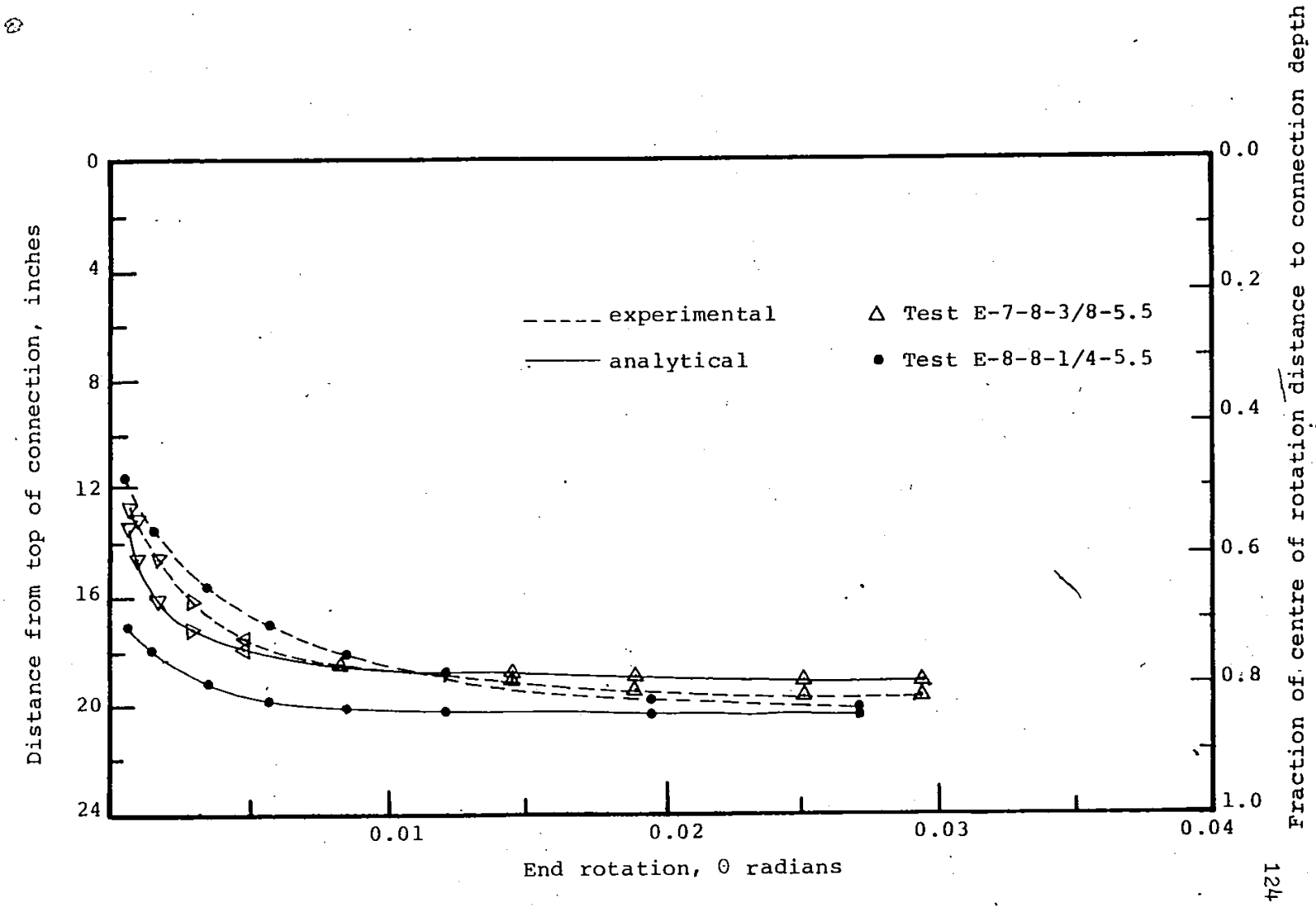

Fig. 3.41. Location of centre of rotation.

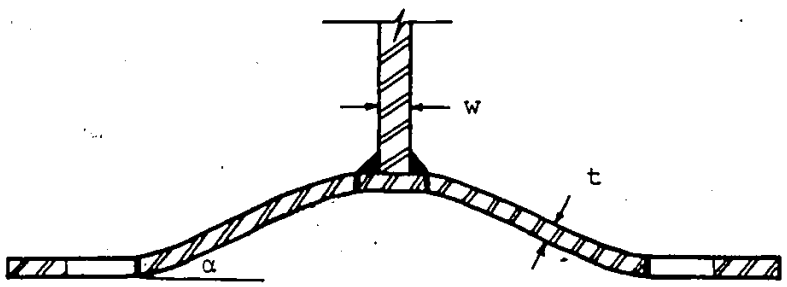

Fig. 4.1 Idealized location of plastic hinges.

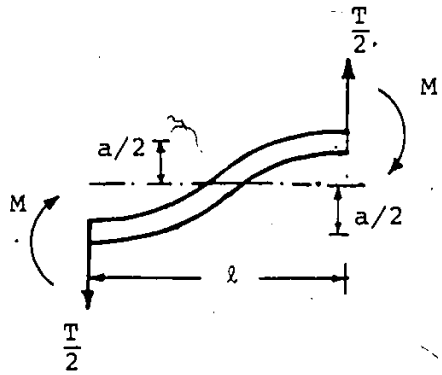

Fig. 4.2 F.B.D. for half the x-section under flexural action.

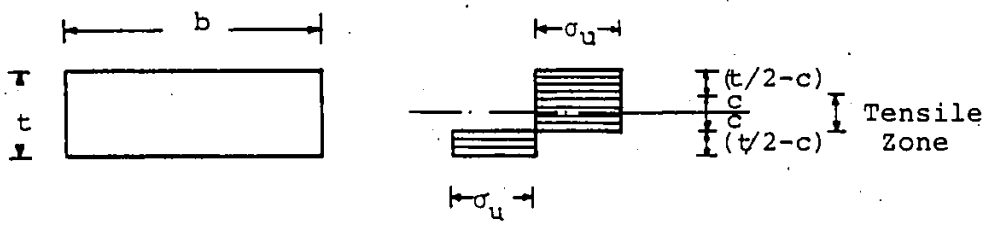

Fig. 4.3 Maximum stresses under the effect of moment and tension force

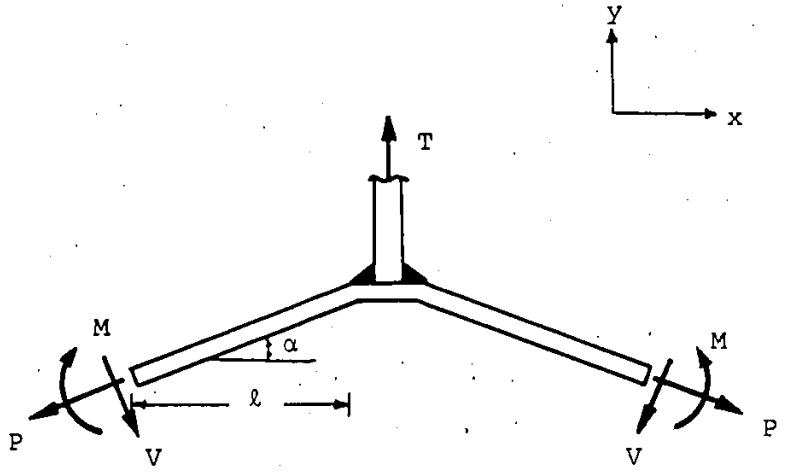

Fig. 4.4 Free body diagram of deformed T specimen.

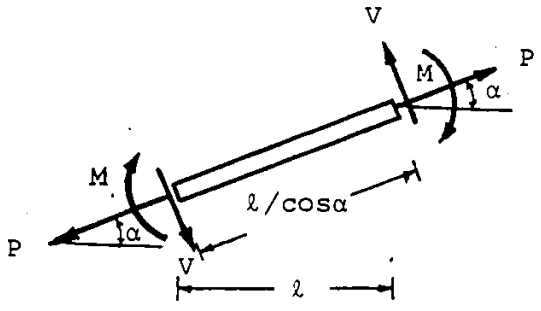

Fig. 4.5 Free body diagram of portion of end plate.

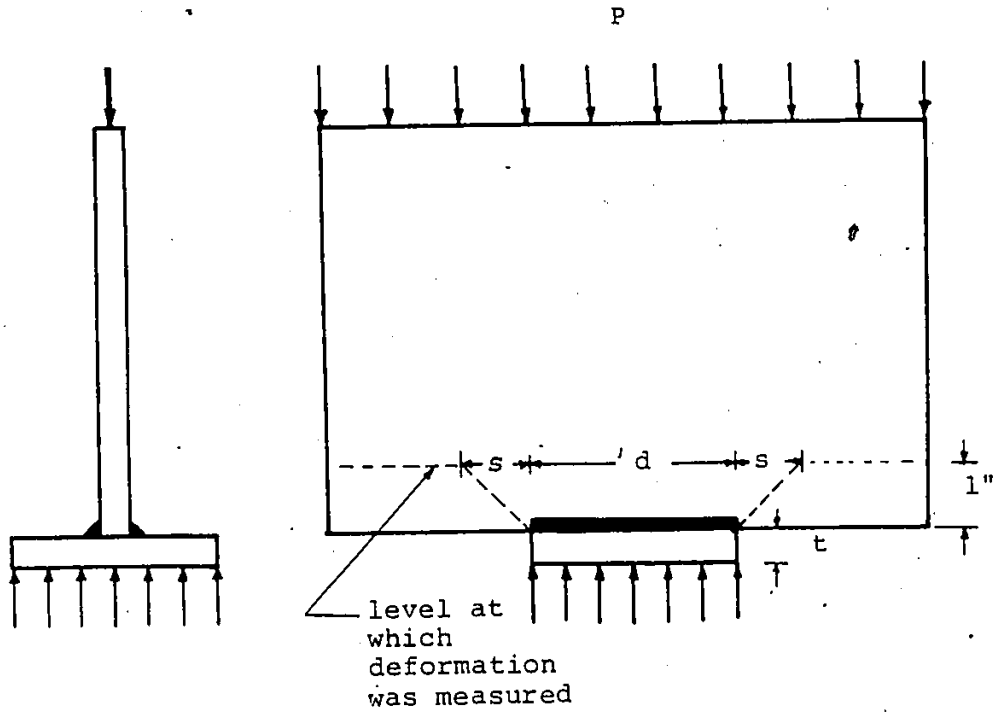

Fig. 4.6 T-section compression test specimen and the force spread out.

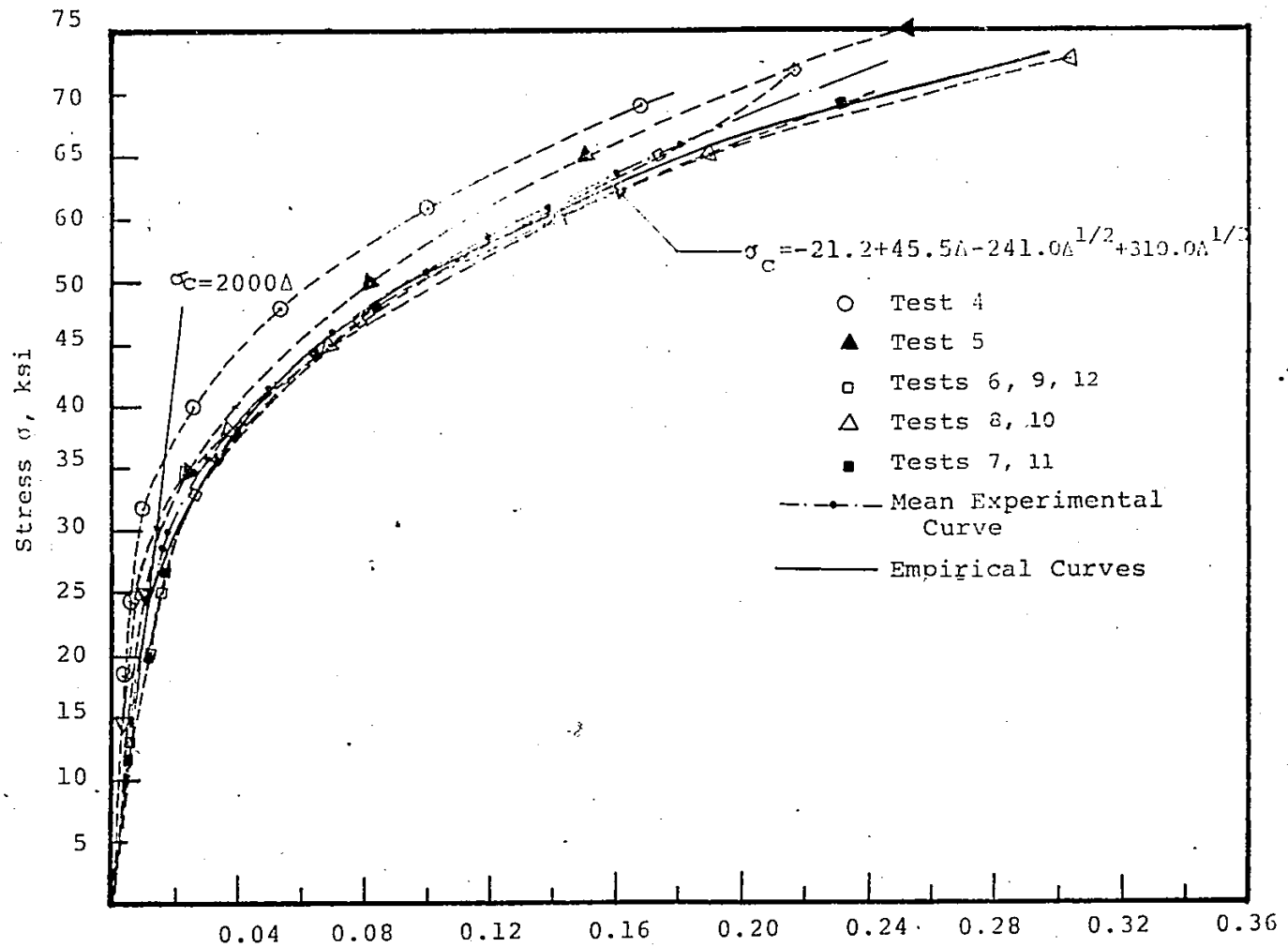

Fig. 4.7 Stress-Displacement Relationship for Compression Test

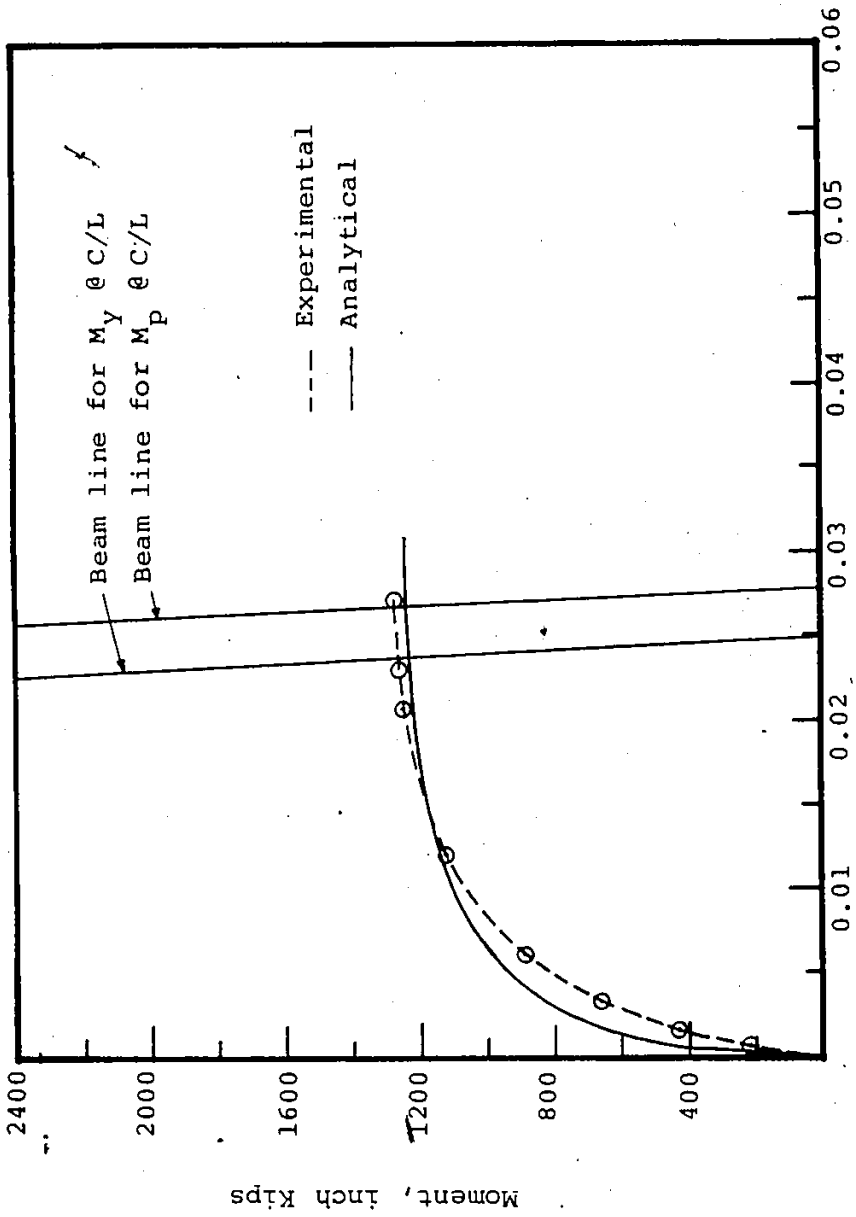

Fig. 4.8. Analytical and experimental moment-rotation curves before bearing for Test E-1-6-3/8-4.

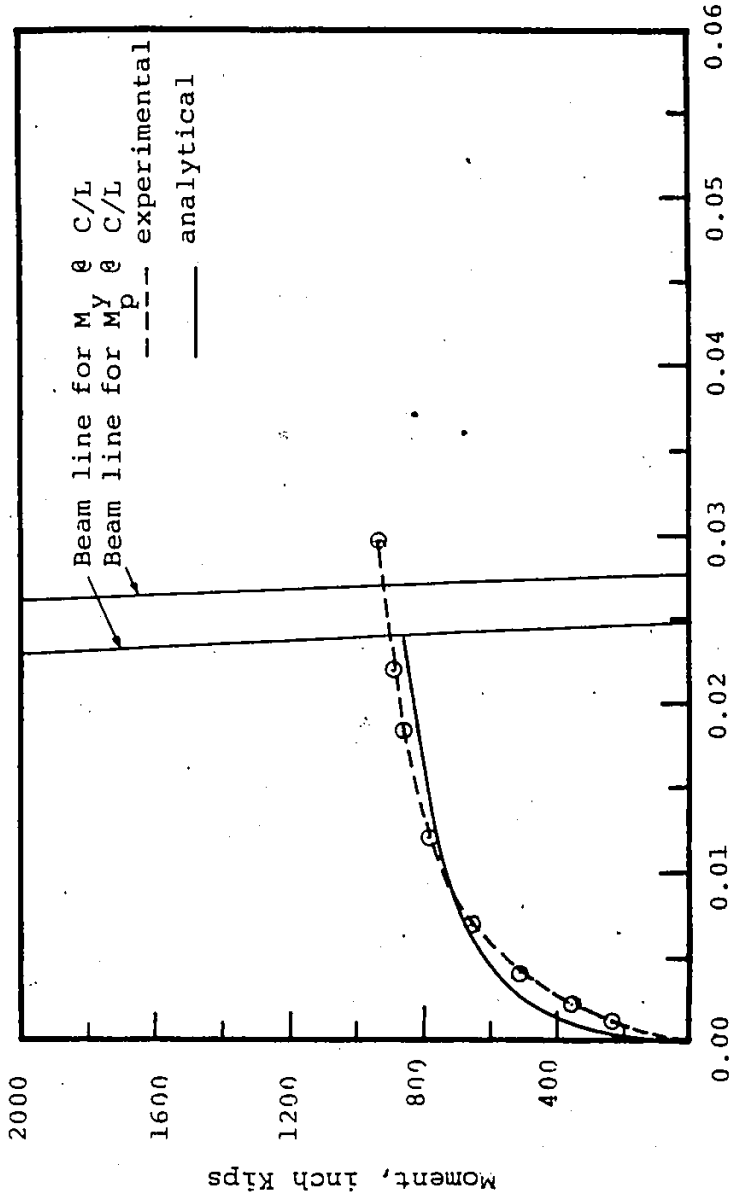

Fig. 4.9 Analytical and experimental moment-rotation curves before bearing for Test E-2-6-1/4-4.

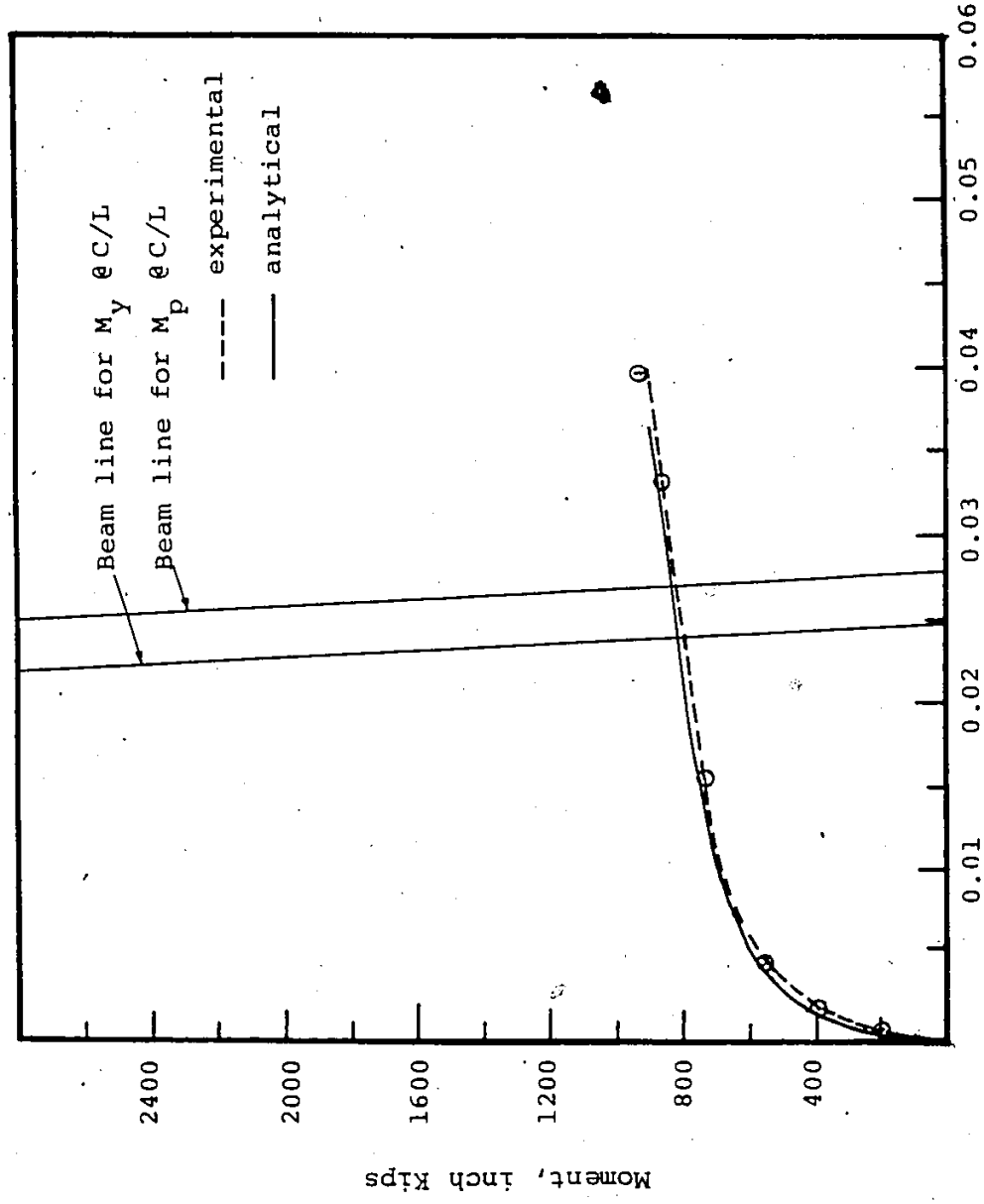

Fig. 4.10. Analytical and experimental moment-rotation curves before bearing for Test E-3-6-3/8-5.5.

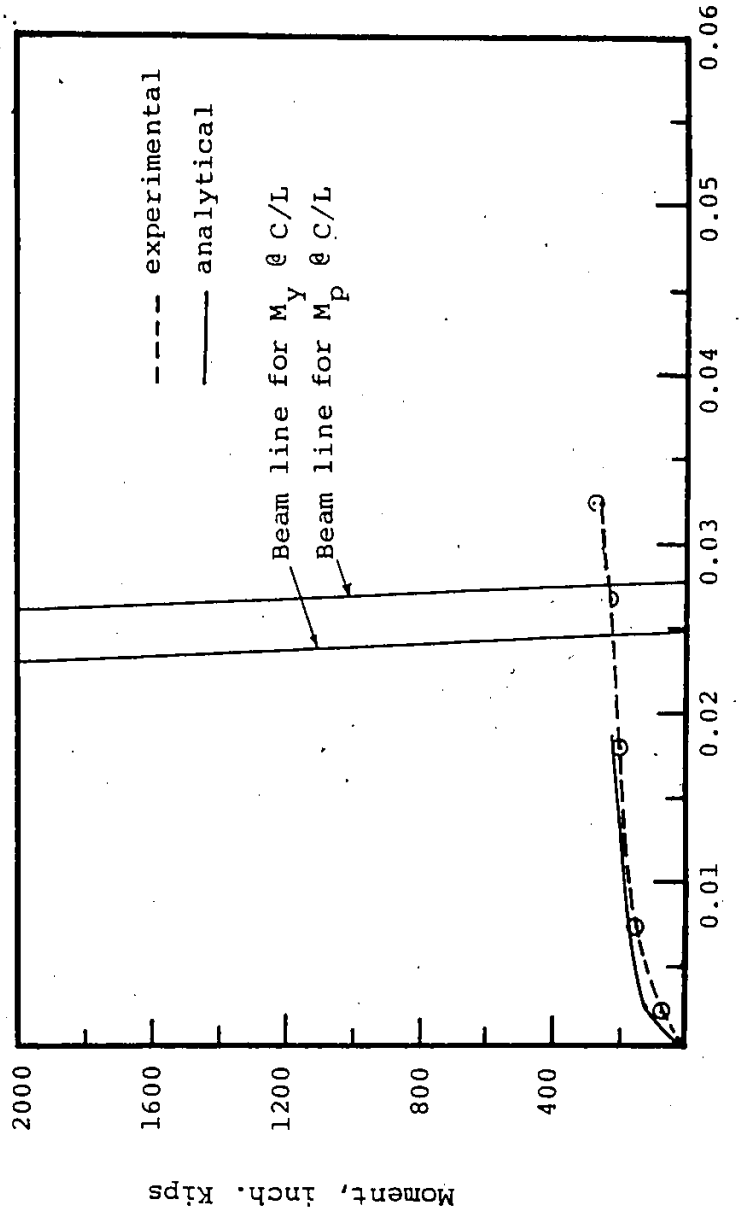

Fig. 4.11. Analytical and experimental moment-rotation curves before bearing for Test E-4-4-1/4-5.5

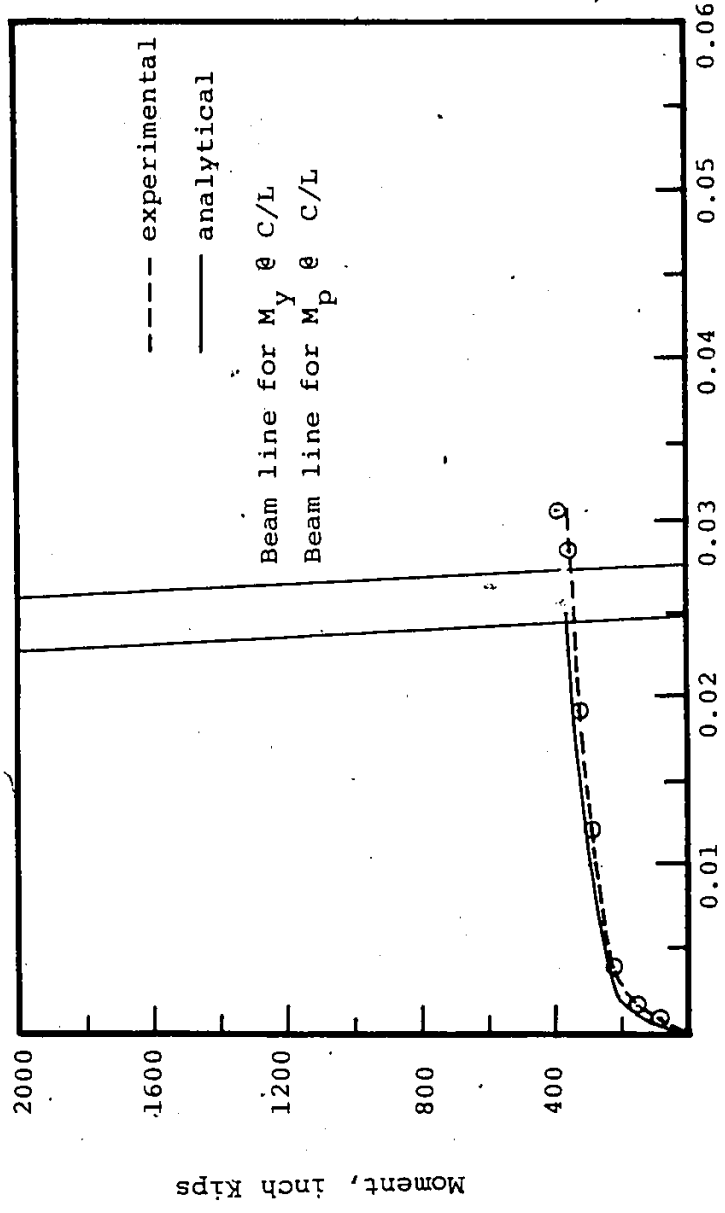

Fig. 4.12. Moment rotation curve for test E-5-4-3/8-5.5

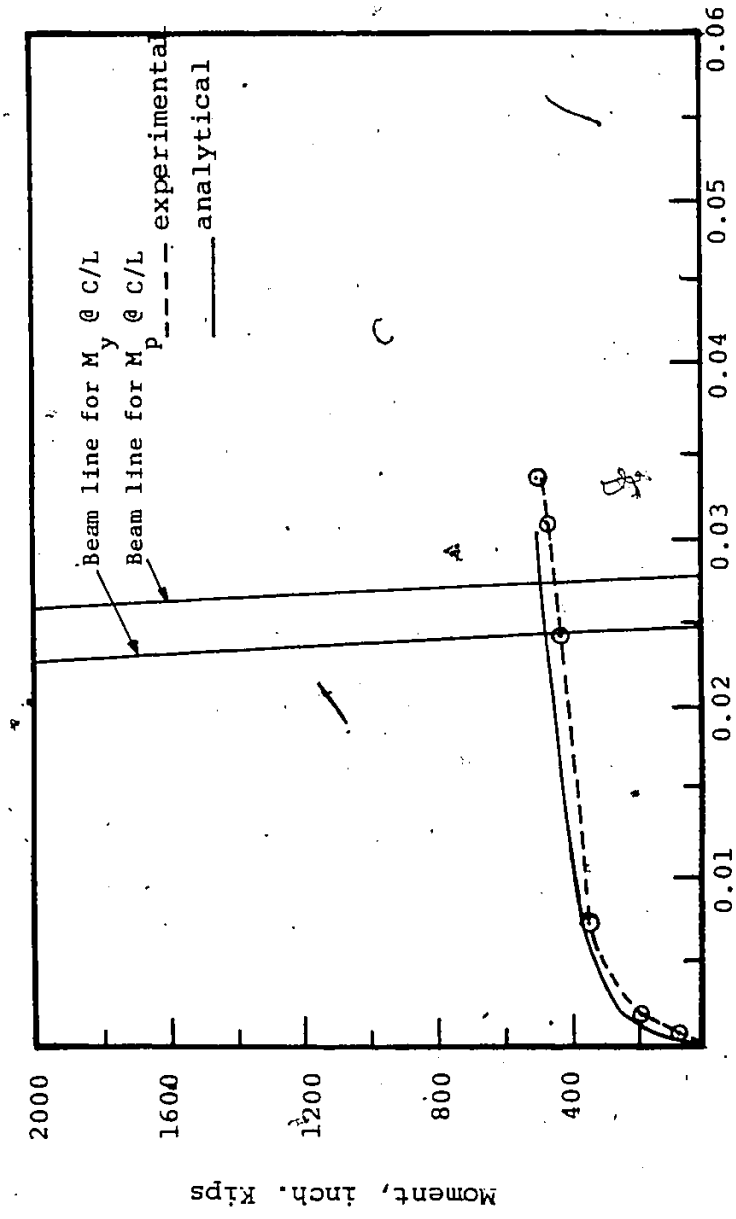

Fig. 4.13. Moment Rotation curve for Test E-6-4-1/2-5.5.

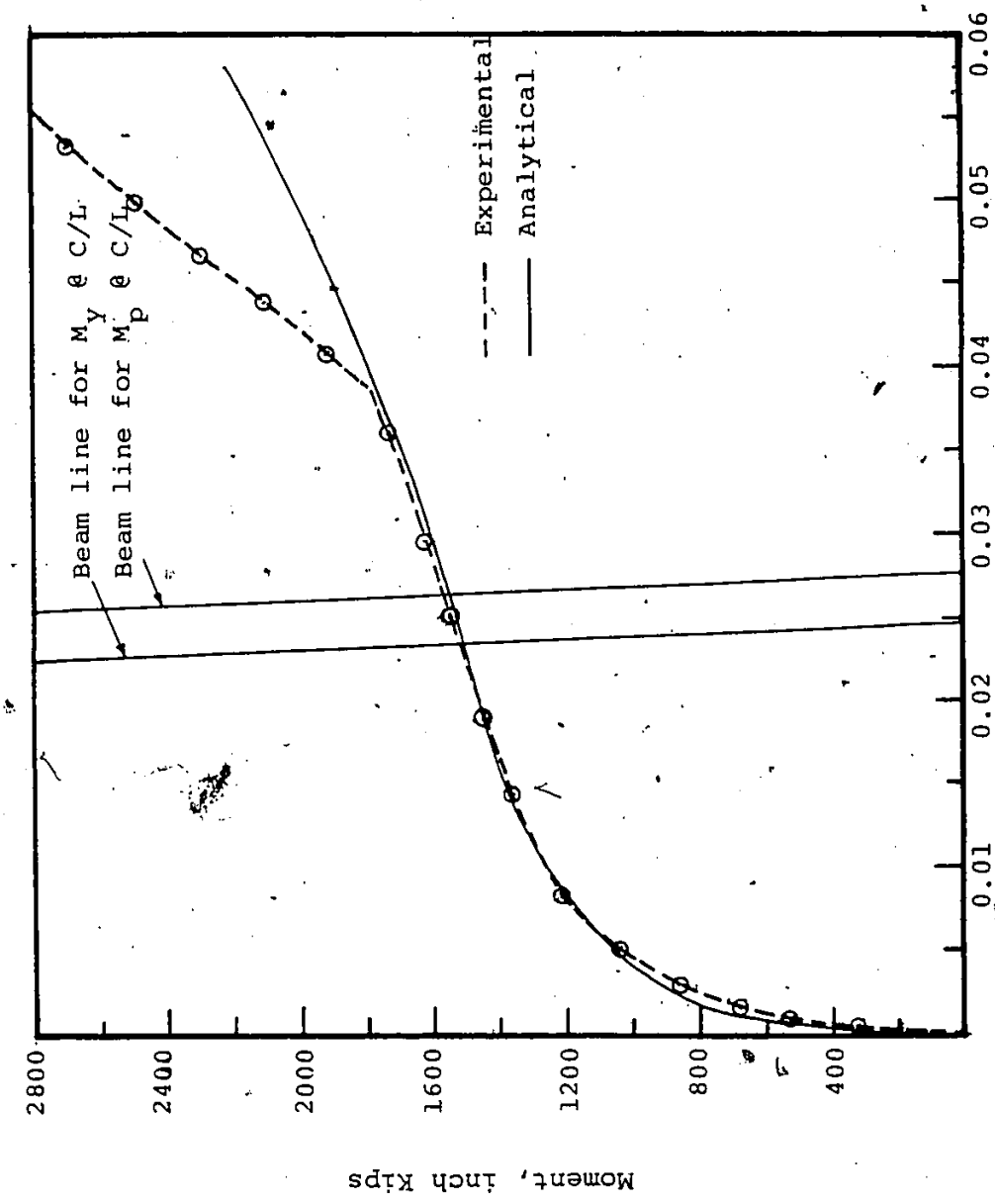

Fig. 4.14. Analytical and experimental moment-rotation curves before bearing for Test -7-8-3/8-5.5

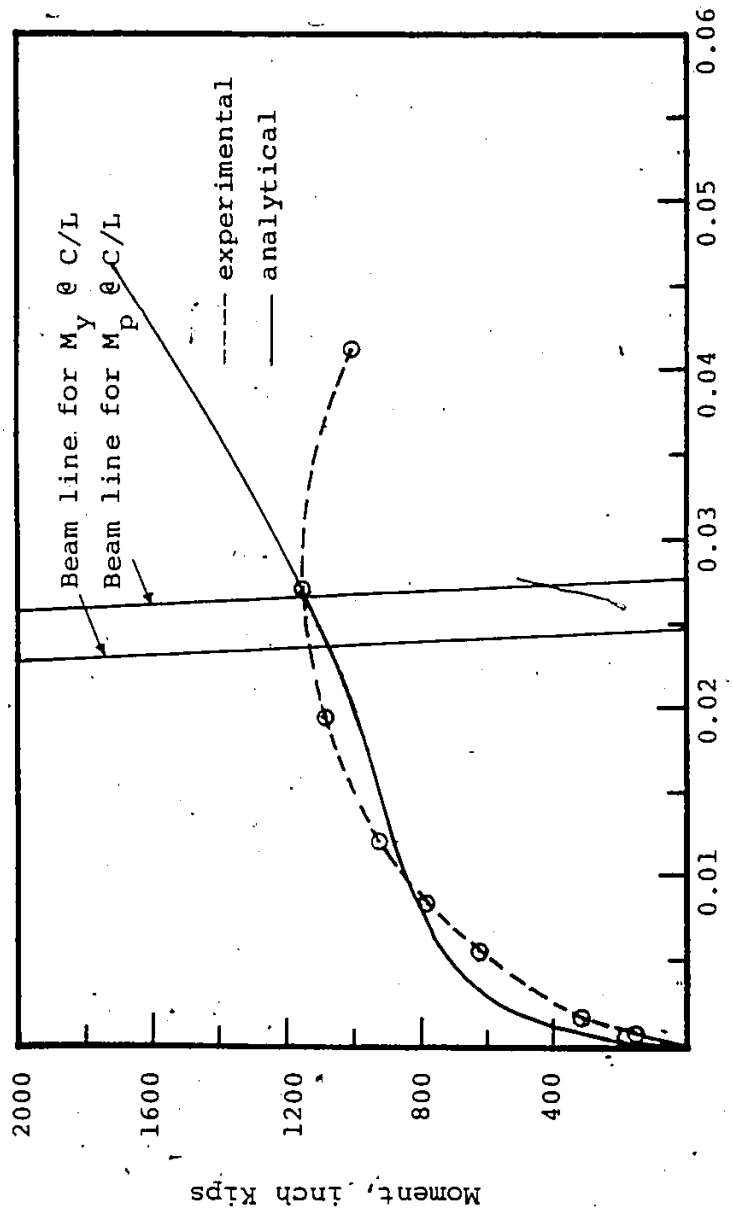

Fig. 4.15. Analytical and experimental moment-rotation curves before bearing for Test E-8-8-1/4-5.5.

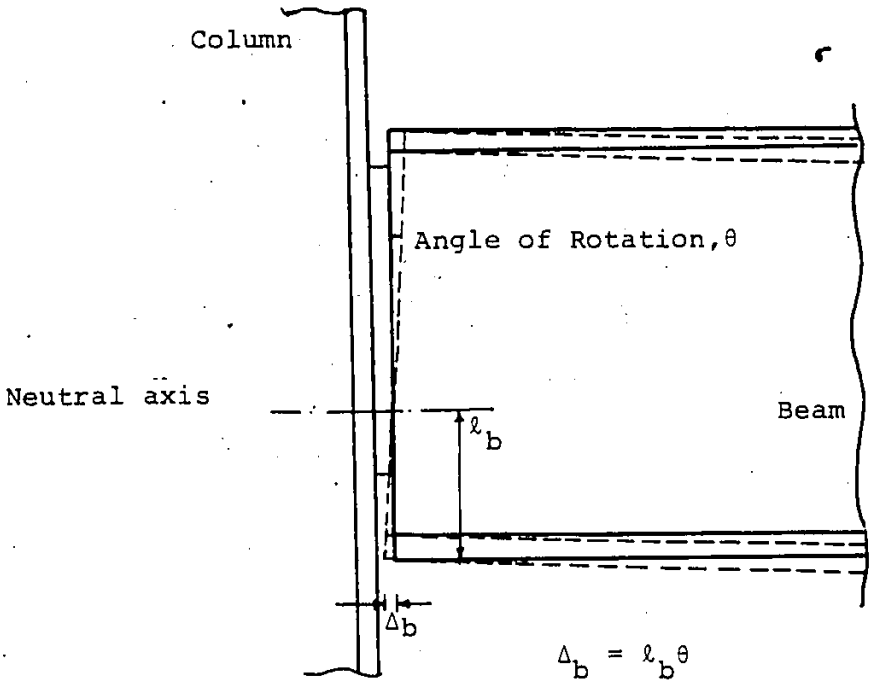

Fig. 4.16 Geometry of Deformation at Contact of Beam with Column.

APPENDIX I

Detailed Observations of End Plate Tests

Notes:

1. Sometimes one of the tips of the beam flange came into contact with against the column before the other. This is designated as east or west bearing respectively.

2. The rows of bolts are numbered from 1 to 8 proceeding from the top to the bottom of the connection. The area where yielding occurred on the connection is related to the rows of bolts; for example, yielding at bolt 1, means yielding occurred in the area of the connection around the first (top) row of bolts.

3. "HAZ" refers to the heat affected zone in the plate material adjacent to the weld.

DETAILED OBSERVATIONS OF TEST 1

TEST E-1-6-3/8-4

Load kips	
24	yielding in plate above bolt 1 for east side
30	significant yielding at bottom west side
32	yielding down to bolt 2 both sides
34	east bearing on column
36	west bearing on column
50	yielding down to bolt 3
65	weld cracked west side of bolt 2 weld cracked east side to bolt 2
72	weld cracked down to bolt 3 west side
73	weld cracked down to bolt 4

Measurement of Weld Size
(in sixteenth of inches)

	East	West
top	4	5
1	4	4
2	4	5
3	4	5
4	5	4
5	4	5
6	5	5
bottom	4	4

DETAILED OBSERVATIONS OF TEST 2

TEST E-2-6-1/4-4

Load kips	Notes
24	yielding in plate above bolt 1 for west side
24	yielding of the beam web around the end of the end plate
25	yielding around the upper bolt at east side
26	crack of weld down to second bolt in east side
26	almost bearing on west side
32	crack of weld to second bolt in west side
32	crack of weld to third bolt for east side
37	maximum load reached with failure in both sides of weld
26	failure in HAZ

Measurement of Weld Size
(in sixteenth of inches)

	East	West
top	4	5
1	5	4
2	4	4
3	5	4
4	4	4
5	4	4
6	5	5
bottom	4	5

DETAILED OBSERVATION OF TEST 3

TEST E-3-6-3/8-5.5

Load kips	Notes
15	yielding in plate above bolt 1 at the west side
18	yield starts at the east side above around bolt 1
20	yielding progressed to third bolt for the west side
25	yielding to bolt 4 in east side
27	west bearing on column
29	east bearing on column
39	crack down to bolt 3 west side
50	crack down to bolt 3 east side
65	failure due to crack in HAZ

Measurements of Weld Size
(in sixteenth of inches)

	East	West
top	4	5
1	4	5
2	4	4
3	5	4
4	4	5
5	4	4
6	4	5
bottom	4	4

143

DETAILED OBSERVATIONS OF TEST 4

TEST E-4-4-1/4-5.5

Load kips	Notes
6	yielding in plate above bolt 1 for east side
6.5	almost bearing for east side
7.0	bearing for west side
10	yielding dawn to bolt 2 both sides
25	weld crack at east side down to bolt 2
26	weld crack down to bolt 2 in west side

Measurements of Weld Size
(in sixteenth of inches)

	East	West
top	4	5
1	5	5
2	4	4
3	5	4
4	4	4
bottom	4	5

DETAILED OBSERVATIONS OF TEST 5

TEST E-5-4-3/8-5.5

Load kips	Notes
9	yielding of the web of the beam around the end of the end plate
10	yielding down to bolt 2 both sides
11	east bearing on column
12	west bearing on column
40	weld cracked down to bolt 3 east side
45	weld cracked down to bolt 3 west side

Measurements of Weld Size
(in sixteenth of inches)

	East	West
top	4	5
1	4	5
2	4	4
3	4	4
4	5	4
bottom	4	5

DETAILED OBSERVATIONS OF TEST 6

TEST 6-4-1/2-5.5

Load kips	Notes
5	yielding in plate above bolt 1 for both sides
10	yielding progressed to bolt 2 for both sides
13	east bearing on column
14	west bearing on column
40	weld cracked to bolt 2 east side
45	weld cracked to bolt 2 west side
72	maximum and failure load reached failure in HAZ

Measurements of Weld Size
(in sixteenth of inches)

	East	West
top	4	5
1	5	5
2	4	4
3	4	4
4	4	5
bottom	4	4

DETAILED OBSERVATIONS OF TEST 7

TEST E-7-8-3/8-5.5

Load kips	Notes
20	yielding in plate above bolt 1 on both sides
30	yielding in plate down to bolt 2 both sides
45	weld cracked down to bolt 2 east side
50	west bearing on column
50	yielding down to bolt 4 both sides
60	weld cracked down to bolt 3 east side
70	weld cracked down to bolt 5 east side
76	failure land reached

Measurements of Weld Size
(in sixteenth of inches)

	East	West
Top	5	4
1	4	5
2	4	5
3	4	4
4	5	4
5	5	4
6	4	5
7	5	4
8	4	4
bottom	5	5

147

DETAILED OBSERVATIONS OF TEST 8

TEST E-8-8-1/4-5.5

Load kips	Notes
7	yielding in plate down to bolt 2 east side
10	yielding in plate to bolt 3 west side
20	weld cracked at the top of the plate.
24	weld cracked down to bolt 2 east side
28	weld cracked extended to bolt 2 west side
30	crack progressed to bolt 3 west side
30	crack extended to bolt 5 east side
30	maximum load reached. Beyond this load, the connection could not transmit more loads, and the load started to decrease

Measurements of Weld Size
(in sixteenth of inches)

	East	West
top	4	5
11	4	4
2	4	4
3	4	5
4	4	4
5	5	4
6	4	4
7	4	4
8	5	5
bottom	5	4

APPENDIX II

FLOW CHART

START

CETA	= End rotation at contact
CF	= Compression force in the end plate connection
CFU	= Compression force in the end plate connection at contact
CIN	= Incremental end rotation assumed during the determination of CETA
CLEAR (I)	= Minimum clearance between the beam and column at rotation No. I
CM	= Compression moment in the end plate connection
CMU	= Compression moment in the end plate connection at contact
DIN	= Distance between assumed positions of neutral axis during two consecutive incremental analyses
FINC	= End rotation increment
FM1 (I)	= Moment at the end plate corresponding to end rotation No. I
FMU	= Moment at the end plate at contact
NL	= Total number of end rotations considered in the analysis
PHI (I)	= End rotation No. I
SPA	= Minimum clearance between the beam and column during the analysis for end rotation at contact
TF	= Tension force in the end plate connection
TFU	= Tension force in the end plate connection at contact
TH	= Thickness of the end plate
TM	= Tension moment in the end plate connection
TMU	= Tension moment in the end plate connection at contact

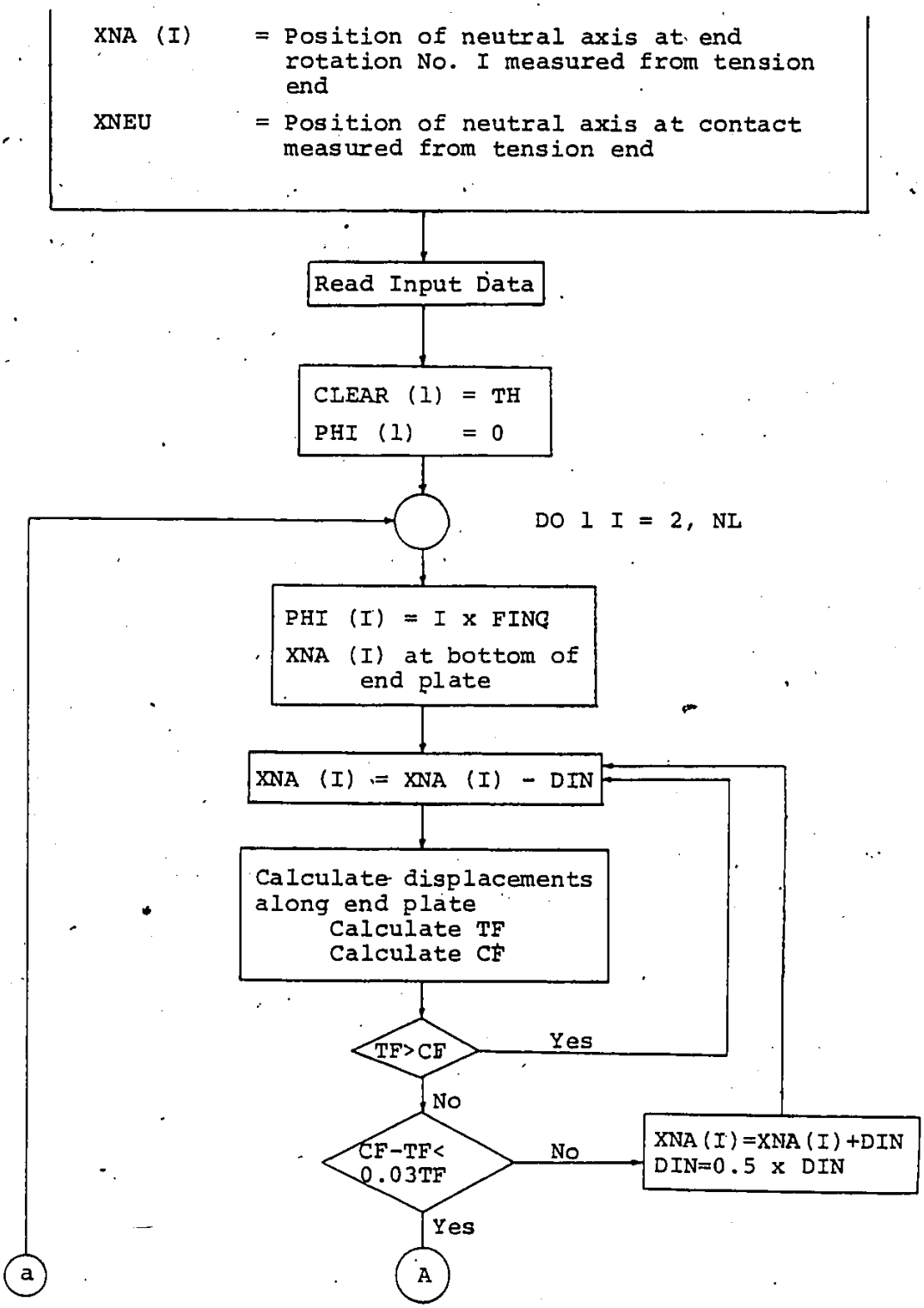
XNA (I) = Position of neutral axis at end rotation No. I measured from tension end
XNEU = Position of neutral axis at contact measured from tension end
Read Input Data
CLEAR (1) = TH
PHI (1) = 0
DO 1 I = 2, NL
PHI (I) = I x FINQ
XNA (I) at bottom of end plate
XNA (I) = XNA (I) - DIN
Calculate displacements along end plate
Calculate TF
Calculate CF
TF>CF
Yes
No
CF-TF< 0.03TF
No
XNA(I)=XNA(I)+DIN
DIN=0.5 x DIN
Yes
a
A

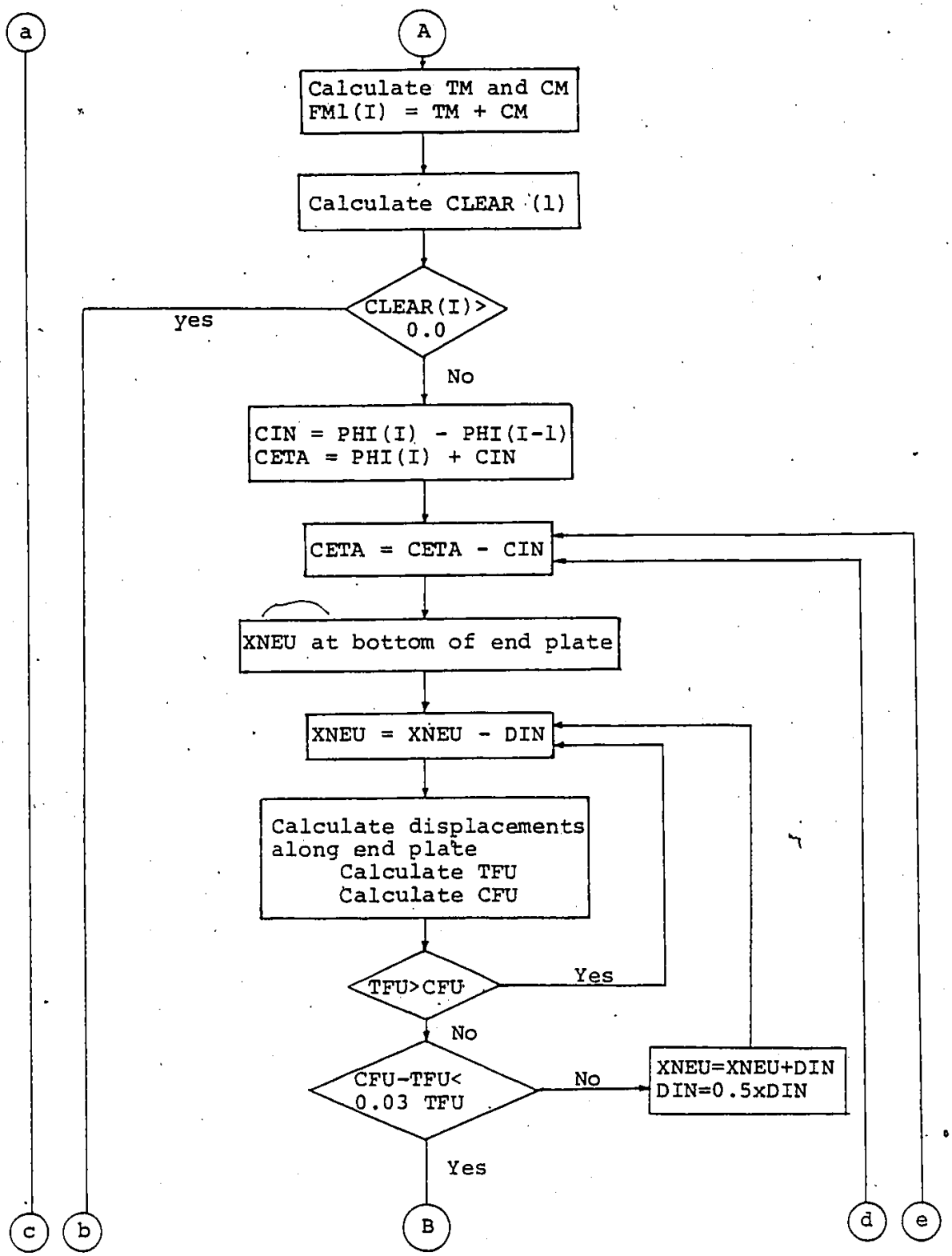
a
A
Calculate TM and CM
FM1(I) = TM + CM
Calculate CLEAR (1)
CLEAR(I)>
0.0
yes
No
CIN = PHI(I) - PHI(I-1)
CETA = PHI(I) + CIN
CETA = CETA - CIN
XNEU at bottom of end plate
XNEU = XNEU - DIN
Calculate displacements
along end plate
Calculate TFU
Calculate CFU
TFU>CFU
Yes
No
CFU-TFU<
0.03 TFU
No
XNEU=XNEU+DIN
DIN=0.5xDIN
Yes
c
b
B
d
e

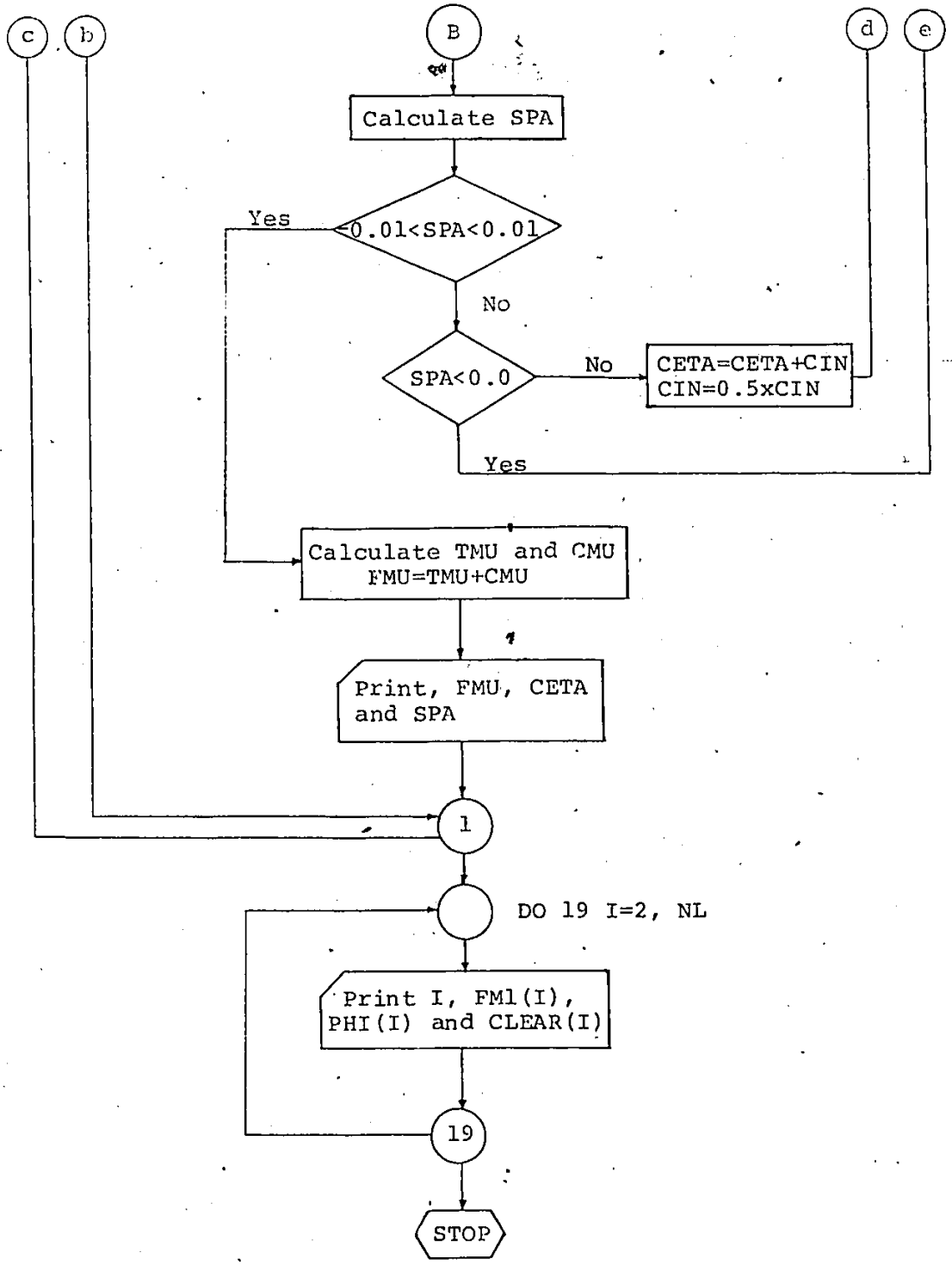
c
b
B
d
e
Calculate SPA
Yes
-0.01<SPA<0.01
No
SPA<0.0
No
CETA=CETA+CIN
CIN=0.5xCIN
Yes
Calculate TMU and CMU
FMU=TMU+CMU
Print, FMU, CETA
and SPA
1
DO 19 I=2, NL
Print I, FM1(I),
PHI(I) and CLEAR(I)
19
STOP

REFERENCES

1. Kennedy, D.J.L., "Welded Header Plate Beam-Column Connections." Report to Niagara Structural Steel Company Limited, A Private Report, March 1966.

2. Sommer, W. H., "Behavior of Welded Header Plate Connections." Thesis presented to the Department of Civil Engineering, University of Toronto, Toronto, Ontario, Canada, in partial fulfillment of the requirements for the degree of M.A.Sc., 1969.

3. Kennedy, D.J.L., "Moment Rotation Characteristics of Shear Connections." Engineering Journal, AISC, Vol. 6, No. 4, Otober 1969.

4. W. McGuire, "Steel Structures." Prentice Hall Inc., 1968.

5. Adams, P. F., Krentz, H. A., and Kulak, G. L., "Limit Slates Design in Structural Steel." Canadian Institute of Steel Construction, 1977.

6. "Handbook of Steel Construction." Canadian Institute of Steel Construction, 1972.

7. Annual Book of ASTM STANDARD, 1976.

8. Gaylord, E. A., and Gaylord, C. N., "Design of Steel Structures." McGraw-Hill Book Company, 1972.

VITA AUCTORIS

Mona Ali Hafez

The author was born on July 18, 1953 in Cairo, Egypt. In 1971, she completed her secondary school education at Sania School, Cairo, Egypt. Then, she joined the Faculty of Engineering, Cairo University, where she was granted undergraduate scholarships for five consecutive years. In 1976, she graduated from Cairo University with a degree of Bachelor of Civil Engineering.

In 1976, she was appointed as a Teaching and Research Assistant in the Civil Engineering Department of the University of Windsor, Windsor, Ontario, Canada. The author prepared this thesis in partial fulfillment of the requirements for the degree of Master of Applied Science at the University of Windsor.